

Real-time Vehicle Steering Sensitivity Adaptation based on Time-Frequency Analysis of Individual Drivers' Steering Behaviour

Master Thesis

Sam Staps



Real-time Vehicle Steering Sensitivity Adaptation based on Time-Frequency Analysis of Individual Drivers' Steering Behaviour

Master Thesis

by

Sam Staps

to obtain the degree of Master of Science
at the Delft University of Technology.
to be defended publicly on Friday May 28, 2021 at 10:00 AM.

Student number: 4175034
Project duration: Oktober, 2019 – May 28, 2021
Thesis committee: Ir. T. Melman, TU Delft, supervisor
Prof. dr. ir. D. A. Abbink, TU Delft, supervisor
Dr. Ir. Michaël Wiertlewski, TU Delft

An electronic version of this thesis is available at <http://repository.tudelft.nl/>.

Acknowledgements

Ik wil Barys Shyrokau bedanken voor zijn hulp en inzichten in de voertuigdynamica, en Joost de Winter bedanken voor zijn enthousiasme en open feedback op het ontwerp van het experiment.

Ik wil Timo Melman heel hartelijk bedanken voor zijn enthousiaste begeleiding, houvast, feedback en sturing die ik heb gekregen tijdens dit project. Ik wil graag David Abbink bedanken voor zijn begeleiding en supervisie, de scherpe ideeën, en ook de motivatie en persoonlijke steun voor en tijdens dit project.

Ik wil de medewerkers van het Cognitive Robotics Lab bedanken voor de technische ondersteuning, en ik wil mijn medestudenten in het Cognitive Robotics Lab bedanken voor de gezelligheid en hun bereidbaarheid om na te denken over ideeën en oplossingen die ik tijdens dit project ben tegen gekomen.

Ik wil al mijn vrienden bedanken voor alle motivatie, steun en hulp tijdens mijn afstudeerproject. Ik wil mijn familie, Bas, Nicole, Zep, Thijs en Dex bedanken voor alle steun en motivatie.

In herinnering aan Thomas Janssen.

Sam Staps
Delft, May 2021

Preface

From the idea that there is more to explore and discover in the behaviour of human movements, I took the challenge to research the steering behaviour of human drivers, limiting myself to the steering movements only. Although this limitation would seem to make this project nearly impossible, this limitation forced me to investigate deeper into the behaviour of human movements. With my experience as a driver, I noticed certain characteristics in my own steering behaviour. I was not able to explain these characteristics with the knowledge I had when I started this project. Through literature, discussions and meetings I found out that these characteristics, were known to exist for a long time but were not clearly explained nor understood. Through exploratory research, methods new to the research field were investigated, tested on available data, and finally incorporated into the final investigation of this study. A human-in-the-loop fixed-base driving simulator study is performed, and the results and findings are hereby proudly presented.

Contents

| | | |
|---|--|----|
| 1 | Research paper | 1 |
| A | Reanalysis of steering behaviour from steering wheel data from the experiment by Kroes (2019). | 15 |
| B | Extraction of intermittent switching by Inoue (2015) | 19 |
| C | Vehicle wheel dynamics | 25 |
| D | Adaptive design algorithm | 37 |
| E | Simulated road environment | 41 |
| F | Experiment remarks | 43 |
| G | Informed Consent form | 45 |
| H | Experiment Questionnaires | 49 |
| I | Individual participant data | 63 |

1

Research paper

Real-time Vehicle Steering Sensitivity Adaptation based on Time-Frequency Analysis of Individual Drivers' Steering Behaviour

Master Thesis

Sam Staps

Department of Cognitive Robotics, Faculty of Mechanical, Maritime and Materials Engineering, Delft University of Technology, Mekelweg 2, 2628 CD Delft, The Netherlands

Abstract—Conventional steering systems in passenger vehicles have a mechanically fixed steering ratio. The steering sensitivity, defined as the amount of vehicle response to the driver's steering wheel input, remains fixed with changing road environments. Research has shown that driving comfort and safety can be improved when the vehicle's steering sensitivity is adapted to the road curvature profile. Current vehicle models can adapt the vehicle's steering sensitivity based on vehicle's speed and driver's steering wheel angle (i.e. variable gear-ratio systems), or on individual selection of driving mode (i.e. sport, comfort). It is hypothesised that adaptation of the steering sensitivity based on frequency measures of individual drivers' steering behaviour could improve driving comfort and safety. In a fixed-base driving simulator experiment involving 24 participants, real-time adaptation of steering wheel sensitivity based on individual drivers' steering behaviour was compared to three different fixed steering sensitivity settings on a road with changing road curvature. Here I show that intermittent switching frequency in drivers' steering movements can be used to adapt the vehicle's steering response to a varying road curvature. Significant differences in intermittent switching were found between different road curvature sections and between different steering sensitivity settings. Driver's positional control and comfort ratings did not significantly increase with the steering sensitivity adaptation strategy.

Index Terms—steering response, motor control, man-machine, wavelet, adaptation

I. INTRODUCTION

A. Steering comfort and safety

Steering systems in passenger vehicles have historically a mechanically fixed steering ratio. The steering ratio and the vehicle speed, among other vehicle parameters, mainly affect the vehicle's lateral and yaw rate response. The amount of vehicle response to the human driver's steering wheel input is defined as the vehicle's steering sensitivity. With a fixed steering ratio, the vehicle's steering sensitivity is generally low at low speed driving and high at high speed driving [1]. This requires drivers to steer with larger steering wheel angle inputs at low speed driving, which increases physical

effort, and more precise steering wheel angle inputs at high speed driving to maintain high-speed stability.

Previous research has shown that adaptation of steering sensitivity to the curvature of the road can increase safety margins and driver acceptance ratings, with higher subjective ratings reported for control safety, ease of control and comfort [2] and steering performance characteristics [3] when driving with a high steering sensitivity on a curved road with a high steering demand, and a low steering sensitivity on a straight road with a low steering demand.

In an effort to improve driving comfort, modern technologies such as Variable Gear-ratio System (VGS) and four-wheel steering (4WS) adapt the steering wheel sensitivity continuously based on vehicle parameters such as vehicle speed and steering wheel angle [3]–[6]. Other modern technologies allow for steering sensitivity adaptation based on individual preference by selecting the driving mode (e.g. comfort, normal, sport) by means of a push-button [7].

While current implementations of steering wheel sensitivity adaptation strategies infer the preference for steering sensitivity through steering wheel angle, speed, and selected driving mode, current implementations do not continuously adapt to the driver's actual preference for the steering sensitivity, in a continuous feedback manner. An objective measure of steering behaviour indicating driver preference for the steering sensitivity is required as basis for this adaptation strategy.

B. Measures of steering behaviour

McLean & Hoffmann (1975) summarised three frequency measures of steering wheel movements that are reflective of steering task difficulty: steer reversal rate (SRR), primary dominant frequency (PDF) and high-frequency area (HFA) [8].

Steering reversal rate (SRR) is measured by the number of times the steering wheel movement changes direction, filtered through a gap of 0.5 - 0.7 deg for most meaningful results for steering tasks [8]. "The steering reversal rate can be a valid criterion for detecting differences in drivers or conditions", as stated by McLean & Hoffmann (1975) [8].

Primary dominant frequency (PDF) is measured by the peak found in the spectral analysis of the steering wheel angle [9]. No consistent effects on the shape of the steering wheel angle spectrum for different steering sensitivities in a circular-course experiment by McLean & Hoffmann (1971) were found [9]. In a straight road driving experiment, PDFs were mainly found in the 0.1 - 0.3 Hz frequency spectrum, and appeared to be associated with control of vehicle heading angle without close attention to lateral error [10].

High frequency area (HFA) is measured by the proportion of high frequency steering movements calculated by taking the area under the steering wheel angle spectral density curve at frequencies greater than 0.4 Hz [10]. The proportion of high frequency (> 0.4 Hz) control movements tend to increase with increasing speed and decreasing lane width, combined referred to as 'tightness' of the driving situation [10]. For extreme situations of task tightness, McLean & Hoffmann (1972) observed an increase in HFA and related this to a change in steering strategy that dominantly involved direct control of lateral error [10].

Review of the frequency measures of steering wheel movements above shows that steering movements in the low frequency spectrum are related to the driving task, and that steering movements in the high frequency spectrum may be related to the control strategy of the driver. Variation of the steering wheel sensitivity will not affect the driving task, but may affect the control strategy of the driver, and therefore create a preference for one steering sensitivity setting over the other. Drivers may have a different driving strategy when driving on a highly curved road with a higher steering sensitivity than with a lower steering strategy. Measurement of high frequency steering behaviour of the driver could provide an estimate for steering strategies that show increased comfort and safety ratings.

C. Time-frequency analysis

The wavelet transform is a signal analysis technique that detects short-lived high frequency phenomena better than the windowed Fourier transform because the analysing functions of the wavelet transform (called wavelets) have their time-widths adapted to their frequency [11]. The wavelet analysis technique is chosen for analysis of driver's steering behaviour because it's ability to detect changes in frequency behaviour of driver's steering wheel movements over time. Inoue & Sakaguchi (2015) published an algorithm using the wavelet analysis technique for detection of intermittent behaviour in control movements of human operators [12]. The frequency spectrum of analysis for detection of intermittency in human control movements is within the 0.5 - 4.0 Hz frequency range. The frequency spectra of analysis of control movements of HFA (> 0.4 Hz) and movement intermittency (0.5 - 4.0 Hz) show a strong overlap. The scope of HFA as meaningful measure

is limited when compared to intermittent switching behaviour. While HFA may correlate with a control strategy of drivers, it provides little meaning compared to intermittent switching behaviour.

The rationale behind the existence of intermittent switching in human movements is that the human brain solves the delay in neuro-muscular feedback by executing movement primitives sequentially in a feed-forward manner to create a continuous smooth movement. This description of intermittent switching in human movements bears close resemblance to human control behaviour not linearly correlated to task behaviour, also called remnant [13]. Remnant is seen as a motor noise component (see fig. 1) that, according to McRuer (1980), appears to be caused by "random time-varying behavior within the operator primarily associated with fluctuations in the effective time delay." [14]. McRuer & Jex (1967) found that "Remnant increases with controlled element gain, with forcing function bandwidth, and with control order." [13]. These relations resemble increase of HFA with task tightness. In a study of deep brain stimulation on patients with Parkinson disease, frequency of intermittent switching has shown it's application as measure of clinical balance impairment while strong correlations of intermittent switching and control gains were found in a quiet standing task [15]. The relationship of intermittent switching frequency and controlled element gain may be a useful property for a measure of steering behaviour that indicates the driver's acceptance of the sensitivity of the steering wheel.

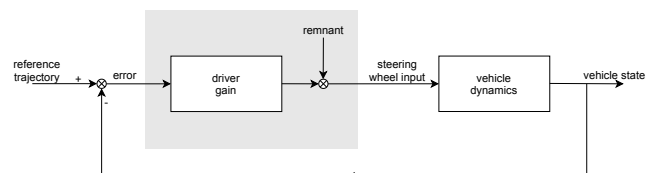


Fig. 1. Driver-vehicle control model with remnant, based on McRuer & Jex (1967) [13].

D. Goal

The aim of this work is to investigate adaptation of the vehicle's steering sensitivity based on driver's steering behaviour to improve driver acceptance.

E. Research question

In this research paper the following questions are investigated:

- What measure of driver steering behaviour is a valid indicator of driver acceptance of the steering wheel sensitivity?
- Does driver acceptance increase when the steering wheel sensitivity is adapted based on real-time measurement of drivers' individual steering behaviour when subjected to changing road curvature profiles?

F. Method

This research paper is structured in two parts, of which each part corresponds to one of the research questions. In the first part, I reanalysed data from Kroes (2019) [2] to investigate the correlation of measures of steering behaviour with driver acceptance and their potential use as basis for a steering sensitivity adaptation strategy. I chose a measure based on this analysis and formulated a hypothesis to the second research question. In the second part, an adaptation strategy based on the measure chosen in the first part is evaluated. The adaptive steering sensitivity strategy based on individual steering behaviour was compared to three fixed steering sensitivity settings in a human-in-the-loop experiment involving twenty-four participants in a fixed-base driving simulator experiment.

II. REANALYSIS OF KROES' DATA

An analysis of three measures of steering behaviour, intermittent switching of steering movements, steering reversal rate and root mean square steering angle, was performed on experiment data from Kroes (2019) [2] to investigate potential correlations with driver acceptance and potential use as basis for adaptation of steering wheel sensitivity.

A. Intermittent switching

Intermittent switching in driver's steering wheel movements were calculated according to [12]. This included (i) the continuous wavelet transform (CWT) of the steering wheel velocity signal by a second-order derivative of a complex Gaussian kernel, which obtains the jerk of the steering wheel angle smoothed by a Gaussian function. (ii) A wavelet scale range that corresponds to the frequency range of 0.5 - 4.0 Hz is chosen to filter out higher frequency kinetic and physiological tremors. A scale range of 10 - 80 is obtained for the Gaussian derivative kernel and a sampling frequency of 100 Hz. (iii) Discontinuities in the signal are marked by points where the phase is undefined (singularity points), shown by a rapid change in phase or peak in instantaneous frequency. The signal's instantaneous frequency is obtained through time differentiation of the unwrapped phase of the CWT. (iv) The frequency of intermittent switching in human movements is given by the amount of signal discontinuities per unit time.

B. Steer reversal rate

Steering reversal rate is a measure of steering task difficulty imposed on the driver [8]. The steering reversal rate is counted as the number of times the direction of steering wheel movement is reversed through a gap size of 0.5 degrees.

C. Root mean square steering angle

Root mean square steering angle is a measure of steering activity. It is calculated by taking the square root of the mean of the squared steering wheel angle values.

D. Data analysis

Steering wheel data from a human-in-the-loop driving simulator experiment of Kroes (2019) was used for analysis of driver's steering behaviour for different steering sensitivities on different road curvature profiles [2]. Three measures of steering behaviour were compared: the frequency of intermittent switching in driver's steering movements, the steering reversal rate (gap size of 0.5 degrees), standard deviation of steering wheel angle. The measures are compared for two steering wheel sensitivity settings, defined in terms of steering ratio, and two road profiles, defined in terms of road curvature. The steering sensitivity settings are denoted by steering ratio, 12:1 for the high steering sensitivity setting, 40:1 for the low steering sensitivity setting. The different road profiles are a curved road (denoted by CR) with road curvatures up to $0.01 m^{-1}$ in magnitude in both directions, and a straight road (denoted by HW) with no road curvature. The vehicle speed was set to a fixed speed of 80 km/h. The steering wheel data from twenty-four participants cropped to equal lengths of 470 seconds from the beginning of the experiment for all conditions was analysed. The driver's subjective acceptance ratings for the steering sensitivity settings (see table I) were used to determine driver's preference to the steering sensitivity settings.

TABLE I
REPORTED DRIVERS' ACCEPTANCE SCORES BY KROES (2019) FOR DRIVERS DRIVING WITH DIFFERENT STEERING SENSITIVITIES (40:1: LOW SENSITIVITY STEERING RATIO, 12:1: HIGH SENSITIVITY STEERING RATIO) AND ON DIFFERENT ROADS PROFILES (HW: STRAIGHT ROAD, CR: CURVED ROAD) [2]. SIGNIFICANT DIFFERENCES ($P < 0.05$) FOR THE MEANS BETWEEN THE STEERING RATIOS WITHIN EACH ROAD PROFILE ARE MARKED BOLD.

| Measure | Condition | | | |
|-----------------|------------------|--------------------|--------------------|------------------|
| | CR 40:1 | CR 12:1 | HW 40:1 | HW 12:1 |
| | <i>Mean (SD)</i> | <i>Mean (SD)</i> | <i>Mean (SD)</i> | <i>Mean (SD)</i> |
| Control safety | 1.21 (1.47) | 2.25 (0.61) | 2.63 (0.49) | 2.17 (0.87) |
| Ease of control | 0.38 (1.64) | 2.04 (1.00) | 2.38 (0.65) | 1.83 (0.96) |
| Comfort | 1.08 (1.41) | 1.92 (0.93) | 2.33 (0.76) | 1.88 (1.36) |

E. Statistical analysis

Means and 95% within-subject confidence intervals for three measures of steering behaviour are shown in fig. 2. Confidence intervals were calculated with the method of Cousineau (2005) [16] and bias-corrected following the method of Morey (2008) [17].

F. Results

The driver's preference for steering sensitivity setting is based on acceptance ratings for control safety, ease of control and comfort reported by Kroes (2019) [2]. The highest values were found for the high steering sensitivity on the curved road (CR 12:1) and the low steering sensitivity on the straight road (HW 40:1), see table I.

The frequency of intermittent switching increases with an increase of steering sensitivity for both the curved road and the straight road, see fig. 2a. Intermittent switching frequency is higher for the straight road compared to the curved road. The conditions with the highest acceptance scores for the steering sensitivity (CR 12:1 and HW 40:1) show similar means for the intermittent switching frequency, while the conditions with the lower acceptance scores (CR 40:1 and HW 12:1) show either lower or higher values of intermittent switching frequency.

The steering reversal rate does not significantly change with the steering sensitivity for both the curved road and the straight road, see fig. 2b. The conditions with the highest acceptance scores cannot be correlated to the steering reversal rate.

The root mean square steering angle decreases with an increase of steering sensitivity for both the curved road and the straight road, see fig. 2c. The magnitude of root mean square steering wheel angle scales approximately linearly with steering sensitivity for the curved road. The difference of root mean square steering angle between the steering sensitivities of the straight road is small compared to the difference of root mean square steering angle between the conditions with the highest acceptance scores (CR 12:1 and HW 40:1).

G. Discussion

Measures of steering behaviour are evaluated for their ability to indicate driver acceptance of the steering sensitivity.

The frequency of intermittent switching increases with the steering sensitivity, which is in line with the relation of remnant power and controlled element gain [13], and the correlation of the proportional control gain of the PID model of a balancing human with intermittent switching frequency [15]. An intermediate value of intermittent switching frequency may indicate high driver acceptance for the steering sensitivity.

Steering reversal rate is not a valid indicator for driver's acceptance of the steering wheel sensitivity, because it does not change with the steering sensitivity.

The root mean square steering wheel angle is strongly dependent on steering ratio. This dependence cannot be used for continuous steering adaptation, because it does not indicate a preference for the steering sensitivity.

Review of the frequency measures of steering wheel movements above shows that from the reviewed measures only the frequency of intermittent switching in

steering movements can be correlated with driver's acceptance of steering sensitivity. An intermediate value of switching frequency may indicate a high driver acceptance. The validity of the frequency of intermittent switching will be tested in a human-in-the-loop simulator experiment.

H. Hypothesis

From the reanalysis of the data of the experiment by Kroes (2019), the following hypotheses are formulated.

- The difference of the frequency of intermittent switching of driver's steering movements from a certain target frequency is inversely correlated with driver's driving comfort and ability to control the vehicle with the sensitivity of the steering wheel.
- Adaptation of the steering wheel sensitivity based on the frequency of intermittent switching in driver's steering movements increases driver's driving comfort and ability to control the vehicle compared to fixed steering sensitivity settings.

III. EXPERIMENTAL INVESTIGATION

A. Participants

Participants were recruited from the group of researchers in and around the Cognitive Robotics research lab. Twenty-four participants (18 male, 6 female) between the ages of 19 and 35 years old ($M = 25.6$, $SD = 3.7$) voluntarily agreed to participate in the experiment. All participants were in possession of a valid driver's licence ($M = 7.0$, $SD = 4.3$ years). The study was approved by the Human Research Ethics Committee of Delft University of Technology. No financial compensation was given to the participants.

B. Apparatus

The experiment was conducted in a fixed-base simulator of the Department of Cognitive Robotics at the faculty of Mechanical, Maritime and Materials Engineering (3ME), Delft University of Technology. The steering wheel used is an electronically actuated Sensodrive SENSO-Wheel SD-LC running at 1000 Hz. A 4K LED 65" screen refreshed at 60 Hz displayed the simulated environment at a 1.0 m viewing distance, see fig. 3. The simulation was developed using JOAN [18], an open-source software framework developed at the TU Delft, which builds on the CARLA open-source simulator (version 0.9.8) [19]. The driving simulator environment was created with Unreal Engine 4 (UE4) [20]. Data were recorded at a sampling rate of 100 Hz. The experiment design, data analysis and image generation code was written in Python [21], with the use of the following packages: NumPy [22], SciPy [23], PyWavelets [24], scikit-image [25], pandas [26], seaborn [27] and matplotlib [28].

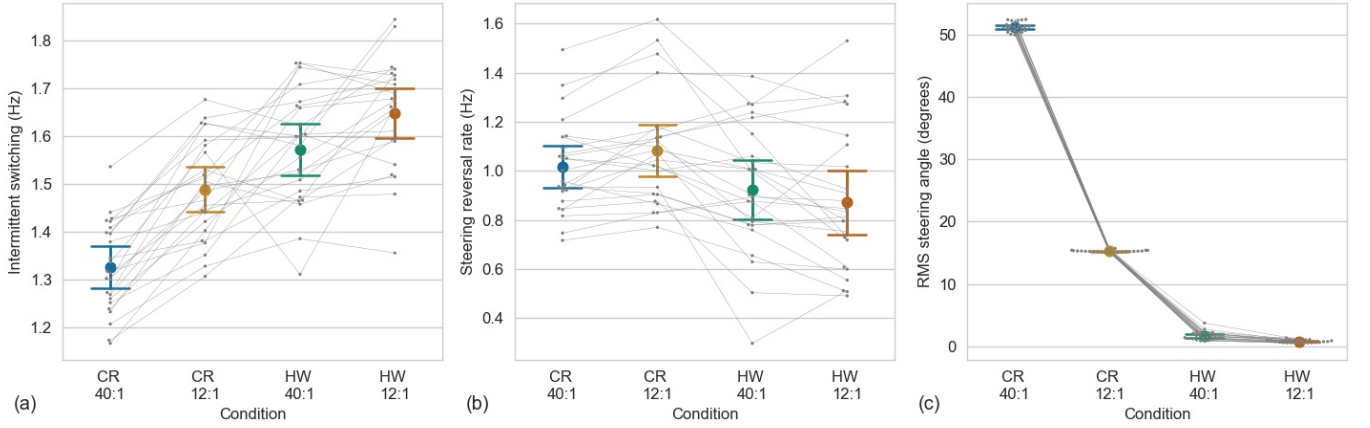


Fig. 2. Within-subject confidence intervals (95%) and means of (a) frequency of intermittent switching in driver’s steering movements, (b) steering reversal rate (0.5 degrees gap), (c) root mean square of the steering wheel angle, for drivers driving with different steering sensitivities (40:1: low sensitivity steering ratio, 12:1: high sensitivity steering ratio) and on different roads profiles (HW: straight road, CR: highly curved road). The data from the experiment by Kroes (2019) [2] were used for analysis.



Fig. 3. Participant driving in the fixed-base driving simulator.

C. Simulated vehicle dynamics

The simulated vehicle is modelled as a 4WS vehicle by a linear bicycle model. The response of yaw rate r and body sideslip β to a steering wheel input can be independently controlled in a four-wheel steering vehicle. Control of the front and rear wheels is done according to a published algorithm by Abe (2015) [29], that results in a vehicle’s lateral acceleration \ddot{y} response to a steering wheel angle δ input to be linear in both transient and steady state given a vehicle speed V . According to the method, the vehicle’s body sideslip and yaw rate response are set to a first-order system response, see eqs. (1) and (2). The lateral acceleration

response is then given by eq. (3).

$$\frac{\beta(s)}{\delta(s)} = \frac{G_\beta}{1 + Ts} \quad (1)$$

$$\frac{r(s)}{\delta(s)} = \frac{G_r}{1 + Ts} \quad (2)$$

$$\frac{\ddot{y}(s)}{\delta(s)} = V \left\{ s \frac{\beta(s)}{\delta(s)} + \frac{r(s)}{\delta(s)} \right\} = \frac{G_r V (1 + \frac{G_\beta}{G_r} s)}{1 + Ts} \quad (3)$$

The time constant T affects the speed of the system’s response. The body sideslip gain G_β and the yaw rate gain G_r are chosen such that eq. (4) is true, so that the vehicle’s response of lateral acceleration will be linear to steering wheel angle input (eq. (5)).

$$G_\beta = G_r T \quad (4)$$

$$\frac{\ddot{y}(s)}{\delta(s)} = G_r V \quad (5)$$

The derivation of the control algorithm for the front and rear wheels were analytically determined and can be found in Appendix C. The vehicle speed is kept constant at 80 km/h. The desired time constant T for both the body sideslip and the yaw rate response is set to 0.030 s. The vehicle is modelled as mid-size sedan, the modelled vehicle parameters can be found in Appendix C. The yaw rate gain value for the middle gain condition is derived from lateral acceleration response data from a commercial four-wheel-steering vehicle reported by Melman et al. (2019) [7], see Appendix C.

D. Independent variables

Four different steering settings are being compared, three steering settings with a fixed gain: low gain, middle gain, high gain, and one steering setting with the gain adapted based on the driver’s steering behaviour: adaptive gain.

1) *Fixed gain settings*: The different yaw rate gain G_r values for the low gain, middle gain and high gain conditions were constant during the whole track. Yaw rate gain values are summarised in table II. The steering wheel force-feedback response was designed to be critically damped ($\zeta = 1.0$) for all steering settings. The force-feedback was equivalent for all steering wheel settings given a certain lateral acceleration response. This is accomplished by adaptation of the steering wheel stiffness k_{sw} and steering wheel damping b_{sw} to the yaw rate gain, see table II. The steering wheel stiffness k_{sw} is proportionally scaled to the yaw rate gain, and the steering wheel damping b_{sw} is proportionally scaled to the square root of the yaw rate gain (see Appendix D). The steering wheel's static friction setting is set to zero.

TABLE II
STEERING SETTINGS FOR DIFFERENT CONDITIONS

| Condition | Steering settings | | |
|---------------|--------------------------|--------------------------|---------------------------|
| | $G_r(\frac{rad/s}{rad})$ | $k_{sw}(\frac{Nm}{rad})$ | $b_{sw}(\frac{Nms}{rad})$ |
| Low gain | 0.16 | 1.20 | 0.30 |
| Middle gain | 0.32 | 2.40 | 0.37 |
| High gain | 0.48 | 3.60 | 0.52 |
| Adaptive gain | 0.16 - 0.48 | 1.20 - 3.60 | 0.30 - 0.52 |

2) *Adaptive gain setting*: The yaw rate gain G_r values for the adaptive gain condition was real-time adapted to the driver's steering behaviour during the driving track. The sensitivity of the steering wheel was adapted to real-time calculated intermittent switching frequency (see fig. 4). Yaw rate gain values are summarised in table II. The steering wheel force-feedback response was designed to be critically damped ($\zeta = 1.0$), similar to section III-D1. The force-feedback parameters were varied according to the adapted yaw rate gain, similar to section III-D1.

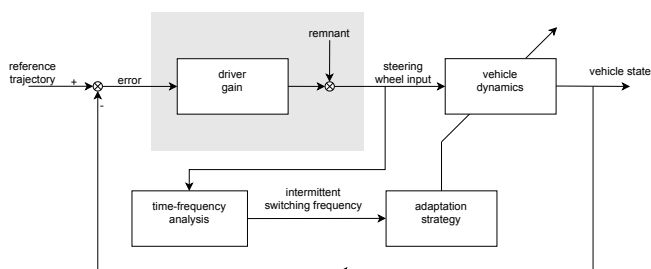


Fig. 4. Schematic of adaptation of steering wheel sensitivity based on measured steering wheel behaviour.

The driver's steering wheel angle was measured and the time-derivative filtered through a second-order Butterworth low-pass filter with a cut-off frequency of 5.0 Hz was taken to obtain the steering wheel velocity. Intermittent switching was calculated according to section II-A. Due to uncertainty of frequency analysis at the edge of the wavelet transform, the wavelet analysis is performed with a delay of approximately 7 seconds to

negate edge effects. The target frequency of intermittent switching is set to 1.80 Hz, which is heuristically tuned.

The wavelet analysis is performed at an update frequency of 100 Hz. The steering sensitivity, determined by the yaw rate gain, is adapted exponentially with an adaptation factor γ ; the yaw rate gain is multiplied by γ when the calculated frequency of intermittent switching is lower than the target frequency and divided by γ when the calculated frequency of intermittent switching is above the target frequency. The value of γ is set to 1.0003, which corresponds with a theoretical time of adaptation between the extremes of 11.5 seconds. The initial steering gain for the adaptive gain condition is set to the steering gain of middle gain condition (see fig. 4). The steering adaptation begins at 220 m from the start of the experiment, corresponding to the start of the first road section. The vehicle dynamics and adaptation of the yaw rate gain are sampled at a frequency of 200 Hz.

E. Road environment

Two road designs are used in the experiment, a training track and an experiment track. The roads are both two-way roads, with having a lane width 3.60 m. The road marking design is similar to the design of national roads in the Netherlands with lanes separated by double solid white lines, and intermittent white lines on both sides (see fig. 3). The training track with length 4.2 km consists of multiple corners with radius 70 m and 100 m, and straight sections of length 50 m and 300 m. The experiment track with total length 13.0 km consists of:

- A straight section of length 220 m.
- The 4.0 km curved road section: road of length 4.0 km with corners with radii between 190 m and 230 m in alternating direction with lengths between 150 m and 170 m.
- The 4.0 km straight road section: straight road of length 4.0 km.
- The 4.0 km mixed road section: alternating straight and curved road sections of length 4.0 km with corners in alternating direction with radii between 360 m and 400 m and lengths between 300 m and 340 m with straight sections of 300 m length after each second corner.
- A final corner of length 160 m and 200 m radius.
- A straight section of length 500 m.

Overall results are calculated from the combined curved, straight and mixed section.

F. Experimental design

Prior to the experiment, participants signed the informed consent form and personal details were obtained. Participants were informed that four different steering settings were being compared with the driver in the loop. A within-subject human-in-the-loop driving simulator research was performed. Four experiment conditions, each condition with a different steering

setting, were compared in a complete counterbalanced measures design. Each condition was assigned a character ('A', 'B', 'C', 'D') which was used throughout the experiment. Participants were requested to take place in the fixed-base driving simulator and were briefed on how to operate it. Participants were instructed to never put their hands through the steering wheel. Prior to driving on the experiment track, participants were made familiar with the steering setting by driving on the training track. Participants were instructed to drive as they would normally do. A self-report driver acceptance questionnaire (see section III-G5) was vocally given to the participants during the experiment trial. Participants were informed on the questions asked and how to answer the self-report questionnaire prior to the experiment. Three sets of three questions of the self-report driver acceptance questionnaire were asked at time 160, 340 and 520 seconds from the starting position, corresponding with each of the road sections with 4.0 km length and a travelled road distance of 3550 m, 7550 m and 11550 m. The vehicle was automatically stopped at the travelled road distance of 12.7 km. A final question of the self-report driver acceptance questionnaire was asked at the end of the experiment track. After driving the experiment track, participants were requested to fill in the NASA Task Load Index (NASA-TLX) questionnaire [30], and motion sickness was assessed by a questionnaire asking for symptoms. Upon clear signs of upcoming motion sickness, a break was strongly suggested. Otherwise, a (coffee) break was honoured whenever the participant felt like it. After the four conditions were performed, the participant was questioned for remarks on the experiment, and then the participant was allowed to ask questions with regards to the goal and meaning of the experiment.

G. Dependent variables

For each of the three 4.0 km road sections, the following metrics were recorded; which can be categorized in Curved section, Straight section, Mixed section, and Overall (see section III-E).

1) *Driver behaviour*: Driver's steering activity is measured by the root mean square of steering wheel angle (degrees). Frequency of intermittent switching (Hz) is measured by the number of jerk peaks per second in the steering wheel angle data in steering movements within the 0.5 - 4.0 Hz frequency spectrum (see section II-A).

2) *Driving behaviour*: Lane-keeping performance is measured by the root mean square lateral deviation from lane centre (m).

3) *Vehicle behaviour*: Adaptation of the vehicle's steering sensitivity is measured by the mean yaw rate gain (rad/s/rad) from per road section.

4) *Task difficulty*: Task difficulty is measured by the raw NASA Task Load Index (NASA-TLX) (%) questionnaire by Hart & Staveland (1988), to estimate sub-

jective workload through combination of six workload-related factors [30], and measured by the mean steer reversal rate (reversals/s), as indicator for the steering task difficulty imposed on the driver, McLean and Hoffman (1975) [8]. It is counted as the number of times the direction of steering wheel movement is reversed through a gap size of 0.5 degrees.

5) *Driver acceptance*: Ease of control, validity, comfort and predictability of the steering settings were measured by participant ratings for the following self-report questionnaire. The participant was requested to rate how much they did agree with the statements on a 1-10 scale (1: 'totally disagree', 10: 'totally agree'). The following statements were asked three times, for every road type section: "I can control my position precisely.", "I find the steering system sensitive.", "I like the steering sensitivity.". The final statement asked after the experiment track end was: "I found the steering behaviour predictable."

H. Statistical analysis

Means and 95% within-subject confidence intervals are reported. Within-subject confidence intervals were calculated with the method of Cousineau (2005) [16] and bias-corrected following the method of Morey (2008) [17]. To improve the reproducibility of this study, non-overlapping 95% confidence intervals were used to indicate statistical significance, corresponding to a p-value of approximately 0.006 [31].

IV. RESULTS

Overall results of the measured variables over the experiment track for the different conditions are given in table III. Relevant results per road section are given in table IV.

A. Fixed steering sensitivity settings

Each driver drove four times on the same experiment road with four different steering settings. Driver's intermittent switching behaviour varied per condition during the experiment road, see fig. 6 for a typical participant. Different steering settings resulted in a difference in steering activity: the root mean square steering angle was higher with conditions with a lower yaw rate gain (see table III and fig. 5). The relation of steering wheel angle and yaw rate gain is approximately inversely proportional. For a given corner radius, the steering wheel angle scales inversely with the steering gain to obtain the lateral acceleration required to take the turn. Based on the results of the NASA-TLX and the steering reversal rate, no significant difference were found between the overall task difficulty of the different fixed gain conditions (see table III). No significant differences were found between overall driver ratings for positional control ability and sensitivity likeability of the different fixed gain conditions (see table III). No significant differences were found between overall

TABLE III

OVERALL RESULTS FOR DIFFERENT CONDITIONS CALCULATED FOR THE COMBINED THREE ROAD SECTIONS (OVERALL). MEASUREMENT MEANS AND 95% WITHIN-SUBJECT CONFIDENCE INTERVALS (CI, ONE-SIDED) ARE REPORTED. *: SENSITIVITY ESTIMATION WAS PERFORMED ON DIFFERENT STEERING GAIN VALUES.

| Measure | Condition (gain setting) | | | | Confidence interval comparison | | | | | |
|---|--------------------------|-------------------------|-----------------------|---------------------------|--------------------------------|-------|-------|-------|-------|-------|
| | Low (1) Mean (CI) | Middle (2) Mean (CI) | High (3) Mean (CI) | Adaptive (4) Mean (CI) | x: non-overlapping CI | | | | | |
| | | | | | 1 - 2 | 1 - 3 | 1 - 4 | 2 - 3 | 2 - 4 | 3 - 4 |
| Mean yaw rate gain (rad/s/rad) | 0.16 (0.00) | 0.32 (0.00) | 0.48 (0.00) | 0.28 (0.04) | x | x | x | x | x | x |
| Root mean square steering angle (degrees) | 22.35 (0.27) | 11.67 (0.16) | 7.93 (0.09) | 13.10 (1.40) | x | x | x | x | | x |
| Mean intermittent switching (Hz) | 1.86 (0.09) | 1.94 (0.11) | 2.06 (0.12) | 1.95 (0.08) | | | | | | |
| Root mean square lateral position (m) | 0.25 (0.03) | 0.24 (0.03) | 0.24 (0.03) | 0.24 (0.03) | | | | | | |
| Mean steer reversal rate (Hz) | 0.92 (0.11) | 0.89 (0.13) | 0.85 (0.11) | 0.87 (0.11) | | | | | | |
| NASA-TLX Mean (%) | 27.01 (7.63) | 24.65 (6.14) | 27.22 (8.12) | 24.76 (7.25) | | | | | | |
| Rating positional control (1-10) | 7.58 (0.52) | 7.71 (0.57) | 7.97 (0.57) | 8.10 (0.45) | | | | | | |
| Rating sensitivity estimation (1-10) | 5.22 (0.94) | 6.33 (0.73) | 6.82 (1.02) | 6.31 (0.82)* | | | | | | |
| Rating sensitivity likeability (1-10) | 6.78 (0.75) | 7.39 (0.58) | 7.25 (0.90) | 7.40 (0.68) | | | | | | |

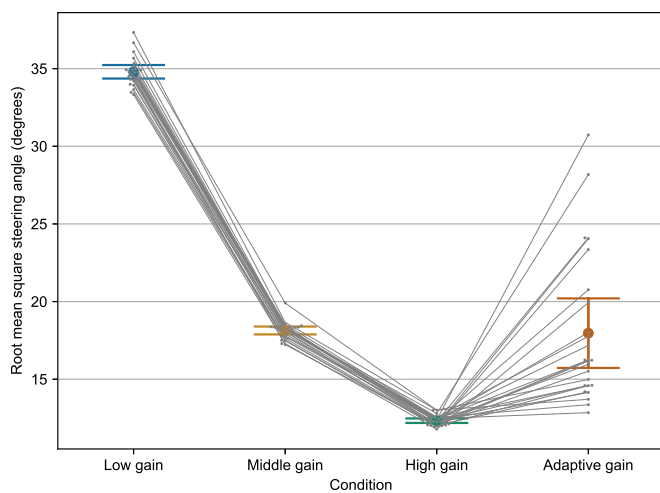


Fig. 5. Within-subject confidence intervals (95%) and means of root mean square steering wheel angle over the curved road section for different steering sensitivity settings.

lane-keeping performance of the different fixed gain conditions (see table III). No significant differences of overall mean intermittent switching between the fixed gain conditions were found (see table III).

With different intermittent steering behaviour observed between road sections (see fig. 7c), analysis of intermittent switching between road sections shows significant differences of intermittent switching between road sections were found between all road sections and for all steering conditions (see table V). No significant differences for the driver acceptance ratings positional control and sensitivity likeability were found between the different fixed gain conditions (see table IV).

B. Adaptive steering sensitivity setting

The mean and 95% confidence interval of intermittent switching frequency for all participants on the experiment road is shown in fig. 7c. Typical adaptation of the steering gain based on measurement of individual's intermittent switching frequency can be seen in fig. 6. The yaw rate gain in the adaptive gain setting did not

significantly change from the initial middle gain setting during driving on the curved road section (see table V). The yaw rate gain value changed significantly from the curved road section to the straight road section (see table V). The yaw rate gain value did not significantly change from the straight road section to the mixed road section (see table V). The intermittent switching frequency for all steering gain conditions was significantly different between all road sections (see table V). No significant differences for the driver acceptance ratings positional control and sensitivity likeability were found between the adaptive gain condition and the fixed gain conditions (see table IV).

V. DISCUSSION

The steering activity for the different steering settings did not linearly scale with the steering sensitivity. Instead, an inverse relation can be found between the steering sensitivity and steering activity by the driver.

Intermittent switching frequency was shown to be a measure of driver's steering behaviour that changes with steering sensitivity and with changes in road curvature. The intermittent switching in the reanalysis of the experiment data of Kroes (2019) [2] shows a significant difference between the steering sensitivity settings on the curved road, using the non-overlapping confidence interval criterion (see fig. 2a). A similar significant difference on the straight road cannot be found, using the non-overlapping confidence interval criterion (see fig. 2a). The human-in-the-loop driving simulator experiment showed a significant difference in intermittent switching frequency between the low and high steering sensitivity settings on the curved road. The steering activity has shown to increase with road curvature. This indicates that the sensitivity of driver's intermittent switching frequency to differences in steering sensitivity is larger when the steering activity is larger.

Significant differences in intermittent switching between the road curvature sections were found for all steering settings in the simulator experiment. A similar significant difference can be found for the reanalysis of

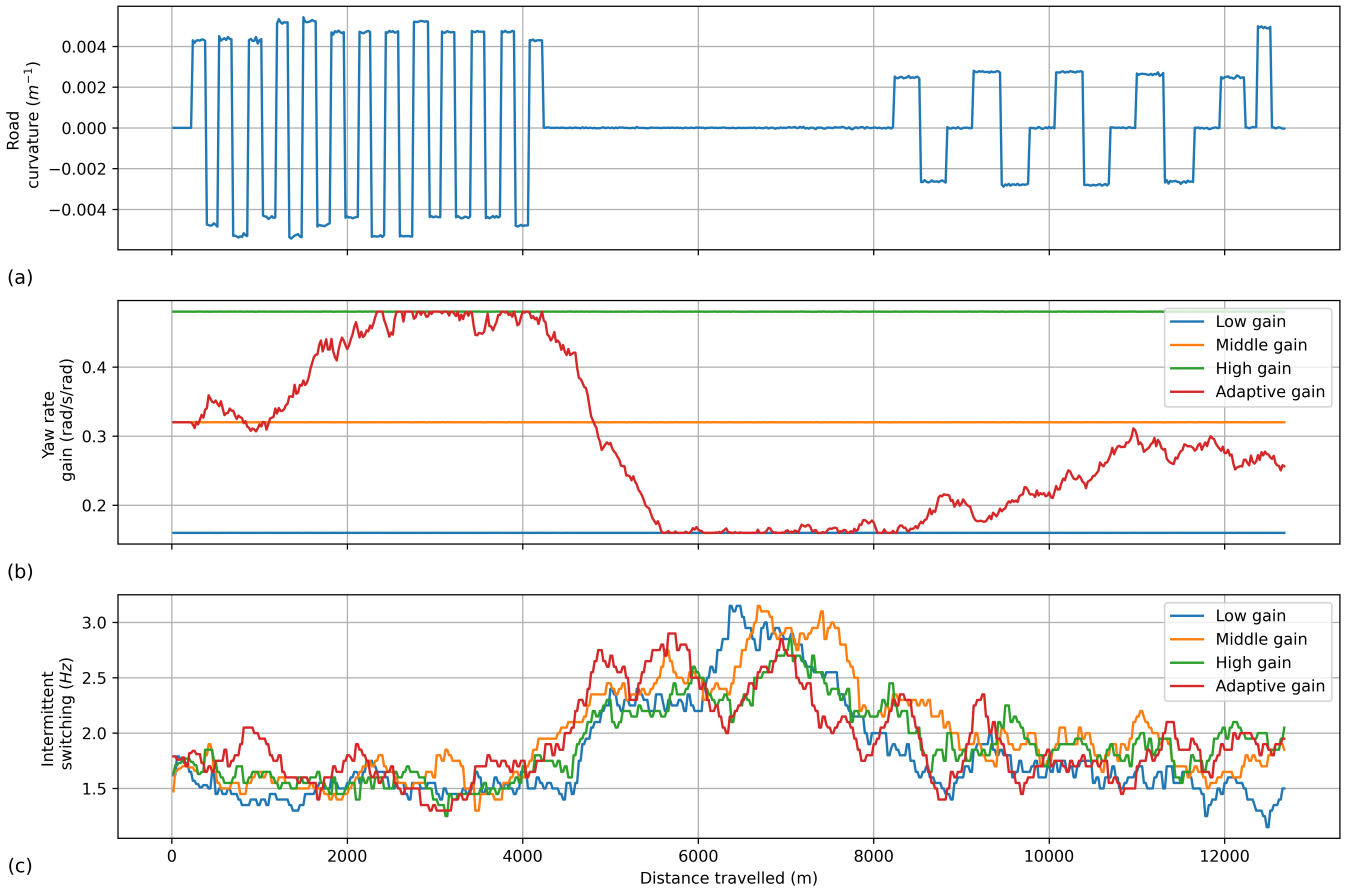


Fig. 6. Raw steering behaviour of typical participant (participant 5) driving the experiment track (a), with different steering sensitivity settings (b), and different intermittent switching behaviour (c). Intermittent switching as shown is filtered with a 20-seconds moving average filter.

TABLE IV

RESULTS FOR MEASURES PER ROAD SECTION BETWEEN CONDITIONS. MEASUREMENT MEANS AND 95% WITHIN-SUBJECT CONFIDENCE INTERVALS (CI, ONE-SIDED) ARE REPORTED. *: SENSITIVITY ESTIMATION WAS PERFORMED ON DIFFERENT STEERING GAIN VALUES.

| Measure | Condition (gain setting) | | | | Confidence interval comparison x: non-overlapping CI 1 - 2 1 - 3 1 - 4 2 - 3 2 - 4 3 - 4 |
|--|--------------------------|-------------------------|-----------------------|---------------------------|--|
| | Low (1) Mean (CI) | Middle (2) Mean (CI) | High (3) Mean (CI) | Adaptive (4) Mean (CI) | |
| Mean intermittent switching (Curved) | 1.67 (0.07) | 1.76 (0.09) | 1.83 (0.09) | 1.77 (0.06) | x |
| Mean intermittent switching (Straight) | 2.05 (0.13) | 2.13 (0.17) | 2.27 (0.19) | 2.18 (0.12) | |
| Mean intermittent switching (Mixed) | 1.86 (0.11) | 1.92 (0.12) | 2.08 (0.12) | 1.89 (0.09) | |
| Rating positional control (Curved) (1-10) | 7.17 (0.68) | 7.46 (0.71) | 7.92 (0.64) | 7.83 (0.54) | |
| Rating positional control (Straight) (1-10) | 8.00 (0.67) | 7.62 (0.65) | 7.88 (0.66) | 8.67 (0.50) | |
| Rating positional control (Mixed) (1-10) | 7.58 (0.53) | 8.04 (0.59) | 8.12 (0.66) | 7.79 (0.58) | |
| Rating sensitivity estimation (Curved) (1-10) | 5.00 (1.00) | 6.38 (0.84) | 6.75 (0.99) | 6.46 (0.84) | |
| Rating sensitivity estimation (Straight) (1-10) | 5.17 (1.03) | 6.33 (0.85) | 6.92 (1.09) | 6.29 (1.03) | |
| Rating sensitivity estimation (Mixed) (1-10) | 5.50 (0.99) | 6.29 (0.81) | 6.79 (1.03) | 6.17 (0.82) | |
| Rating sensitivity likeability (Curved) (1-10) | 6.38 (0.99) | 7.29 (0.82) | 7.38 (0.99) | 7.25 (0.77) | |
| Rating sensitivity likeability (Straight) (1-10) | 6.92 (0.82) | 6.92 (0.79) | 6.79 (1.08) | 7.67 (0.87) | |
| Rating sensitivity likeability (Mixed) (1-10) | 7.04 (0.73) | 7.96 (0.55) | 7.58 (0.87) | 7.29 (0.88) | |

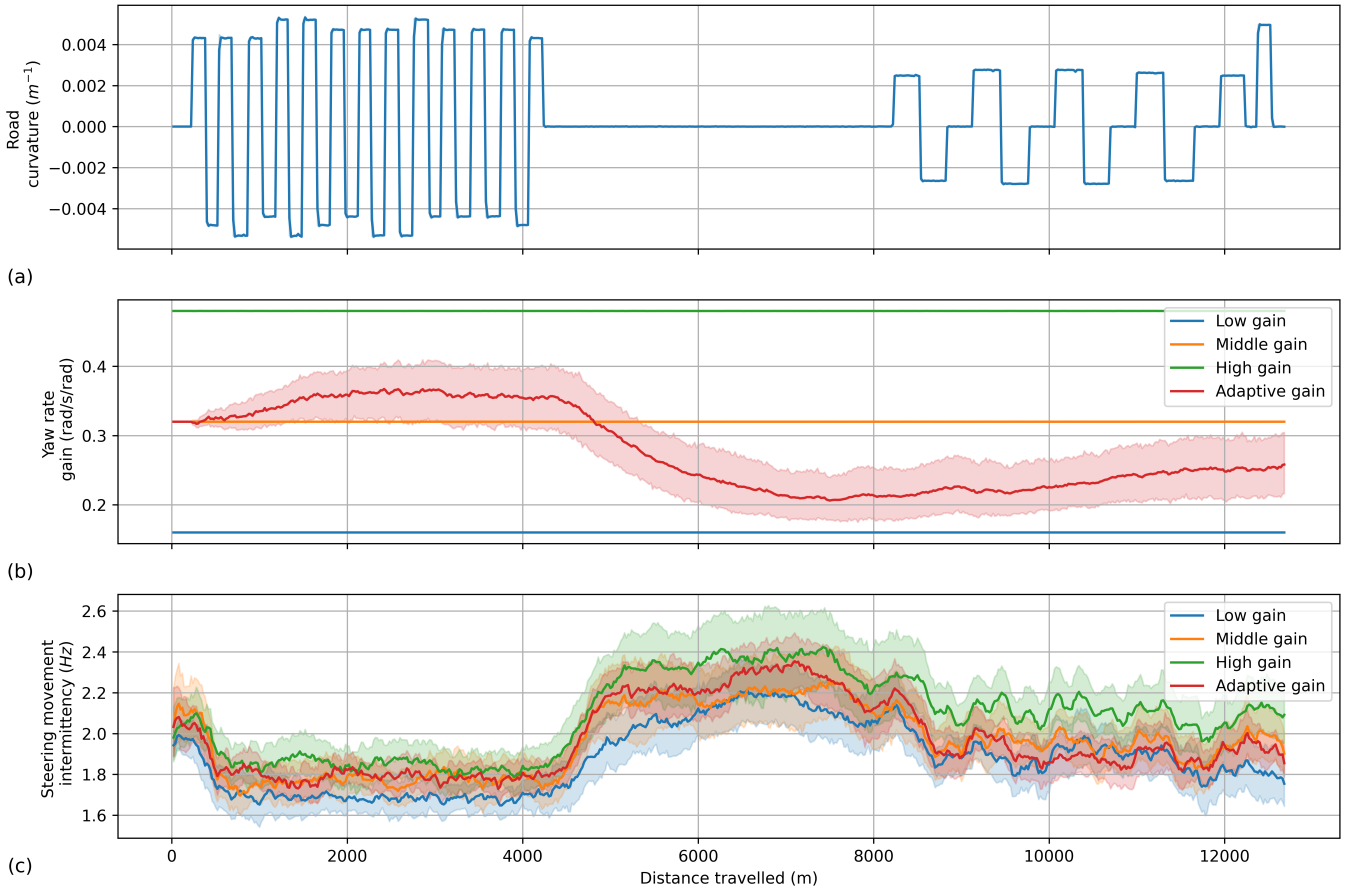


Fig. 7. Road curvature of the experiment track (a) on which all participants drove, with different steering sensitivity settings (b), and different intermittent switching behaviour (c). Mean and 95% confidence interval are shown. Intermittent switching as shown is filtered with a 20-seconds moving average filter.

TABLE V
RESULTS ANALYSED BETWEEN ROAD SECTIONS. MEASUREMENT MEANS AND 95% WITHIN-SUBJECT CONFIDENCE INTERVALS (CI, ONE-SIDED) ARE REPORTED.

| Measure | Road section | | | Confidence interval comparison | | |
|--|-------------------------|---------------------------|------------------------|--------------------------------|-------|-------|
| | Curved (1) Mean (CI) | Straight (2) Mean (CI) | Mixed (3) Mean (CI) | x: non-overlapping CI | | |
| | | | | 1 - 2 | 1 - 3 | 2 - 3 |
| Mean yaw rate gain (Adaptive) | 0.35 (0.04) | 0.25 (0.04) | 0.23 (0.05) | x | x | |
| Mean intermittent switching (Low) | 1.67 (0.04) | 2.05 (0.08) | 1.86 (0.06) | x | x | x |
| Mean intermittent switching (Middle) | 1.76 (0.06) | 2.13 (0.10) | 1.92 (0.07) | x | x | x |
| Mean intermittent switching (High) | 1.83 (0.05) | 2.27 (0.11) | 2.08 (0.08) | x | x | x |
| Mean intermittent switching (Adaptive) | 1.77 (0.03) | 2.18 (0.07) | 1.89 (0.06) | x | x | x |

the experiment data of Kroes (2019) [2] which shows a significant difference between the curved road and the straight road, using the non-overlapping confidence interval criterion (see fig. 2a). These findings show that the variation of road curvature has a strong effect on driver's intermittent switching behaviour. It is shown that the adaptation of the steering sensitivity responded to the larger difference in intermittent switching between the road profiles.

While the reanalysis the experiment data of Kroes (2019) [2] suggested that intermittent switching behaviour could indicate driver acceptance, no relation has been proven. Both the experiment by Kroes (2019) [2] and in the human-in-the-loop driving simulator ex-

periment of this study simulated a perfectly straight road. This may have caused that drivers use different steering strategies (control of lateral error) than what would be expected from real-world roads (control of yaw rate). This is also noted during the simulator experiment trials, where participant 4 stated that he was "following the midline closely" while driving on the straight road section. This may have had an effect on the values found for intermittent switching on the straight road.

A. Recommendations

Calculation of intermittent switching was performed through time-differentiation of the steering wheel angle,

filtering with a low-pass filter and convoluted with a second-order complex Gaussian wavelet to obtain the wavelet transform. A more direct approach would be to convolute the steering wheel angle with a third-order complex Gaussian wavelet to obtain the wavelet transform.

VI. CONCLUSION

The goal of this study was to investigate adaptation of the vehicle's steering sensitivity based on driver's steering behaviour to improve driver acceptance. Intermittent switching frequency is a measure of driver's steering behaviour that has been shown to change with steering sensitivity and with road curvature. Variation of road curvature was shown to have a larger effect on intermittent switching compared to variation of steering sensitivity. The human-in-the-loop driving simulator experiment showed no significant improvement in driver acceptance when adapting the steering wheel sensitivity to the driver's individual intermittent switching frequency when driving on a road with changing road curvature.

VII. FUTURE RESEARCH

Future research could reveal whether adaptation based on intermittency increases driver acceptance in real-world situations. An alternative adaptation strategy could be compared to the adaptation strategy presented in this study. The relation of intermittent switching and road curvature size, road width, and other road environmental parameters could be studied.

ACKNOWLEDGMENT

I would like to thank R. Kroes for the use of his experiment data. I would like to thank B. Shyrokau for his feedback on vehicle dynamics. I would like to thank J. de Winter for his feedback on the experiment design. I would like to thank D. Abbink for his feedback during this project. I would like to thank T. Melman for his continuous support, feedback and supervision during this project.

REFERENCES

- [1] P. Koehn and M. Eckrich, "Active steering-the bmw approach towards modern steering technology," SAE technical paper, Tech. Rep., 2004.
- [2] R. Kroes, "The impact of steering ratio variability to road profiles on driver acceptance and driving behaviour," 2019.
- [3] A. Heathershaw, "Optimizing variable ratio steering for improved on-centre sensitivity and cornering control," *SAE transactions*, pp. 1140–1151, 2000.
- [4] Y. Shimizu, T. Kawai, and J. Yuzuriha, "Improvement in driver-vehicle system performance by varying steering gain with vehicle speed and steering angle: Vgs (variable gear-ratio steering system)," *SAE transactions*, pp. 630–639, 1999.
- [5] M. Azzalini, G. Gissinger, V. Boussouar, and P. Coutant, "Computation of a variable steering ratio with a fuzzy logic method," in *Intelligent Vehicle Symposium, 2002. IEEE*, IEEE, vol. 1, 2002, pp. 259–267.
- [6] Y. Furukawa, N. Yuhara, S. Sano, H. Takeda, and Y. Matsushita, "A review of four-wheel steering studies from the viewpoint of vehicle dynamics and control," *Vehicle system dynamics*, vol. 18, no. 1-3, pp. 151–186, 1989.
- [7] T. Melman, J. de Winter, X. Mouton, A. Tapus, and D. Abbink, "How do driving modes affect the vehicle's dynamic behaviour? comparing renault's multi-sense sport and comfort modes during on-road naturalistic driving," *Vehicle System Dynamics*, pp. 1–19, 2019.
- [8] J. R. McLean and E. R. Hoffmann, "Steering reversals as a measure of driver performance and steering task difficulty," *Human Factors*, vol. 17, no. 3, pp. 248–256, 1975.
- [9] J. McLean and E. Hoffmann, "Analysis of drivers' control movements," *Human Factors*, vol. 13, no. 5, pp. 407–418, 1971.
- [10] J. McLean and E. Hoffmann, "The effects of lane width on river driving steering control and performance," in *Australian Road Research Board Conference Proc*, vol. 6, 1972.
- [11] I. Daubechies, *Ten lectures on wavelets*. SIAM, 1992.
- [12] Y. Inoue and Y. Sakaguchi, "A wavelet-based method for extracting intermittent discontinuities observed in human motor behavior," *Neural Networks*, vol. 62, pp. 91–101, 2015.
- [13] D. T. McRuer and H. R. Jex, "A review of quasi-linear pilot models," *IEEE transactions on human factors in electronics*, no. 3, pp. 231–249, 1967.
- [14] D. McRuer, "Human dynamics in man-machine systems," *Automatica*, vol. 16, no. 3, pp. 237–253, 1980.
- [15] T. Perera, J. L. Tan, M. H. Cole, S. A. Yohanandan, P. Silberstein, R. Cook, R. Peppard, T. Aziz, T. Coyne, P. Brown, *et al.*, "Balance control systems in parkinson's disease and the impact of pedunculopontine area stimulation," *Brain*, vol. 141, no. 10, pp. 3009–3022, 2018.
- [16] D. Cousineau *et al.*, "Confidence intervals in within-subject designs: A simpler solution to loftus and masson's method," *Tutorials in quantitative methods for psychology*, vol. 1, no. 1, pp. 42–45, 2005.
- [17] R. D. Morey *et al.*, "Confidence intervals from normalized data: A correction to cousineau (2005)," *reason*, vol. 4, no. 2, pp. 61–64, 2008.
- [18] N. Beckers, O. Siebinga, J. Giltay, and A. Van der Kraan, *JOAN, a human-automated vehicle experiment framework (version 1.0)*, 2021. [Online]. Available: <https://github.com/tud-hri/joan> (visited on 12/28/2020).

- [19] A. Dosovitskiy, G. Ros, F. Codevilla, A. Lopez, and V. Koltun, “CARLA: An open urban driving simulator,” in *Proceedings of the 1st Annual Conference on Robot Learning*, 2017, pp. 1–16.
- [20] Epic Games, Inc. (2020). Unreal engine, [Online]. Available: <https://www.unrealengine.com> (visited on 12/28/2020).
- [21] G. Van Rossum and F. L. Drake, *Python 3 Reference Manual*. Scotts Valley, CA: CreateSpace, 2009, ISBN: 1441412697.
- [22] C. R. Harris, K. J. Millman, S. J. van der Walt, R. Gommers, P. Virtanen, D. Cournapeau, E. Wieser, J. Taylor, S. Berg, N. J. Smith, R. Kern, M. Picus, S. Hoyer, M. H. van Kerkwijk, M. Brett, A. Haldane, J. Fernández del Río, M. Wiebe, P. Peterson, P. Gérard-Marchant, K. Sheppard, T. Reddy, W. Weckesser, H. Abbasi, C. Gohlke, and T. E. Oliphant, “Array programming with NumPy,” *Nature*, vol. 585, pp. 357–362, 2020. DOI: 10.1038/s41586-020-2649-2.
- [23] P. Virtanen, R. Gommers, T. E. Oliphant, M. Haberland, T. Reddy, D. Cournapeau, E. Burovski, P. Peterson, W. Weckesser, J. Bright, S. J. van der Walt, M. Brett, J. Wilson, K. J. Millman, N. Mayorov, A. R. J. Nelson, E. Jones, R. Kern, E. Larson, C. J. Carey, Í. Polat, Y. Feng, E. W. Moore, J. VanderPlas, D. Laxalde, J. Perktold, R. Cimrman, I. Henriksen, E. A. Quintero, C. R. Harris, A. M. Archibald, A. H. Ribeiro, F. Pedregosa, P. van Mulbregt, and SciPy 1.0 Contributors, “SciPy 1.0: Fundamental Algorithms for Scientific Computing in Python,” *Nature Methods*, vol. 17, pp. 261–272, 2020. DOI: 10.1038/s41592-019-0686-2.
- [24] G. R. Lee, R. Gommers, F. Waselewski, K. Wohlfahrt, and A. O’Leary, “Pywavelets: A python package for wavelet analysis,” *J. Open Source Softw*, vol. 4, no. 36, p. 1237, 2019.
- [25] S. Van der Walt, J. L. Schönberger, J. Nunez-Iglesias, F. Boulogne, J. D. Warner, N. Yager, E. Goullart, and T. Yu, “Scikit-image: Image processing in python,” *PeerJ*, vol. 2, e453, 2014.
- [26] W. McKinney *et al.*, “Data structures for statistical computing in python,” in *Proceedings of the 9th Python in Science Conference*, Austin, TX, vol. 445, 2010, pp. 51–56.
- [27] M. Waskom, O. Botvinnik, D. O’Kane, P. Hobson, S. Lukauskas, D. C. Gemperline, T. Augspurger, Y. Halchenko, J. B. Cole, J. Warmenhoven, J. de Ruiter, C. Pye, S. Hoyer, J. Vanderplas, S. Villalba, G. Kunter, E. Quintero, P. Bachant, M. Martin, K. Meyer, A. Miles, Y. Ram, T. Yarkoni, M. L. Williams, C. Evans, C. Fitzgerald, Brian, C. Fonnesbeck, A. Lee, and A. Qalieh, *Mwaskom/seaborn: V0.8.1 (september 2017)*, version v0.8.1, Sep. 2017. DOI: 10.5281/zenodo.883859. [Online]. Available: <https://doi.org/10.5281/zenodo.883859>.
- [28] J. D. Hunter, “Matplotlib: A 2d graphics environment,” *Computing in science & engineering*, vol. 9, no. 3, pp. 90–95, 2007.
- [29] M. Abe, *Vehicle handling dynamics: theory and application*. Butterworth-Heinemann, 2015.
- [30] S. G. Hart and L. E. Staveland, “Development of nasa-tlx (task load index): Results of empirical and theoretical research,” in *Advances in psychology*, vol. 52, Elsevier, 1988, pp. 139–183.
- [31] M. E. Payton, M. H. Greenstone, and N. Schenker, “Overlapping confidence intervals or standard error intervals: What do they mean in terms of statistical significance?” *Journal of Insect Science*, vol. 3, no. 1, 2003.

A

Reanalysis of steering behaviour from steering wheel data from the experiment by Kroes (2019).

Raw steering wheel behaviour

Raw steering behaviour for different steering ratio's was compared using the experiment data from Kroes (2019) **kroes2019impact**, see fig. A.1. The difference in magnitude of the steering wheel movements for the different ratio's can clearly be observed. A closer inspection suggests that the frequency behaviour is also different, with the 40:1-ratio showing an increased number of lower frequency movements (high overshoots and smooth oscillations).

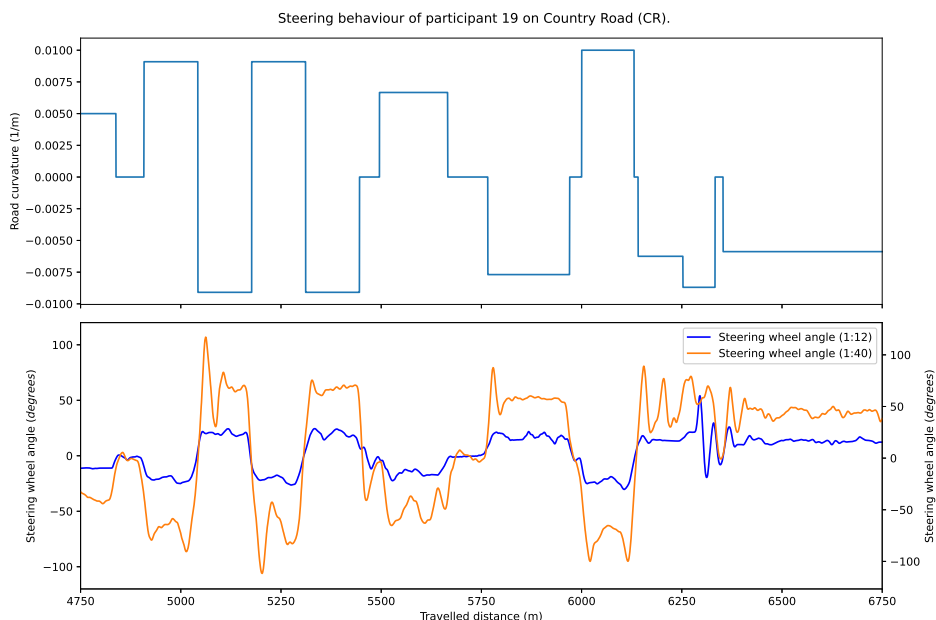


Figure A.1: Comparison of raw steering behaviour for different steering sensitivities (40:1: low sensitivity steering ratio, 12:1: high sensitivity steering ratio) on a highly curved road (CR) profile, calculated using experiment data from Kroes (2019) **kroes2019impact**.

Steering reversal rate

The steering wheel angle data is used from time 0 – 470s. The measured steering input angle is filtered with a Butterworth filter with a cut-off frequency of 2.0 Hz. Local peaks are identified, and filtered with a 0.5 degree difference threshold to be counted as reversal. The effect of a change in steering ratio on the mean steer reversal rate (0.5 degrees gap) for the country road (CR), is shown in fig. A.2, calculated using the steering wheel data from Kroes (2019) **kroes2019impact**.

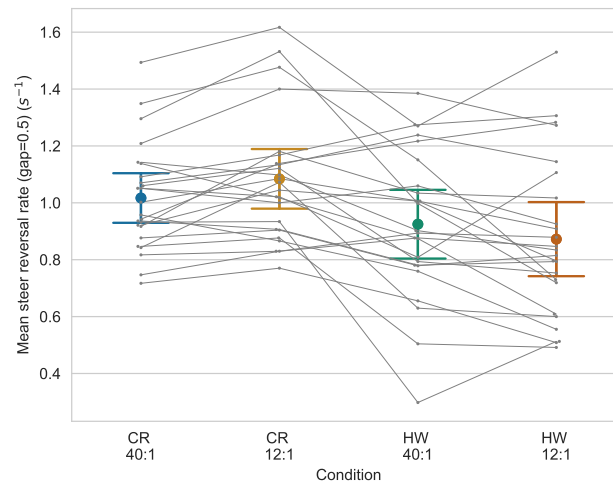


Figure A.2: Within-subject confidence intervals (95%) and means of mean steer reversal rate (using a 0.5 degrees threshold gap) for different steering sensitivities (40:1: low sensitivity steering ratio, 12:1: high sensitivity steering ratio) and on different roads profiles (HW: straight road, CR: highly curved road), calculated using experiment data from Kroes (2019) **kroes2019impact**.

Usage of steering wheel reversal rate as metric

The mean steer reversal rate is a metric commonly used for task difficulty. Steering reversal rate (SRR) filtered through a gap size of 0.5 - 0.7 deg yields most meaningful results for steering tasks **mclean1975steering**. McLean & Hoffmann (1975) stated that "the steering reversal rate can be a valid criterion for detecting differences in drivers or conditions" **mclean1975steering**.

The steering reversal rate should be used with caution when interpreting differences **mclean1975steering**.

The measured outcome of the steering reversal rate is affected by the choice of gap size, which can be seen in fig. A.3. Note that statistic results also differ for different choices of the gap size. The threshold gap acts as a low-pass filter to the steer reversals. The choice of the threshold gap has different effects on different conditions. From fig. A.3 it deduced that the steering reversals on the country road were generally bigger than 5.0 degrees and that the amount of measured reversals was barely impacted by a change in steering sensitivity, while the steering reversals on the highway were generally smaller than 2.0 degrees and that the amount of measured reversals was greatly impacted by changing the steering sensitivity for a gap size of 2.0 and 5.0 degrees. Kroes (2019) reported the steering reversal rate with a gap size of 2.0, and reported significant differences of the steering reversal rate for different steering sensitivities on both the country road and the highway **kroes2019impact**.

From this example (fig. A.3) and previous literature warning that caution is needed when interpreting differences in steering reversal rate between conditions **mclean1975steering**, it should be clear that the steering reversal rate can be a measure of task difficulty or workload (objective perspective), or a measure of to what extent drivers were able to maintain a certain level of performance given the task difficulty (subjective perspective).

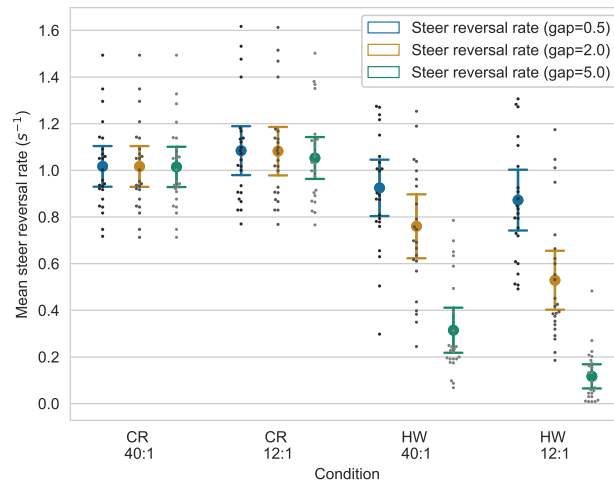


Figure A.3: Within-subject confidence intervals (95%) and means of mean steer reversal rate with different gap sizes (deg) for different steering sensitivities (40:1: low sensitivity steering ratio, 12:1: high sensitivity steering ratio) and on different roads profiles (HW: straight road, CR: highly curved road), calculated using experiment data from Kroes (2019) **kroes2019impact**.

Steering demand

Analysis of the standard deviation of steering wheel angle is shown in fig. A.4.

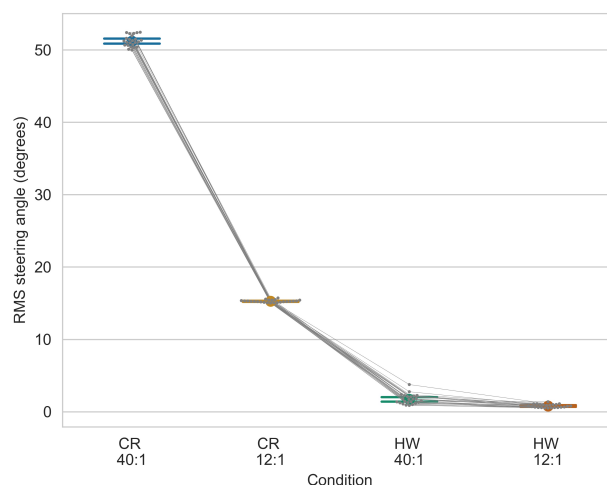


Figure A.4: Within-subject confidence intervals (95%) and means of standard deviation of steering wheel angle for different steering sensitivities (40:1: low sensitivity steering ratio, 12:1: high sensitivity steering ratio) and on different roads profiles (HW: straight road, CR: highly curved road), calculated using experiment data from Kroes (2019) **kroes2019impact**.

Power spectral density

The power spectral density (PSD) of the steering wheel angle is shown in fig. A.5.

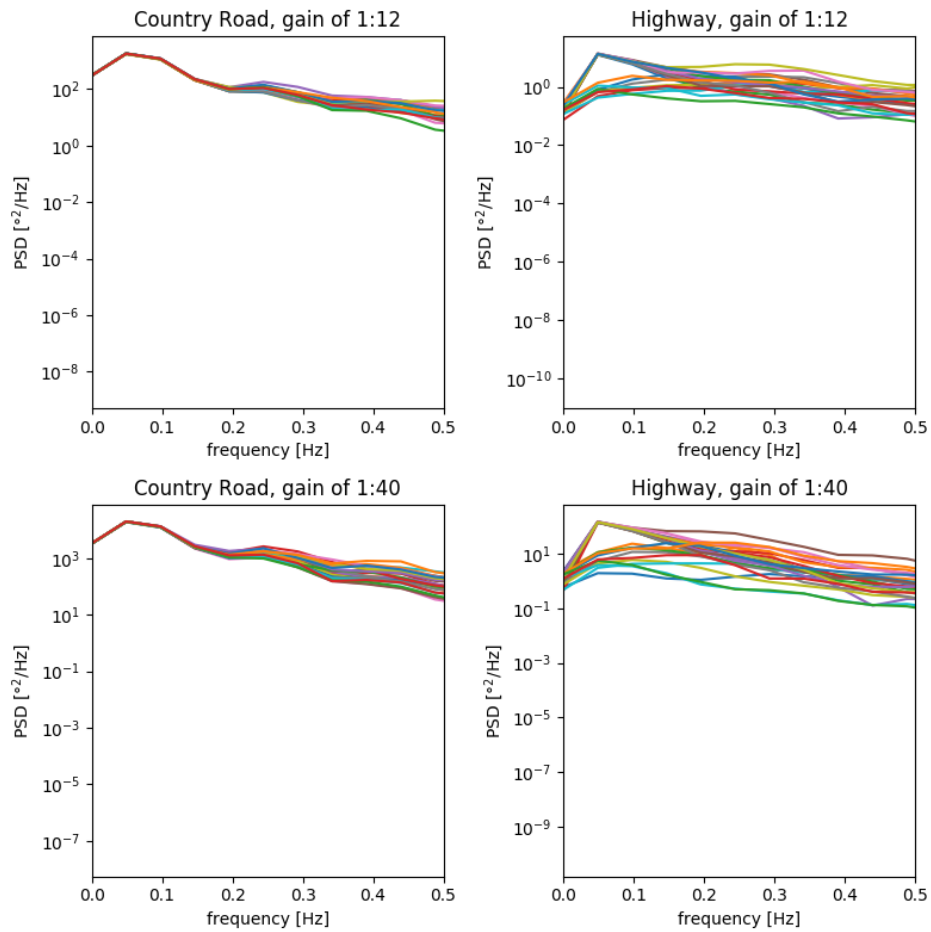


Figure A.5: Power spectral density for different steering sensitivities (40:1: low sensitivity steering ratio, 12:1: high sensitivity steering ratio) and on different roads profiles (HW: straight road, CR: highly curved road), calculated using experiment data from Kroes (2019) **kroes2019impact**.

B

Extraction of intermittent switching by Inoue (2015)

Human motor movement discontinuities can be detected as jerk peaks in the movement profile, pointing to the transition of one motor sub-movement to the next one. Detection of motor movement intermittency according to a published algorithm by Inoue & Sakaguchi (2015) **inoue2015wavelet**. The continuous wavelet transform (CWT) with second-order derivative complex Gaussian wavelet (fig. B.2) with scales corresponding to centre frequencies of 0.5-4.0 Hz of human movement velocity data is taken. An artificial velocity profile based on Inoue & Sakaguchi (2015) **inoue2015wavelet** was created to validate the detection of movement discontinuity peaks, see fig. B.1. The movement discontinuities are extracted by the detection of peaks in instantaneous frequency (time-derivative of instantaneous phase) which correspond with the amplitude minima of the wavelet coefficients. The onset of the sub-movements can be detected by tracing one of the equi-phase lines of 0 and π from the singularity point to lower scales. The chosen line should be the one other than the one going towards the greater scales.

Analytical background of the continuous wavelet transform

Here the analytical background to wavelet analysis and the complex wavelet transform is given, which lead to the calculation of instantaneous frequencies that were used in the estimation of human motor movement intermittency for this research. The analytical background of the continuous wavelet transform published by Prieto-Guerrero & Espinosa-Paredes (2008) and Prieto-Guerrero & Espinosa-Paredes (2018) (Chapter 6.4, pages 292 - 298) are summarised here.

References:

Prieto-Guerrero, A., & Espinosa-Paredes, G. (2008). Decay ratio estimation of bwr signals based on wavelet ridges. *Nuclear science and engineering*, 160(3), 302-317.
Prieto Guerrero, A., & Espinosa Paredes, G. (2018). *Linear and Non-Linear Stability Analysis in Boiling Water Reactors*.

A wavelet is a function that satisfies the following conditions:

- The mother wavelet has finite energy: $E_\psi = \int_{-\infty}^{\infty} |\psi(t)|^2 dt < \infty$.

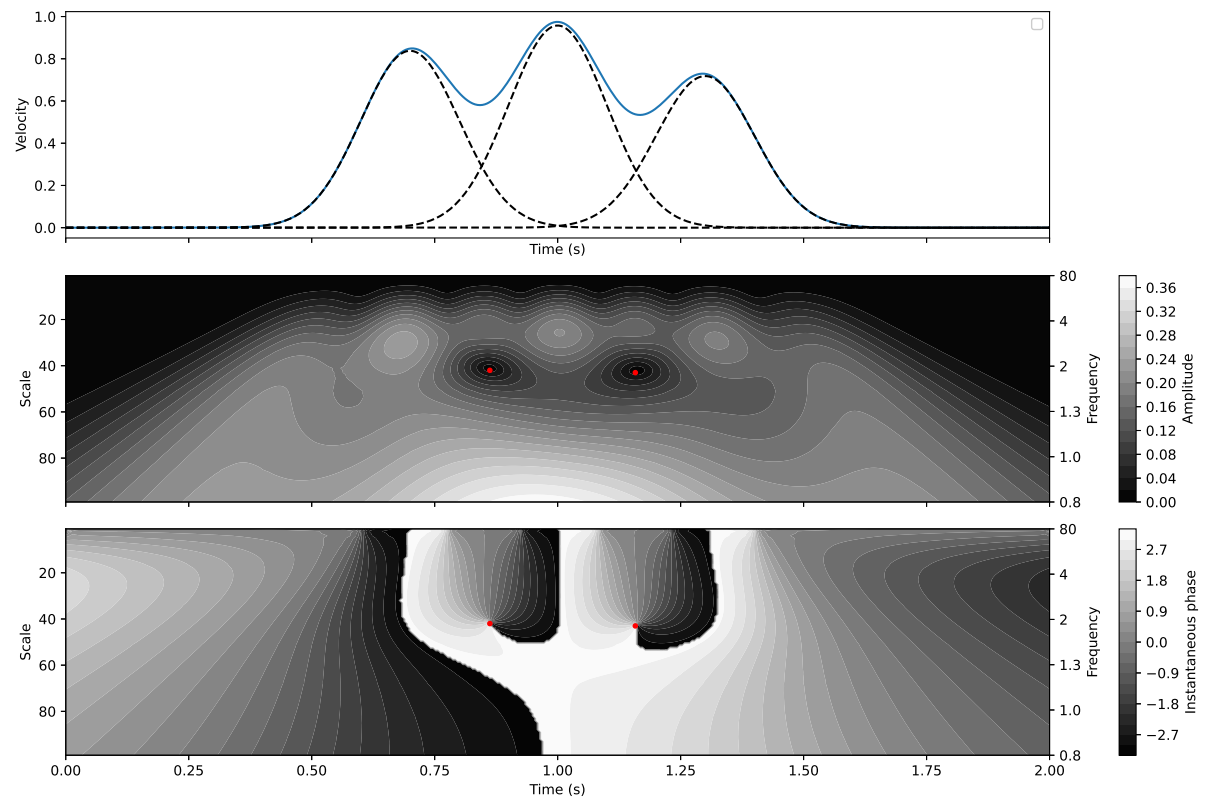


Figure B.1: Artificial velocity profile with overlapping sub-movements based on Inoue & Sakaguchi (2015) **inoue2015wavelet**. The first plot shows an example signal made up from three sub-movements. The second and third plot show the respective amplitude and phase information of the CWT of the signal with the complex second-order Gaussian wavelet. The discontinuities are obtained from the unwrapped phase information and are marked with red dots. Equi-phase lines of 0 and π may be followed from the discontinuity positions towards the lower scaled to obtain the onset of the sub-movements.

- The function satisfies the admissibility condition: $C_\psi = \int_{-\infty}^{\infty} \frac{|\hat{\psi}(\omega)|^2}{\omega} d\omega < \infty$.
- For analytic (complex) wavelets, the Fourier transform must be real and vanish for negative frequencies.

According to Prieto Guerrero, A., & Espinosa Paredes, G. (2018, p. 292 - 298): "A complex (or analytic) wavelet is a function whose spectrum has only positive frequencies. Since a complex wavelet responds only to the nonnegative frequencies of a given signal, then it produces a transform whose modulus is less oscillatory than in the case of a real wavelet. This property is a real advantage to detect and track instantaneous frequencies contained in the signal."

A wavelet ψ is a function in time with zero average value.

$$\int_{-\infty}^{\infty} \psi(t) dt = 0 \quad (\text{B.1})$$

This wavelet function, the mother wavelet ψ , is dilated by scale parameter a , and translated in time by parameter b .

$$\psi_{a,b}(t) = \frac{1}{\sqrt{a}} \psi\left(\frac{t-b}{a}\right) \quad (\text{B.2})$$

The continuous wavelet transform (CWT) of signal $x(t)$ is obtained by convolution of $x(t)$ with a scaled and translated version of ψ , with $\psi^*(t)$ being the complex conjugate of $\psi(t)$.

$$CWT_x(a, b) = \int_{-\infty}^{\infty} x(t) \psi^*\left(\frac{t-b}{a}\right) dt = x(t) * \left[\frac{1}{\sqrt{a}} \psi\left(\frac{-t}{a}\right)\right] \quad (\text{B.3})$$

Note the normalisation factor $1/\sqrt{a}$, which ensures that the integral energy given by each wavelet $\psi_{a,b}(t)$ remains independent of scale a .

The wavelet used in this research was the second-order derivative of a complex Gaussian wavelet, shown in fig. B.2. The algebraic convolution property of the relationship with differentiation (eq. (B.4)) is used to obtain steering wheel jerk smoothed by a Gaussian function from the steering wheel velocity.

$$(f * g)' = f' * g = f * g' \quad (\text{B.4})$$

Note that the same result would have been obtained if a third-order derivative of a complex Gaussian wavelet was used with the steering wheel angle as input.

The pseudo-frequency f_a (Hz) linked to scale a , which is the approximated frequency at the scale a , can be calculated by eq. (B.5) with the central frequency (Hz) of the wavelet f_c (depends on the number of oscillations in the wavelet) and the sampling frequency of the signal (Hz) f_s .

$$f_a = \frac{f_c f_s}{a} \quad (\text{B.5})$$

The instantaneous frequency is obtained from the instantaneous phase information obtained from the CWT of the signal by the complex wavelet by eqs. (B.6) and (B.7).

$$\omega_{inst}(t) = \frac{d\phi(t)}{dt} \quad (\text{B.6})$$

$$f_{inst}(t) = \frac{1}{2\pi} \frac{d\phi(t)}{dt} \quad (\text{B.7})$$

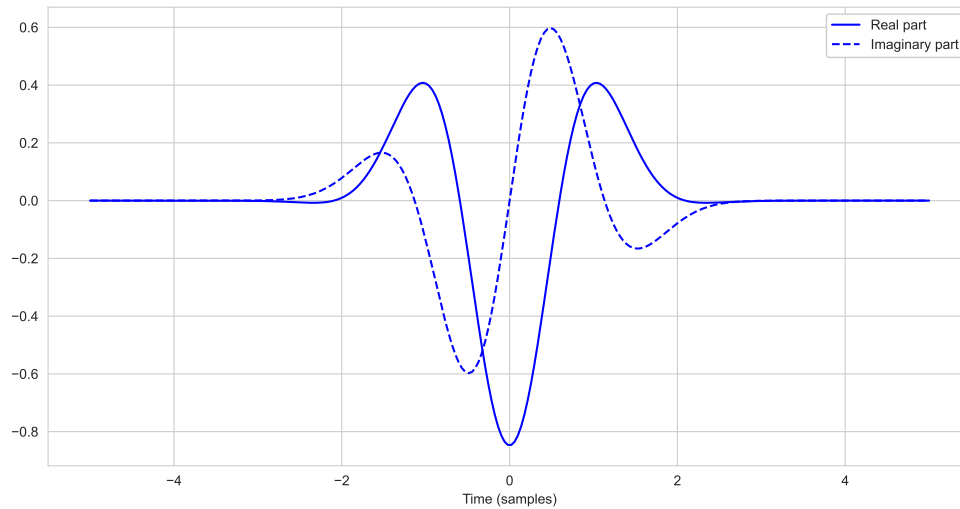


Figure B.2: Second-order derivative complex Gaussian wavelet used for the continuous wavelet transform (CWT).

The n -th order derivative of the complex Gaussian wavelet is calculated by n -th derivation of the function:

$$\psi(t) = C e^{-jt} e^{-t^2} \quad (\text{B.8})$$

with C being a normalisation constant **lee2019pywavelets**.

Cone of influence

Wavelet decomposition is done using the Pywavelets python package **lee2019pywavelets**. A real-time analysis is done by analysing 5 seconds of steering signal every 2 seconds in a batch-like process, for which edge effects are negated by ignoring discontinuity peaks within 1.5 seconds to the edges of the analysing window. The discontinuity peaks are identified using the Scikit-image python package **van2014scikit**.

Disturbance artefacts

Spikes in the steering wheel angular velocity profile are caused by the increased computation time required for the CWT analysis every 2.0 seconds. Since the spikes are of such high frequency, they do not cause unwanted behaviour in the time-instantaneous phase and time-instantaneous frequency plot.

Noise artefacts

The default value for the precision of the wavelet integration using the Pywavelets package introduced noise in the time-instantaneous phase and time-instantaneous frequency plot (see figs. B.3 to B.6). The expected result of the CWT of the steering wheel velocity data with the Gaussian wavelet is a smooth time-phase plot. Increasing the precision value should have removed the artefacts, see <https://github.com/PyWavelets/pywt/issues/531>.

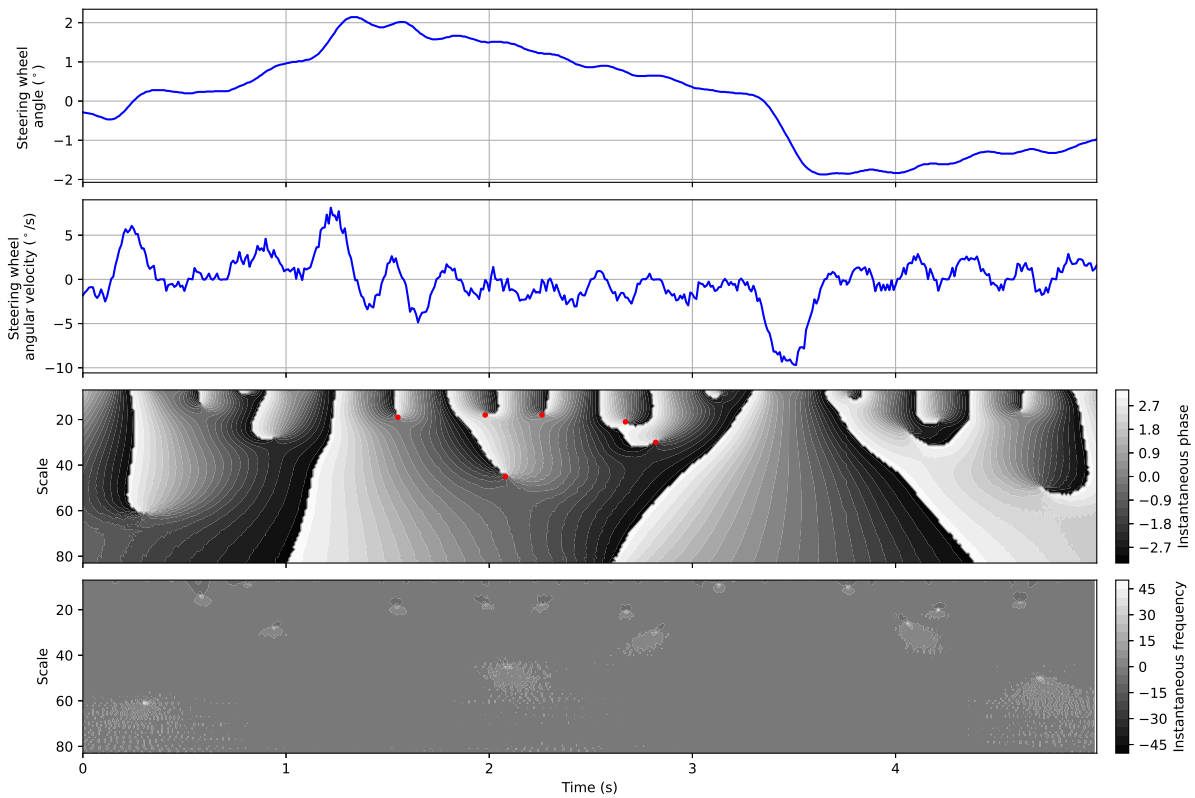


Figure B.3: Detection of movement discontinuities for "Middle gain" condition, participant #3 on curved section, by algorithm published by Inoue (2015) **inoue2015wavelet**.

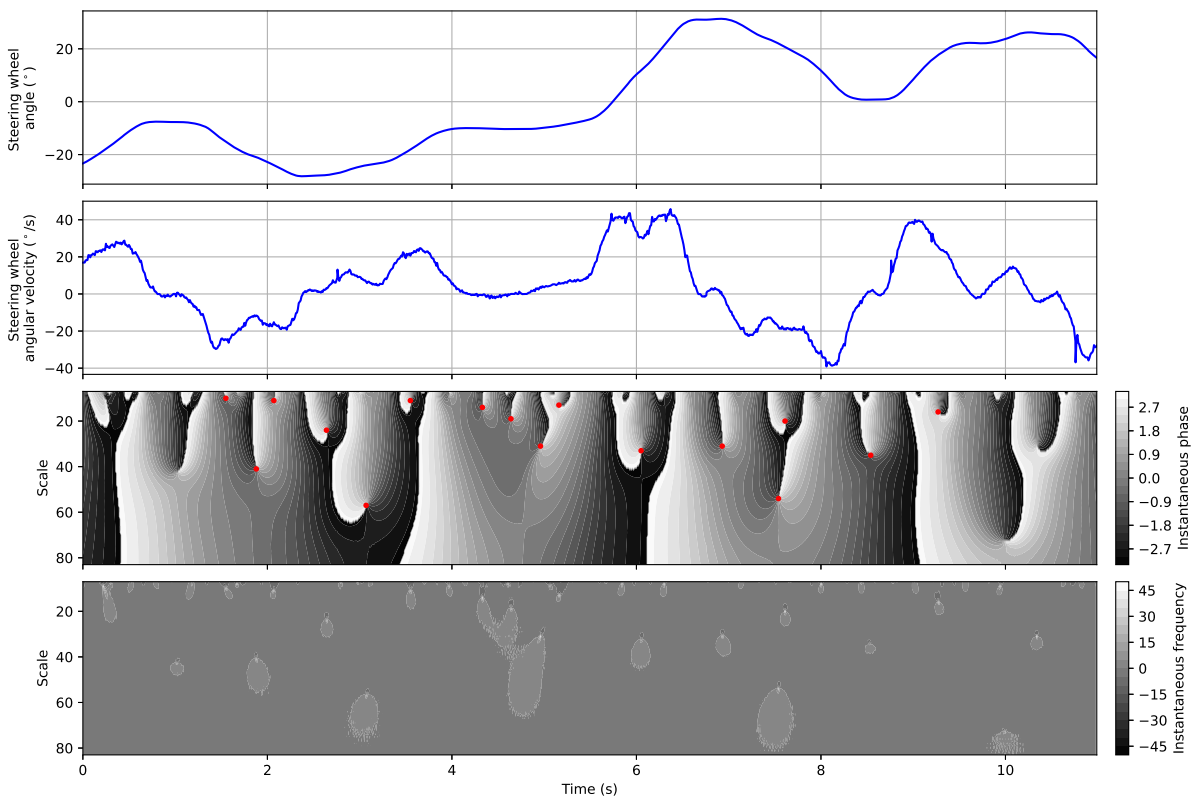


Figure B.4: Detection of movement discontinuities for "Middle gain" condition, participant #3 on straight section, by algorithm published by Inoue (2015) **inoue2015wavelet**.

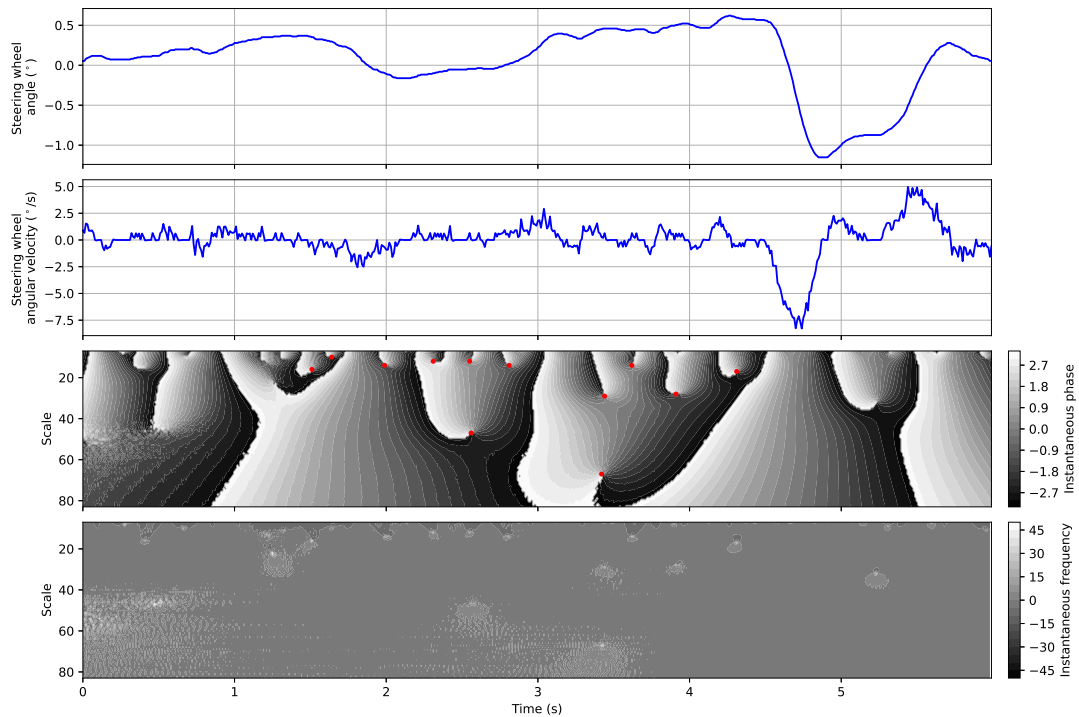


Figure B.5: Detection of movement discontinuities for "Middle gain" condition, participant #3 on balanced section, by algorithm published by Inoue (2015) **inoue2015wavelet**.

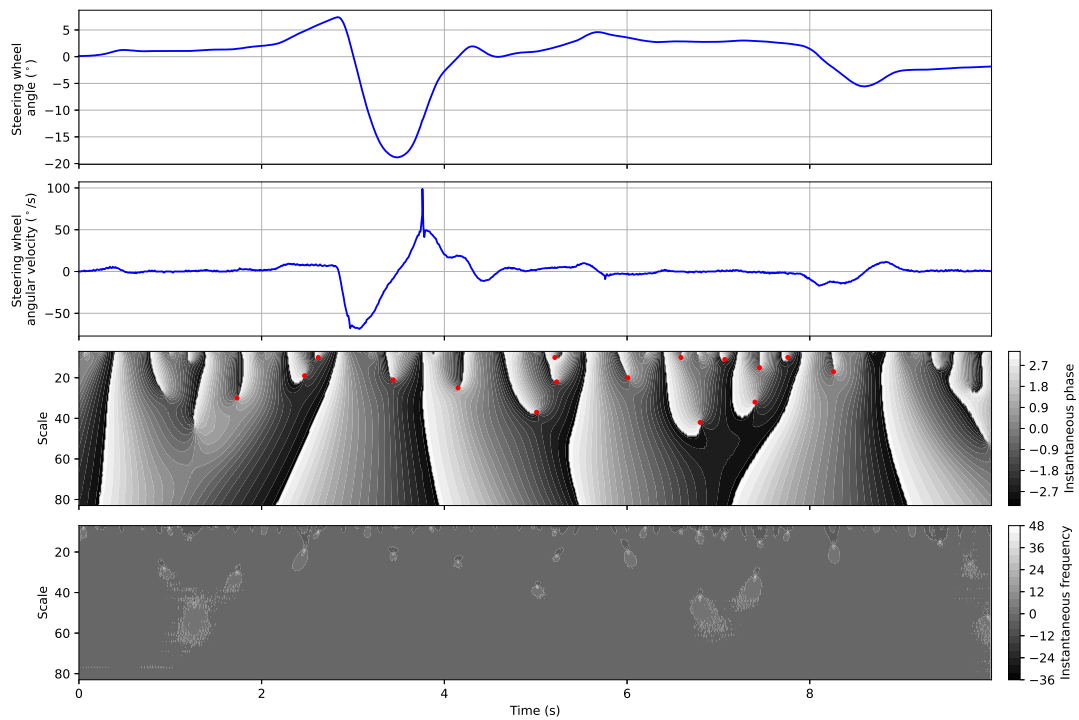


Figure B.6: Detection of movement discontinuities for "Middle gain" condition, participant #3 on curved section, by algorithm published by Inoue (2015) **inoue2015wavelet**.

C

Vehicle wheel dynamics

Four-wheel steering dynamics modelling

The vehicle is modelled as a bicycle model as in fig. C.1 with the front- and rear wheel steering relationship according to a published algorithm by Abe (2015) **abe2015vehicle**. The algorithm is checked and corrected for errors, and the control laws for the front and rear wheels as a function of the steering wheel input, steering gains, vehicle speed, and vehicle parameters are obtained.

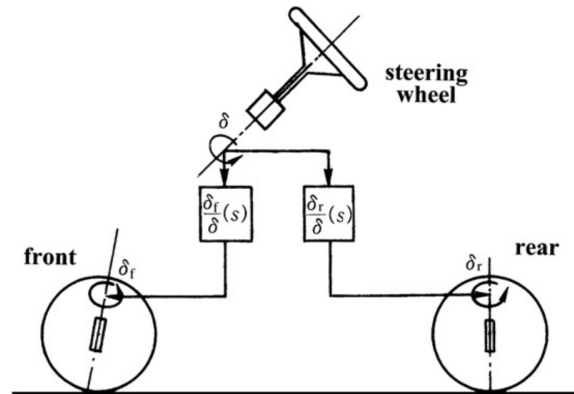


Figure C.1: Model of front- and rear-wheel active steering, adapted from Abe (2015) **abe2015vehicle**.

This section shows the derivation of the control laws for the front and rear wheels of the 4WS vehicle using the bicycle model, see fig. C.2.

The lateral and rotational equations of motions are given by eqs. (C.1) and (C.2).

$$m\ddot{y} = mV\left(\frac{d\beta}{dt} + r\right) = 2C_f + 2C_r \quad (C.1)$$

$$I\frac{dr}{dt} = 2C_f l_f - 2C_r l_r \quad (C.2)$$

$$C_f = k_f\left(\delta_f - \beta - \frac{l_f r}{V}\right) \quad (C.3)$$

$$C_r = k_r\left(\delta_r - \beta + \frac{l_r r}{V}\right) \quad (C.4)$$

The front and rear wheel slip angles are given by eqs. (C.5) and (C.6).

$$\alpha_f = \delta_f - \beta - \frac{l_f r}{V} \quad (C.5)$$

$$\alpha_r = \delta_r - \beta + \frac{l_r r}{V} \quad (C.6)$$

State-space form:

$$\begin{bmatrix} \dot{\beta} \\ \dot{r} \end{bmatrix} = \begin{bmatrix} -\frac{2(k_f+k_r)}{mV} & \frac{-2l_f k_f + 2l_r k_r}{mV^2} - 1 \\ \frac{-2l_f k_f + 2l_r k_r}{I} & -\frac{2l_f^2 k_f + 2l_r^2 k_r}{IV} \end{bmatrix} \begin{bmatrix} \beta \\ r \end{bmatrix} + \begin{bmatrix} \frac{2k_f}{mV} & \frac{2k_r}{mV} \\ \frac{2k_f l_f}{I} & -\frac{2l_r k_r}{I} \end{bmatrix} \begin{bmatrix} \delta_f \\ \delta_r \end{bmatrix} \quad (C.7)$$

Rewrite eqs. (8.48) to (8.50) in Abe (2015) **abe2015vehicle**.

$$\begin{bmatrix} \frac{2k_f}{mV} & \frac{2k_r}{mV} \\ \frac{2k_f l_f}{I} & -\frac{2l_r k_r}{I} \end{bmatrix} \begin{bmatrix} \delta_f(s) \\ \delta_r(s) \end{bmatrix} = \begin{bmatrix} s \frac{\beta(s)}{\delta(s)} \\ s \frac{r(s)}{\delta(s)} \end{bmatrix} - \begin{bmatrix} -\frac{2(k_f+k_r)}{mV} & \frac{-2l_f k_f + 2l_r k_r}{mV^2} - 1 \\ \frac{-2l_f k_f + 2l_r k_r}{I} & -\frac{2l_f^2 k_f + 2l_r^2 k_r}{IV} \end{bmatrix} \begin{bmatrix} \beta(s) \\ \delta(s) \\ r(s) \\ \delta(s) \end{bmatrix} \quad (C.8)$$

Which rewrites:

$$\begin{bmatrix} 2k_f & 2k_r \\ 2k_f l_f & -2l_r k_r \end{bmatrix} \begin{bmatrix} \delta_f(s) \\ \delta_r(s) \end{bmatrix} = \begin{bmatrix} mVs + 2(k_f + k_r) & mV + \frac{2}{V}(l_f k_f - l_r k_r) \\ 2(l_f k_f - l_r k_r) & Is + \frac{2}{V}(l_f^2 k_f + l_r^2 k_r) \end{bmatrix} \begin{bmatrix} \beta(s) \\ \delta(s) \\ r(s) \\ \delta(s) \end{bmatrix} \quad (C.9)$$

Solving as system of linear equations:

$$\begin{bmatrix} \delta_f(s) \\ \delta_r(s) \\ \delta(s) \end{bmatrix} = \begin{bmatrix} \frac{2k_f(l_f+l_r)+Vl_r ms}{2k_f(l_f+l_r)} & \frac{l_r mV + Is + \frac{2k_f l_f(l_f+l_r)}{V}}{2k_f(l_f+l_r)} \\ \frac{2k_r(l_f+l_r)+Vl_f ms}{2k_r(l_f+l_r)} & \frac{-Is + \frac{2k_r l_r(l_f+l_r)}{V} - l_f mV}{2k_r(l_f+l_r)} \end{bmatrix} \begin{bmatrix} \beta(s) \\ \delta(s) \\ r(s) \\ \delta(s) \end{bmatrix} \quad (C.10)$$

Following Abe (2015): taking the desired responses for the side-slip and yaw rate as a first-order lag system response, see eqs. (C.11) and (C.12), the response for the lateral acceleration becomes eq. (C.13):

$$\frac{\beta(s)}{\delta(s)} = \frac{G_\beta}{1 + Ts} \quad (C.11)$$

$$\frac{r(s)}{\delta(s)} = \frac{G_r}{1 + Ts} \quad (C.12)$$

$$\frac{\ddot{y}(s)}{\delta(s)} = V \left\{ s \frac{\beta(s)}{\delta(s)} + \frac{r(s)}{\delta(s)} \right\} = \frac{G_r V (1 + \frac{G_\beta}{G_r} s)}{1 + Ts} \quad (C.13)$$

The front and rear wheel control laws become:

$$\dot{\delta}_f = -\frac{\delta_f}{T} + \frac{G_\beta}{T} \frac{2k_f(l_f+l_r)\delta + ml_r V \dot{\delta}}{2k_f(l_f+l_r)} + \frac{G_r}{T} \frac{I\dot{\delta} + (ml_r V + \frac{2k_f l_f(l_f+l_r)}{V})\delta}{2k_f(l_f+l_r)} \quad (C.14)$$

$$\dot{\delta}_r = -\frac{\delta_r}{T} + \frac{G_\beta}{T} \frac{2k_r(l_f+l_r)\delta + ml_f V \dot{\delta}}{2k_r(l_f+l_r)} + \frac{G_r}{T} \frac{-I\dot{\delta} + (ml_f V - \frac{2k_r l_r(l_f+l_r)}{V})\delta}{2k_r(l_f+l_r)} \quad (C.15)$$

When the body side-slip is chosen such as in eq. (C.16), the vehicle's lateral acceleration response is proportional to the steering wheel angle (eq. (C.17)).

$$G_\beta = G_r T \quad (C.16)$$

$$\frac{\ddot{y}(s)}{\delta(s)} = G_r V \quad (C.17)$$

Steering gain parameters

The lateral acceleration to steering angle response values for a 2015 Renault Talisman are $\frac{\ddot{y}}{\delta_{sw}} = 0.1468 \frac{m/s^2}{deg}$ and $\frac{\ddot{y}}{\delta_{sw}} = 0.116 \frac{m/s^2}{deg}$ for the sport and comfort setting respectively, at a speed of 80 – 90 *km/h*, reported by Melman (2019) **melman2019driving**. Assuming that the 2015 Renault Talisman follows the response pattern similar to four-wheel-steering algorithm proposed by Abe (2015), the yaw rate gain values for the sport and comfort mode are approximated by substituting the vehicle speed (85 *km/h*) and the lateral acceleration to steering wheel angle response values into eq. (C.17) to obtain the yaw rate gain G_r values. The approximated yaw rate gain G_r values are $G_r = 0.36 \frac{rad/s}{rad}$ for the sport setting, $G_r = 0.28 \frac{rad/s}{rad}$ for the comfort setting. The mean value of the sport and comfort setting is $G_r = 0.32 \frac{rad/s}{rad}$, this value is taken for the Middle gain condition in the experiment.

Vehicle response modelling

The lateral acceleration is made up from the sum of lateral acceleration due to yaw rate and lateral acceleration due to body side-slip. The theoretical response is modelled with yaw rate gain values from the Renault Talisman (fig. C.3), as well as the yaw rate gain values used in the experiment (fig. C.4).

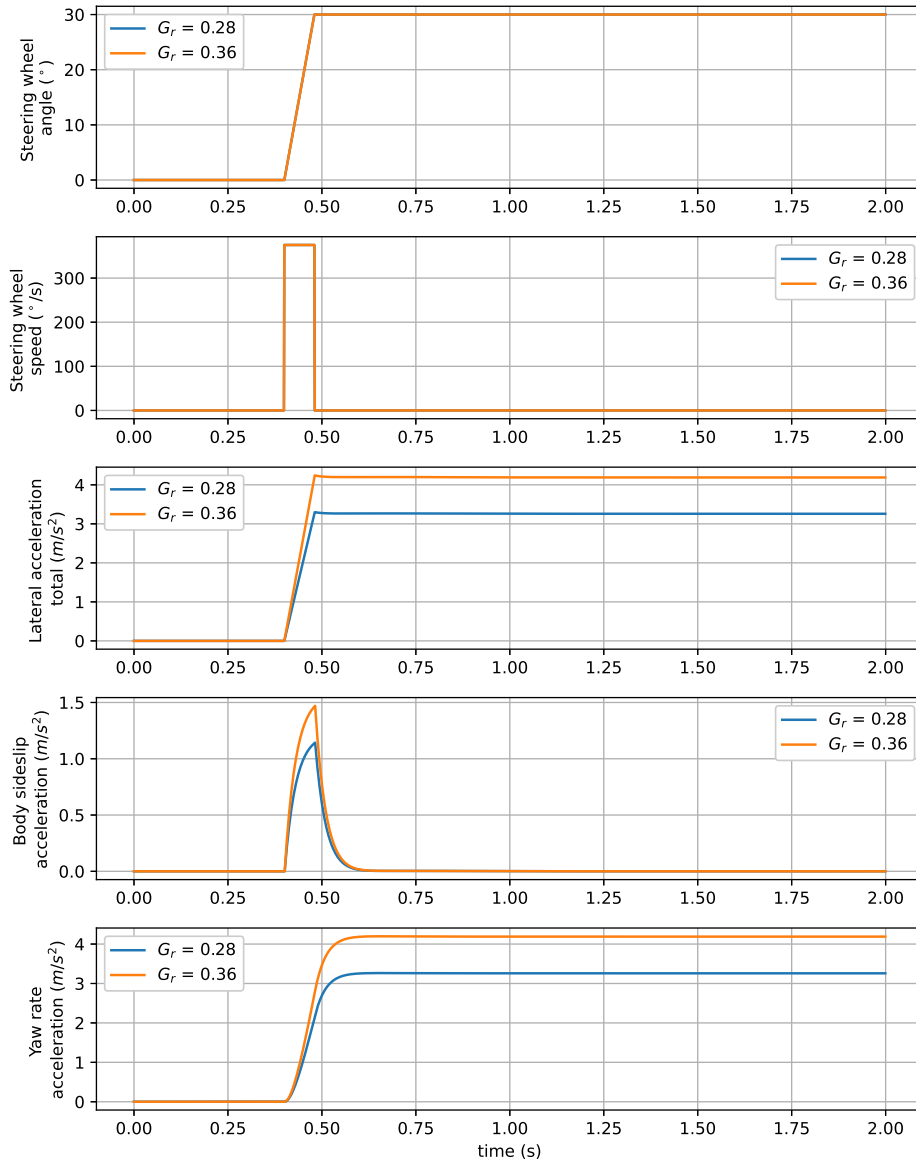


Figure C.3: Vehicle model with yaw rate gains approximated from a 2015 Renault Talisman.

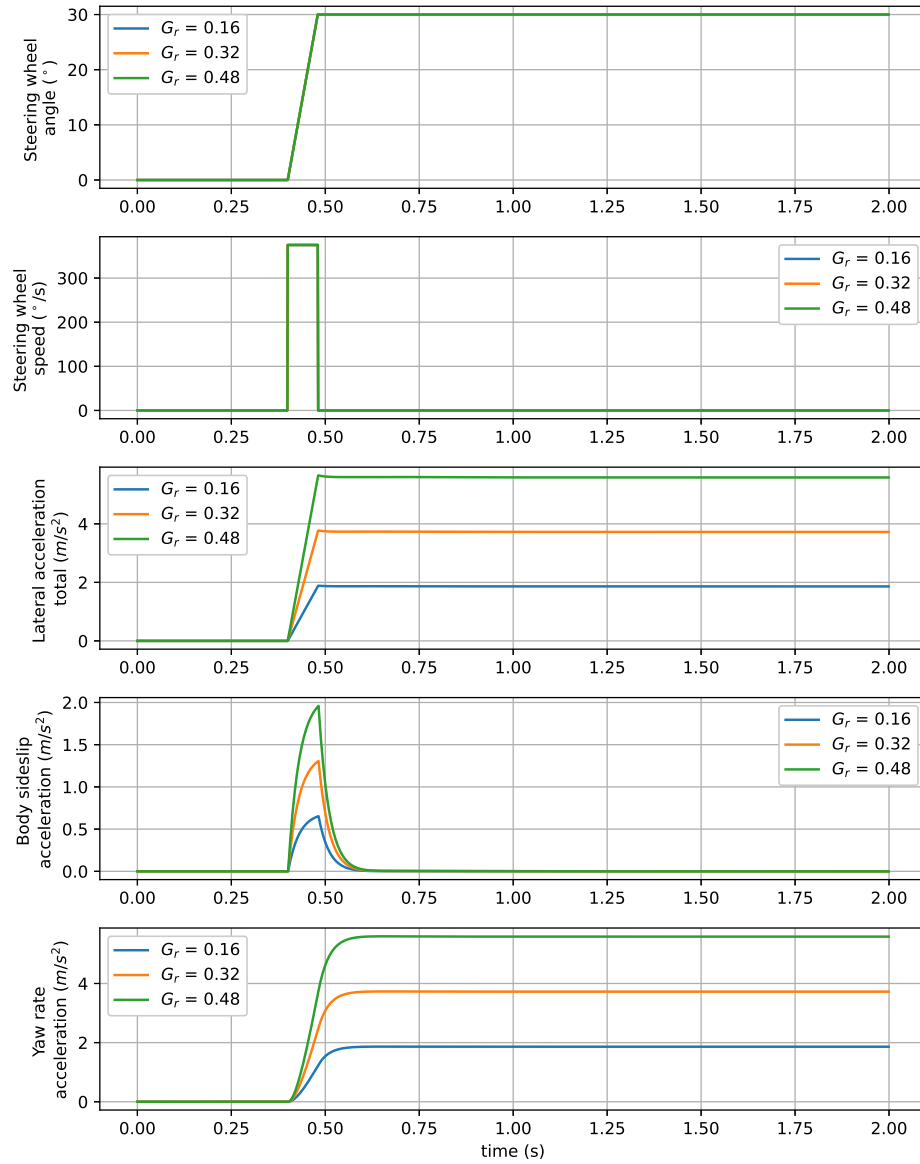


Figure C.4: Vehicle model with yaw rate gains according to the experiment conditions.

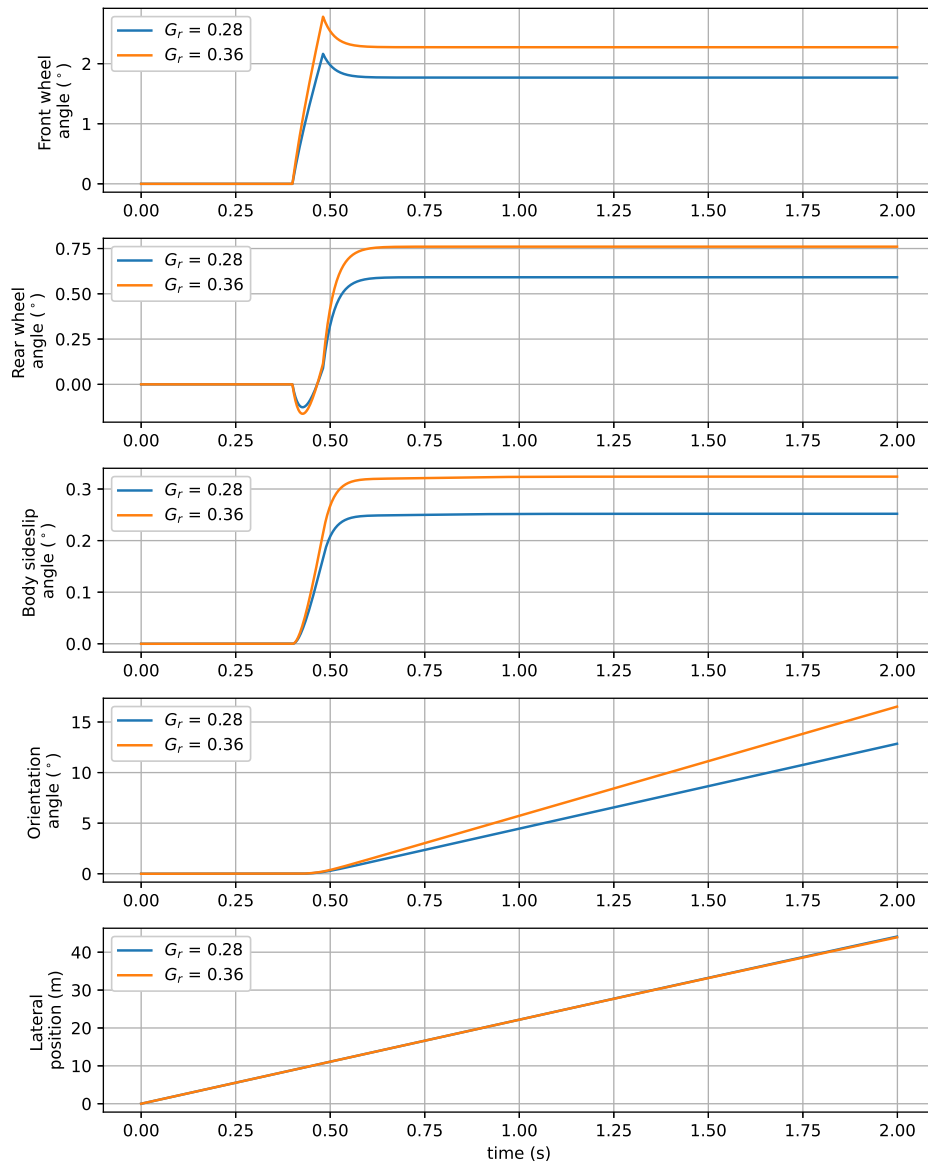


Figure C.5: Response of vehicle model variables with yaw rate gains approximated from a 2015 Renault Talisman.

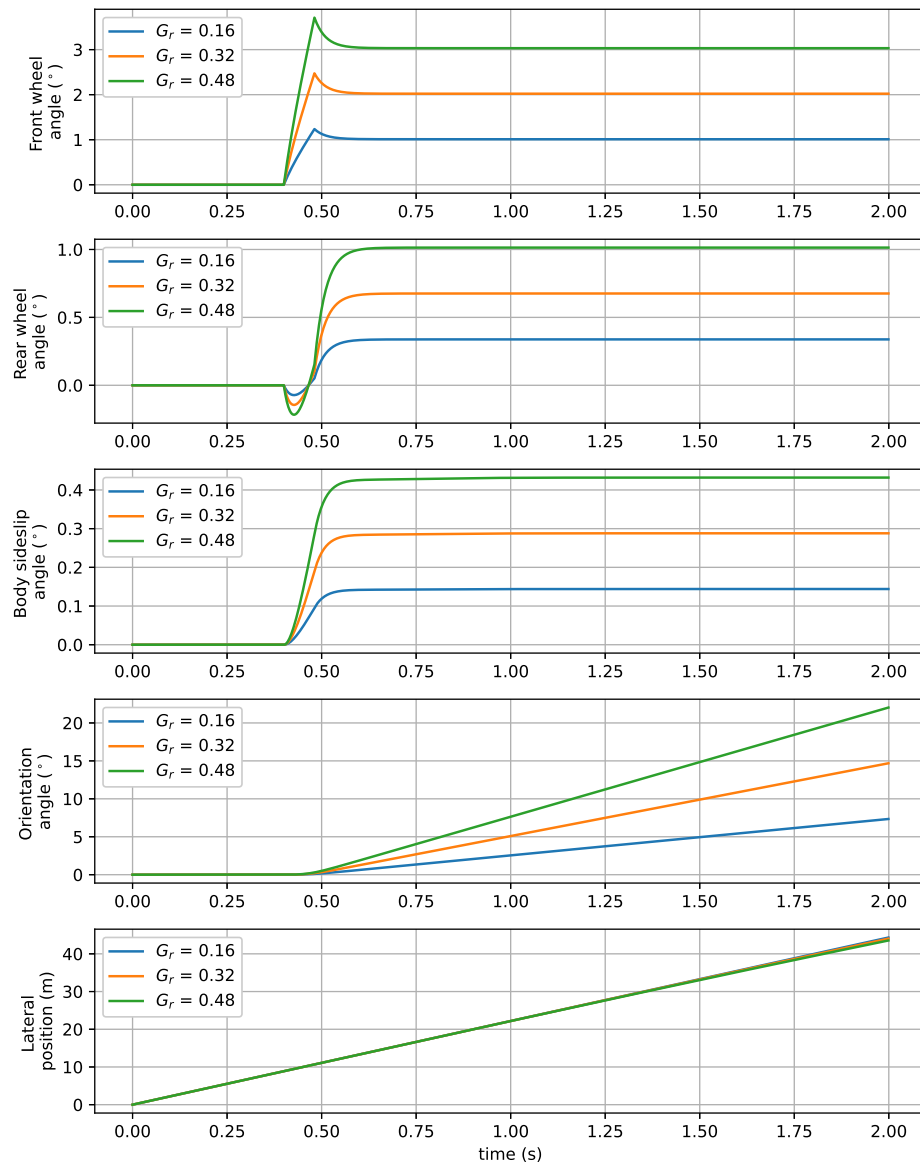


Figure C.6: Response of vehicle model variables with yaw rate gains used in the experiment.

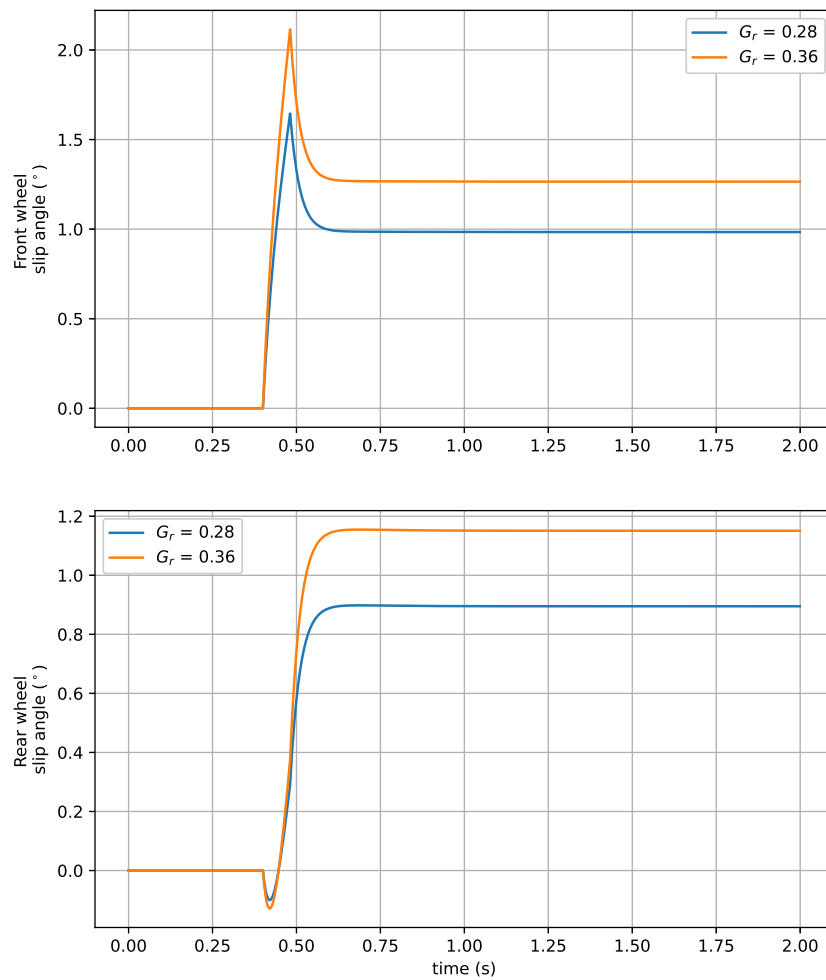


Figure C.7: Wheel slip angles of the vehicle model with yaw rate gains approximated from a 2015 Renault Talisman.

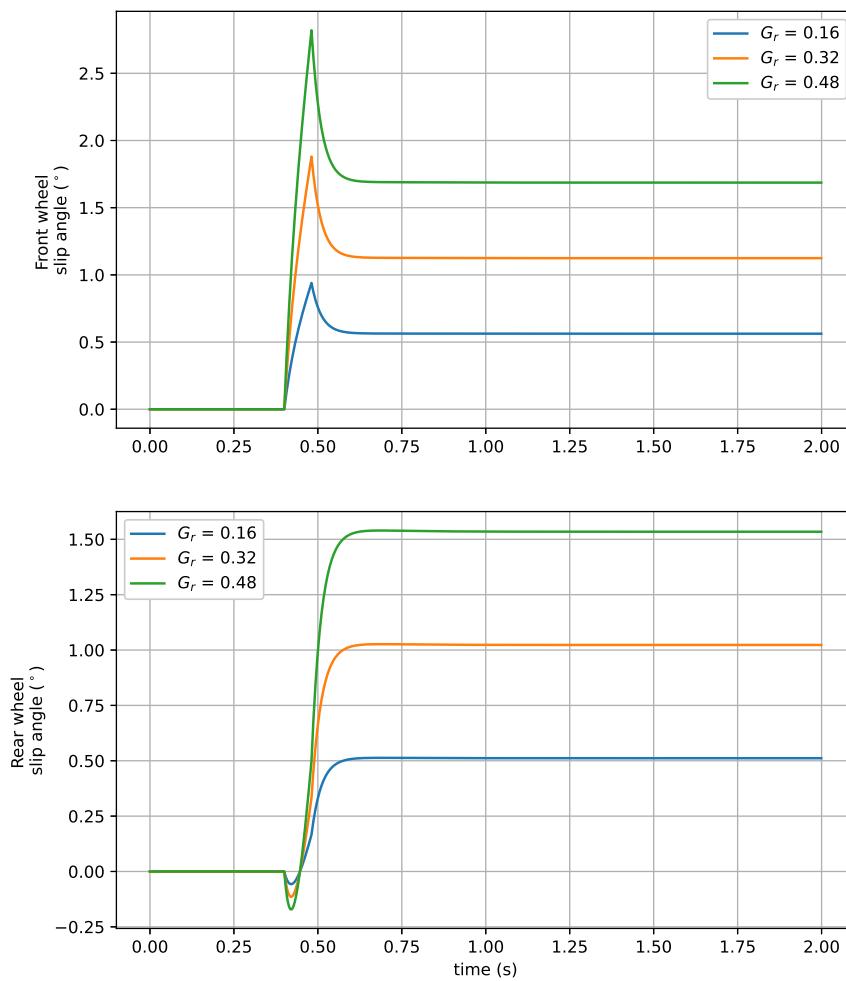


Figure C.8: Wheel slip angles of the vehicle model with yaw rate gains used in the experiment.

Table C.2: Vehicle parameters

| Symbol | Value | Unit | Description |
|----------|-------------|---------|---|
| w | 1.80 | m | Vehicle width |
| l_f | 1.41 | m | Distance from front axle to centre of mass |
| l_r | 1.47 | m | Distance from rear axle to centre of mass |
| L | $l_f + l_r$ | m | Wheelbase |
| m | 1900 | kg | Vehicle mass |
| I_{zz} | 3500 | kgm^2 | Inertia moment of vehicle about vertical axis |
| k_f | 92000 | N/rad | Front wheel cornering stiffness |
| k_r | 97000 | N/rad | Rear wheel cornering stiffness |

Vehicle position and orientation

Derivatives of position and orientation of the vehicle on the road:

$$\begin{bmatrix} \dot{\phi}_{car} \\ \dot{x}_{car} \\ \dot{y}_{car} \end{bmatrix} = \begin{bmatrix} r \\ V \cos(\phi_{car} + \beta) \\ V \sin(\phi_{car} + \beta) \end{bmatrix} \quad (C.18)$$

The vehicle speed is set to be constant. The vehicle does not pitch or roll. The vehicle's tires operate in the linear spectrum. The cornering stiffness does not change. The vehicle parameters remain constant. The vehicle states are updated at 200 Hz, using the RK4 method. Vehicle speeds are sent to the simulated environment. Cumulative errors are corrected for by using the body sideslip constraint (eq. (C.19)).

$$-\sin(\phi_{car})\dot{x} + \sin(\phi_{car})\dot{y} - V\beta = 0 \quad (C.19)$$

Vehicle model validation

Linear vehicle response and overlapping model and carla implementation positions, see fig. C.9.

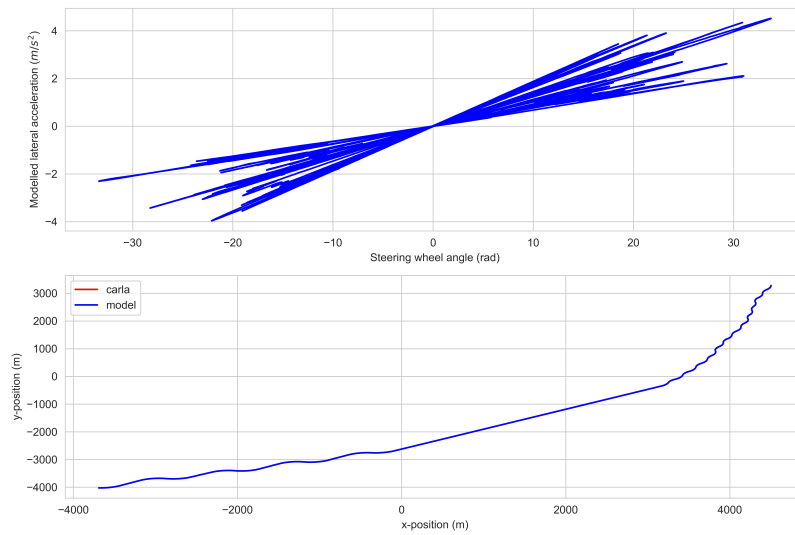


Figure C.9: Plot of vehicle dynamics validation

D

Adaptive design algorithm

Theoretical adaptation speed

1.0003^(200 * 6.8)

The adaptation of the steering gain changes exponentially, by the factor γ (1.0003) each timestep (0.005 s). The theoretically fastest time to change the steering gain by a factor of 1.5 (Middle to High gain) is 6.8 seconds. For γ -values of 1.0002 and 1.0004 this was 10 seconds and 5 seconds respectively.

Note that Theoretically, adaptation to and from lower yaw rate gains takes "longer".

Steering wheel force-feedback

The steering wheel feedback stiffness and gain are adapted to maintain an equivalent steering response while adapting the vehicle gain. The steering wheel system's equation of motion is given by eq. (D.1). The damping for a critically damped system followseq. (D.2). The damping ratio is given by eq. (D.3). The steering wheel force-feedback response should not change per condition, only scaled (inverse) proportionally to the steering wheel gain. The static feedback force to steering wheel angle is scaled inversely with the steering wheel gain, while the dynamic response is kept equal by keeping the damping ratio constant. When the steering gain is scaled by a factor S , the range of steering wheel angles is scaled by a factor $1/S$. The steering wheel stiffness k is scaled by a factor S to keep the static feedback force equal for all steering gains. To keep the damping ratio equal, the steering wheel damping c is scaled by a factor \sqrt{S} , see eq. (D.4).

$$F = \ddot{x} + \frac{c}{m} \dot{x} + \frac{k}{m} x = 0 \quad (\text{D.1})$$

$$c_c = 2\sqrt{km} \quad (\text{D.2})$$

$$\zeta = \frac{c}{c_c} \quad (\text{D.3})$$

$$c = \zeta c_c = 2\zeta\sqrt{km} \quad (\text{D.4})$$

Implementation force-feedback

The root mean square of the steering torque during the experiments is shown in fig. D.1. The feedback forces for each steering setting correspond to the lateral accelerations of the vehicle (fig. D.3), except for the two instances where the torque controller failed.

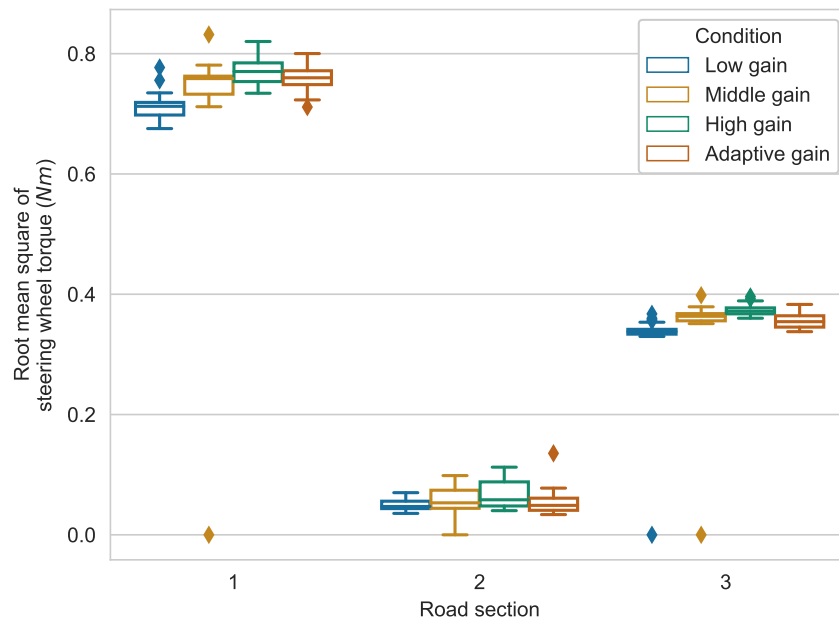


Figure D.1: Root mean square of steering torque per road section for different steering conditions. Note the outliers on the zero line caused by failure of the torque controller during these experiment runs.

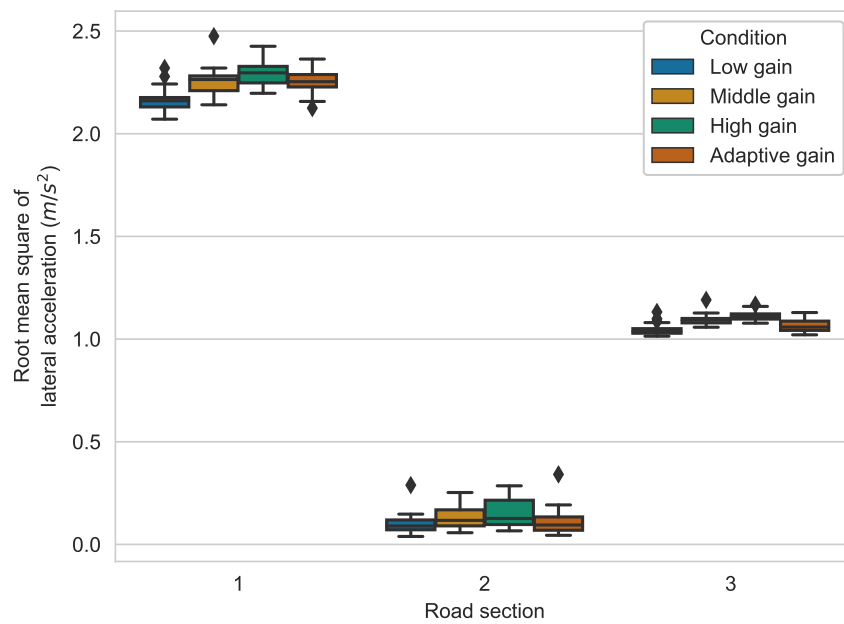


Figure D.2: Root mean square of vehicle lateral acceleration per road section for different steering conditions.

Implementation vehicle dynamics

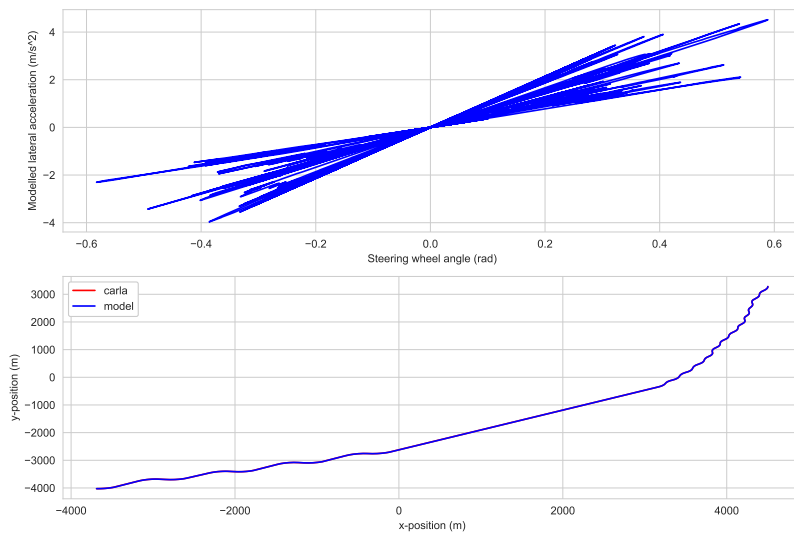


Figure D.3: (A) Plot of modelled lateral acceleration to the steering wheel angle, (B) plot of vehicle position as modelled and as measured, for participant 5, adaptive gain condition.

E

Simulated road environment

The training track is a two-lane (lane width of 3.60 m) road with length 4.2 km consist of multiple corners with radius 70 m and 100 m, and straight sections of length 50 m and 300 m, see fig. E.1.

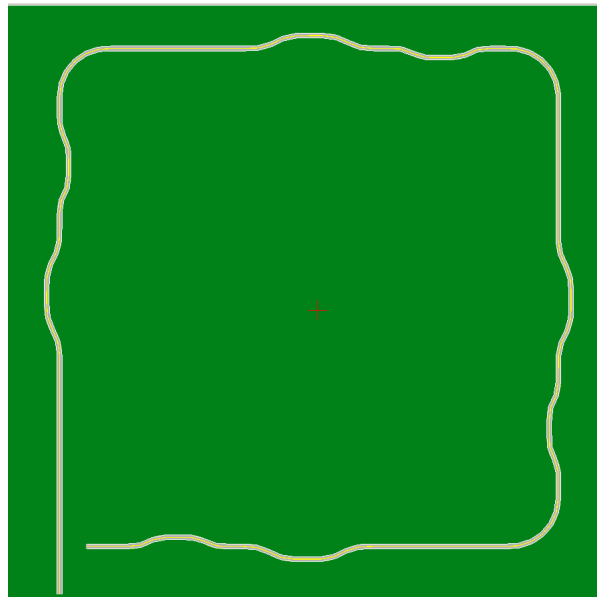


Figure E.1: Training track curvature.

The experiment track is a two-lane (lane width of 3.60 m) road with length of 12.7 km consisting of 220 m straight, three sections of 4.0 km length, and one section with one corner, see fig. E.2.

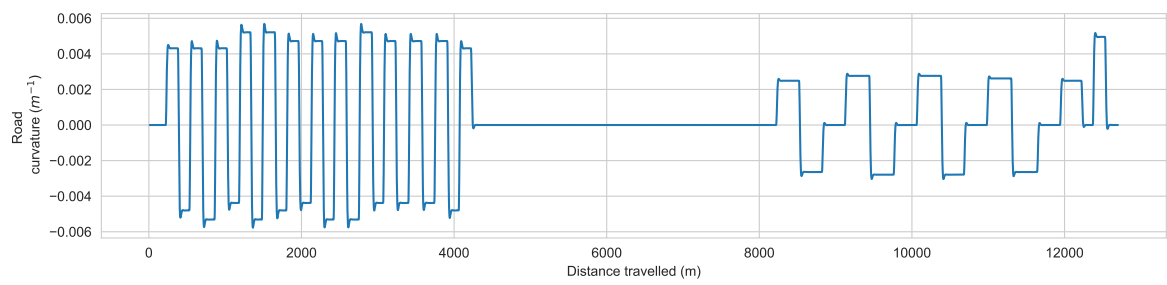
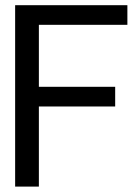


Figure E.2: Road curvature over travel distance.



Experiment remarks

Unforeseen deviations from the experiment protocol, and remarks from participants.

- For participant 1 to participant 4, the carlainterfaceaction module was set to 10 Hz. This caused the visualisation of the movement of the vehicle's steering wheel on the screen to jitter, and the carlainterface data was effectively recorded at 10 Hz. The road waypoints and vehicle position data was recovered using the vehicle model position data.
- From participant 19 to participant 24, the Unreal render quality settings have been set from "Cinematic" to "Epic" with no impact on visual quality, but rendering frame rates seemed to be more stable.
- During three experiments, the vehicle suddenly stopped for a few seconds (while driving 80 km/h), and re-accelerated back to 80 km/h; this was caused by a background windows update. This happened during the trial and experiment run with condition D with participant 11, during the experiment run with condition D with participant 19, and during the experiment run with condition B with participant 22. With participant 11, I decided to restart the experiment run. Later, however, it happened again (approximately at $s = 2000$ m), and it was decided to continue the experiment run. With participant 19, it happened at approximately $s = 5000$ m, and I decided to let the experiment continue. With participant 22, the slow-down was brief, but the lag in the system caused the participant to lose control of the vehicle ($s = 10000$ m). I decided to redo the experiment run of task B. Then, it happened again ($s = 500$ m), but did not cause major problems, and thus I decided to continue with the experiment run.
- Participant 4 did not seem to drive as he normally would have done, and upon asking, he admitted that he was "following the midline closely". Participant 22 did let go of the steering wheel quite often.
- For this experiment, the screen frame rate is normally set to 60 Hz, and the screen resolution is set to native 3840 x 2160. However, this is different for other experiment takers as there are differences in performance and visualisation requirements. During two participants, different screen settings were used. During condition C with

participant 13 and condition C with participant 16 the screen update frequency was 30 Hz, and the resolution was 1920 x 1080. I decided to change this back to 60 Hz and a resolution of 3840 x 2160 after I noticed the difference and after the participant performed the experiment run. The importance of a higher screen update frequency is mainly to counter head-ache and motion sickness, while providing a better simulator experience. Also, normally, the screens vibrancy (boost) is set to 68%, providing a more colourful simulator experience. For participant 13, the screen's vibrancy (boost) remained at the default 50% for all conditions.

- The NASA-TLX has a counter-intuitive axis direction for “Performance”, that participants tend to overlook. Upon noticing the misinterpretation by participant 14 for condition C and condition A and by participant 19 for condition D, the following manual adjustments to the participant scores have been performed: The scores for “Performance” from participant 14 for condition C and condition A, and from participant 19 for condition D have been mirrored on the 50-score at the request of the participants.
- Participant 16 remarked that steering to the left was different than steering to the right. Participant 22 found that the higher steering sensitivity was also tougher to steer, which he found was annoying, and might have affected his answers.
- Participant 21 remarked to feel a slight headache after performing condition B (second task). Participant 22 remarked to feel sleepy after performing task B (for the second time). For both cases, I decided to suggest to have a break, which we took.
- A network error caused the answers to the self-reported questionnaire asked during the experiment of participant 15, for (if remembered correctly) condition C, to get lost. The participant remembered and recalled the answered scores, these scores have been reported.
- The measured torque measurements started reporting zero-values for participant 19 condition D, and for participant 22 condition A. It is unsure whether the actual feedback torque was reduced to zero. Close inspection of the steering wheel angle data of participant 22 condition A at the time that the reported torque measurement started to report zero values, shows an unlikely jump of the steering wheel angle, which points to a loss of feedback torque for this experiment trial.

G

Informed Consent form

Consent Form for a driving simulator study

Researchers

Sam Staps – MSc student

E-mail: s.j.staps@student.tudelft.nl

Tel: +31639680028

Ir. T. Melman – Supervisor

E-mail: t.melman@tudelft.nl

Prof.dr.ir. D.A. Abbink – Supervisor

E-mail: d.a.abbink@tudelft.nl

This document describes the purpose, procedures, benefits, risks and possible discomforts of a driving simulator study. It also describes the right to withdraw from the study at any time in any case. Before agreeing to participate in this study, it is important that the information provided in this document is fully read and understood.

Location of the experiment

TU Delft, Faculty of Mechanical, Maritime and Materials Engineering (3mE)

Department of Cognitive Robotics

Cognitive Robotics Lab, room F-0-220

Mekelweg 2, 2628CD Delft

Purpose of the study

The purpose of this study is to investigate the driver's driving behaviour to different steering settings. The results will be statistically analysed and published in, but not limited to, a Master thesis.

Procedure

You will be requested to take place in a fixed-base driving simulator and you will be briefed on how to operate it. The experiment consists of four trials (duration of 10 minutes each). Prior to each trial, you will drive training trials to become familiar with the steering systems (duration of 3 minutes).

The simulator car will be given a constant speed, you (the driver) only need to control the steering wheel. You are asked to drive as you would normally do. During each trial you are asked questions about your opinion of the steering system. After each trial you are asked to fill out a questionnaire, and a final questionnaire after all trials.

Task instructions

During the entire track you are requested to drive as you normally would.

Duration

The total experiment, including filling out a questionnaires, will take approximately 75 minutes.

Risk and discomforts

Virtual environments like driving simulators can cause motion sickness, due to a difference between actual and expected motion. Symptoms commonly include nausea, vomiting, cold sweat, headache,

sleepiness, yawning, loss of appetite, and increased salivation. Risk factors include pregnancy, migraines, and Meniere's disease. Behavioural measures to decrease motion sickness include holding the head still and lying on the back.

If you feel uncomfortable in any way during the experiment, you are advised to stop the experiment or rest for several minutes. If you do not feel well, please take sufficient rest before leaving the laboratory.

Confidentiality

I understand that personal information collected about me that can identify me, such as my name, will not be shared beyond the study team. The collected data in this experiment will be published. The collected data will also be anonymised i.e. you will be identified by a subject number.

Right to refuse or withdraw

Your participation is strictly voluntary and you may withdraw from or stop this experiment at any time, without having to give a reason, without consequences.

Questions

If you have any questions regarding this experiment, feel free to contact Sam Staps (contact details are provided at the top of this document).

**I have read and understood the information provided above.
I give permission to process the data for the purpose described above.
I voluntary agree to participate in this study.**

Name of the participant:

Signature:

Date:

Name of researcher: Sam Staps

Signature:

Date:

H

Experiment Questionnaires

Driving Simulator Study

Thank you for joining the simulator study! Please read the Informed Consent form and answer the following questions.

*Vereist

Participant number *

Jouw antwoord

I have read the Consent Form: <https://drive.google.com/file/d/1xvtvyrlrzeZ4Y9aAytmkNI9SEbMclQf/view?usp=sharing> *

- Yes
- I will do so now...

What is your sex? *

- Male
- Female

What is your age? *

Jouw antwoord



In which year did you obtain your first driver's licence? *

Jouw antwoord

What is your primary mode of transportation? *

- Private automobile
- Private motorcycle
- Public transport
- Human powered transportation (e.g. walking, cycling)
- Anders:

On average, how often did you drive a vehicle in the last 3 months? *

- Every day
- 4 to 6 days a week
- 1 to 3 days a week
- Once a month to once a week
- Less than once a week
- Less than once a month
- Never



Roughly how many kilometers did you drive in the last 12 months? *

- 0
- 1-1000
- 1001-5000
- 5.001-10.000
- 10.001-15.000
- 15.001-20.000
- 20.001-25.000
- 25.001-35.000
- 35.001-50.000
- 50.001-100.000
- More than 100.000

Have you ever heard of a sport mode in vehicles? *

- Yes
- No

What is your experience in driving in a driving simulator? *

- I am an experienced driver in driving simulators / (racing) games with a steering wheel.
- I have driven in a simulator before/have some experience in (racing) games with a steering wheel.
- No experience at all



Verzenden



Motion sickness questionnaire:

Please check if you feel you are experiencing one/more of these symptoms.

To what extent do you feel symptoms of motion sickness? - Run 1

Please circle the most fitting to your feeling.

1. No symptoms
2. Arising feel in abdomen, no nausea / yawning
3. Slightly nauseous / sleepiness / slight headache
4. Nauseous / headache

To what extent do you feel symptoms of motion sickness? - Run 2

Please circle the most fitting to your feeling.

1. No symptoms
2. Arising feel in abdomen, no nausea / yawning
3. Slightly nauseous / sleepiness / slight headache
4. Nauseous / headache

To what extent do you feel symptoms of motion sickness? - Run 3

Please circle the most fitting to your feeling.

1. No symptoms
2. Arising feel in abdomen, no nausea / yawning
3. Slightly nauseous / sleepiness / slight headache
4. Nauseous / headache

To what extent do you feel symptoms of motion sickness? - Run 4

Please circle the most fitting to your feeling.

1. No symptoms
2. Arising feel in abdomen, no nausea / yawning
3. Slightly nauseous / sleepiness / slight headache
4. Nauseous / headache

During-experiment questionnaire

The researcher will mark the questions.

For each road section, three questions are asked.

Ask these at road section 1 (curves), section 2 (straight), section 3 (medium curves).

The road sections are defined as:

0: short first straight part

1: curves

2: straight road

3: medium curves

4: final sharp curve

Questions:

Q1, rate: "I can control my position precisely".

Q2, rate: "I find the steering system sensitive".

Q3, rate: "I like the steering sensitivity".

For this road section (during trial)

On a scale of 1 to 10 (totally disagree .. totally agree), what is your rating for:

1. I can control my position precisely

Ik kan mijn positie precies controleren

2. I find the steering system sensitive

Ik vind het stuursysteem gevoelig

3. I like the steering sensitivity

Ik vind de gevoeligheid fijn

For the road section/type transitions (post-trial)

On a scale of 1 to 10 (totally disagree .. totally agree), what is your rating for:

10. I found the steering behaviour predictable

Ik vond het stuurgedrag voorspelbaar

***Vereist**

Participant number *

Jouw antwoord



Task *

- Task A
- Task B
- Task C
- Task D

I can control my position precisely (1) *

Ik kan mijn positie precies controleren

1 2 3 4 5 6 7 8 9 10

Totally disagree Totally agree

I find the steering system sensitive (1) *

Ik vind het stuursysteem gevoelig

1 2 3 4 5 6 7 8 9 10

Totally disagree Totally agree

I like the steering sensitivity (1) *

Ik vind de stuurgevoeligheid fijn

1 2 3 4 5 6 7 8 9 10

Totally disagree Totally agree



I can control my position precisely (2) *

Ik kan mijn positie precies controleren

1 2 3 4 5 6 7 8 9 10

Totally disagree

Totally agree

I find the steering system sensitive (2) *

Ik vind het stuursysteem gevoelig

1 2 3 4 5 6 7 8 9 10

Totally disagree

Totally agree

I like the steering sensitivity (2) *

Ik vind de stuurgevoeligheid fijn

1 2 3 4 5 6 7 8 9 10

Totally disagree

Totally agree

I can control my position precisely (3) *

Ik kan mijn positie precies controleren

1 2 3 4 5 6 7 8 9 10

Totally disagree

Totally agree



I find the steering system sensitive (3) *

Ik vind het stuursysteem gevoelig

1 2 3 4 5 6 7 8 9 10

Totally disagree Totally agree

I like the steering sensitivity (3) *

Ik vind de stuurgevoeligheid fijn

1 2 3 4 5 6 7 8 9 10

Totally disagree Totally agree

I found the steering behaviour predictable *

Ik vond het stuurgedrag voorspelbaar

1 2 3 4 5 6 7 8 9 10

Totally disagree Totally agree

Verzenden

Verzend nooit wachtwoorden via Google Formulieren.

Deze content is niet gemaakt of goedgekeurd door Google. [Misbruik rapporteren](#) - [Servicevoorwaarden](#) - [Privacybeleid](#)

Google Formulieren



Workload questionnaire (NASA-TLX)

A driving simulator study

There is a description for each of these subscales that the subject should read before rating. They are rated *for each task* within a 100-points range with 5-point steps. These ratings are then combined to the task load index. These descriptions are as follows:

Mental Demand

How much mental and perceptual activity was required? Was the task easy or demanding, simple or complex?

Physical Demand

How much physical activity was required? Was the task easy or demanding, slack or strenuous?

Temporal Demand

How much time pressure did you feel due to the pace at which the tasks or task elements occurred? Was the pace slow or rapid?

Overall Performance

How successful were you in performing the task? How satisfied were you with your performance?

Effort

How hard did you have to work (mentally and physically) to accomplish your level of performance?

Frustration Level

How irritated, stressed, and annoyed versus content, relaxed, and complacent did you feel during the task?

Hart, S. G., & Staveland, L. E. (1988). Development of NASA-TLX (Task Load Index): Results of empirical and theoretical research. In *Advances in psychology* (Vol. 52, pp. 139-183). North-Holland.

Participant number

Task

- Task A Task B Task C Task D

Mental Demand

How mentally demanding was the task?

Very Low

Very High

0 5 10 15 20 25 30 35 40 45 50 55 60 65 70 75 80 85 90 95 100



Physical Demand

How physically demanding was the task?

Very Low

Very High

0 5 10 15 20 25 30 35 40 45 50 55 60 65 70 75 80 85 90 95 100



Temporal Demand

How hurried or rushed was the pace of the task?

Very Low

Very High

0 5 10 15 20 25 30 35 40 45 50 55 60 65 70 75 80 85 90 95 100



Performance
to do?

How successful were you in accomplishing what you were asked

Perfect

Failure

0 5 10 15 20 25 30 35 40 45 50 55 60 65 70 75 80 85 90 95 100



Effort
performance?

How hard did you have to work to accomplish your level of

Very Low

Very High

0 5 10 15 20 25 30 35 40 45 50 55 60 65 70 75 80 85 90 95 100



Frustration
you?

How insecure, discouraged, irritated, stressed and annoyed were

Very Low

Very High

0 5 10 15 20 25 30 35 40 45 50 55 60 65 70 75 80 85 90 95 100



Powered by Qualtrics [↗](#)



Individual participant data

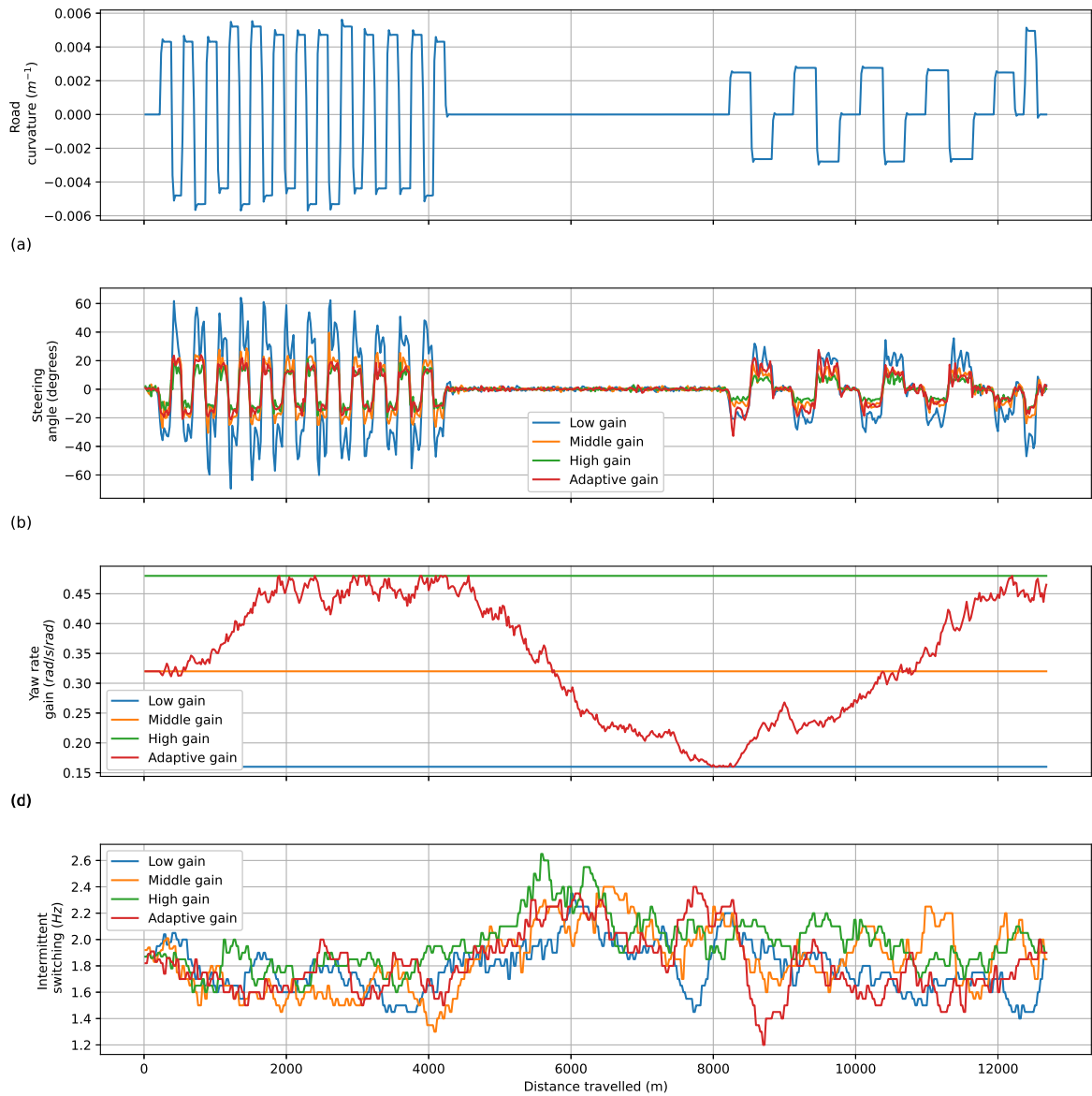


Figure I.1: Raw participant data on the experiment trials (participant 1).

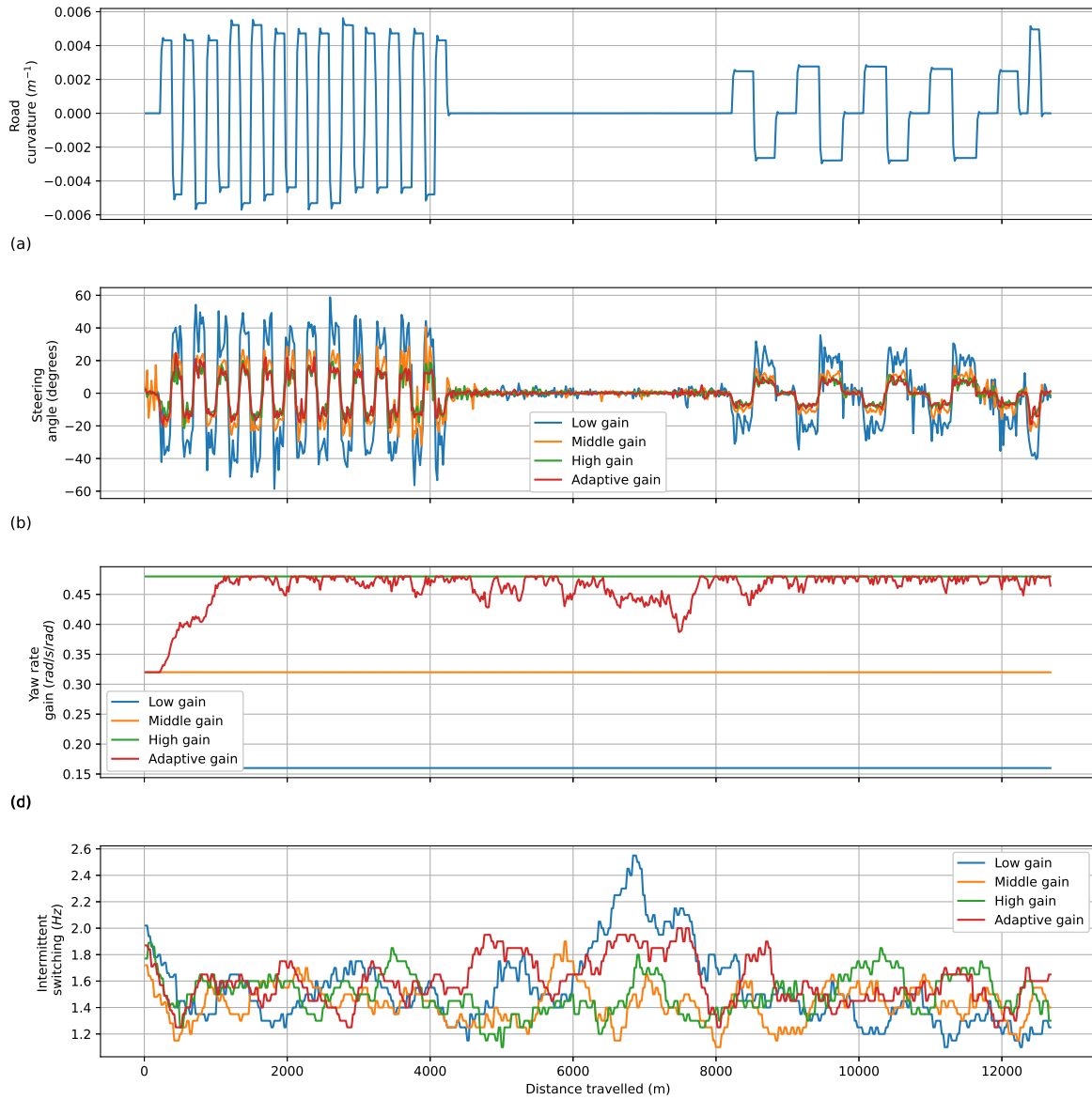


Figure I.2: Raw participant data on the experiment trials (participant 2).

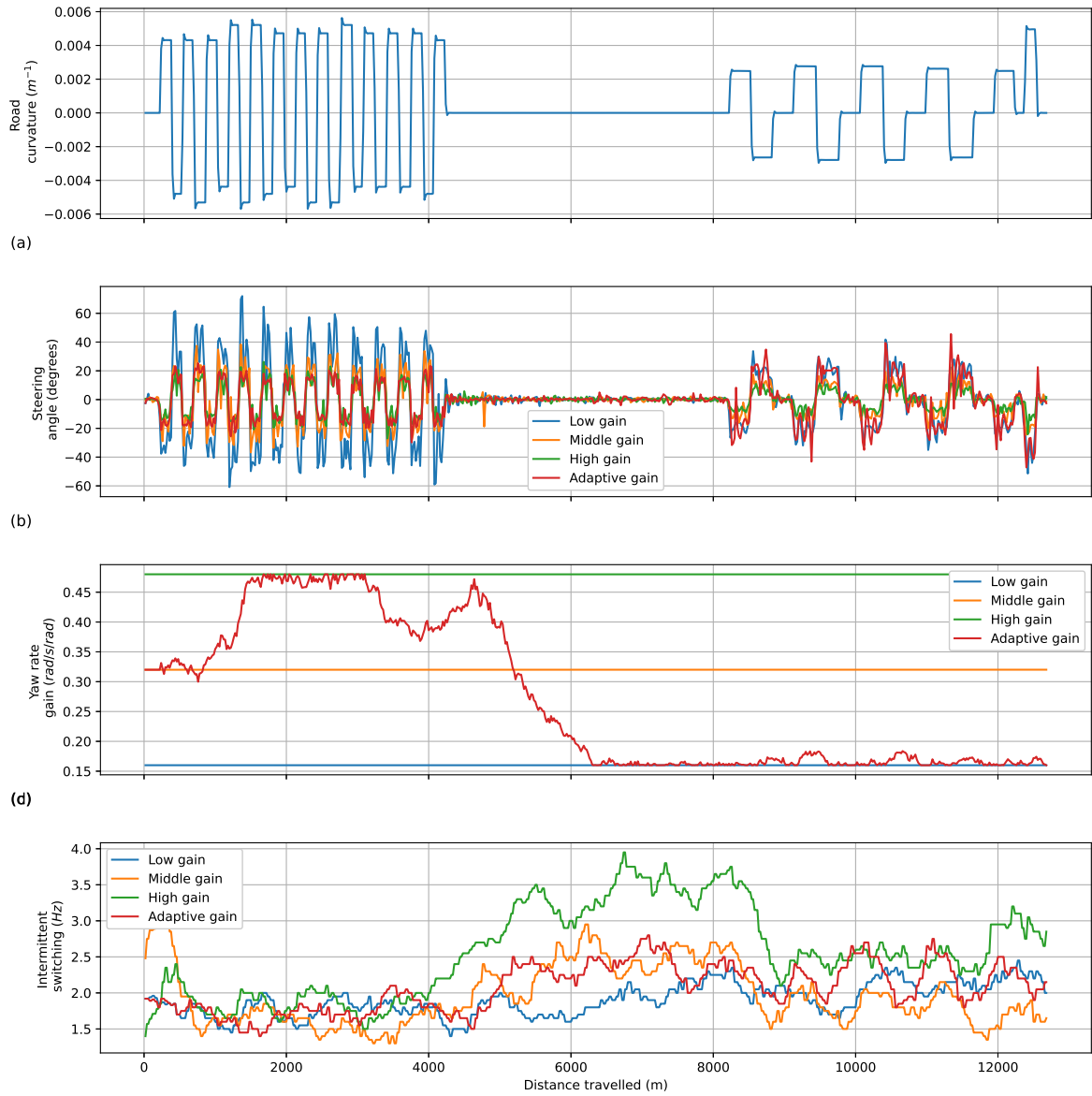


Figure I.3: Raw participant data on the experiment trials (participant 3).

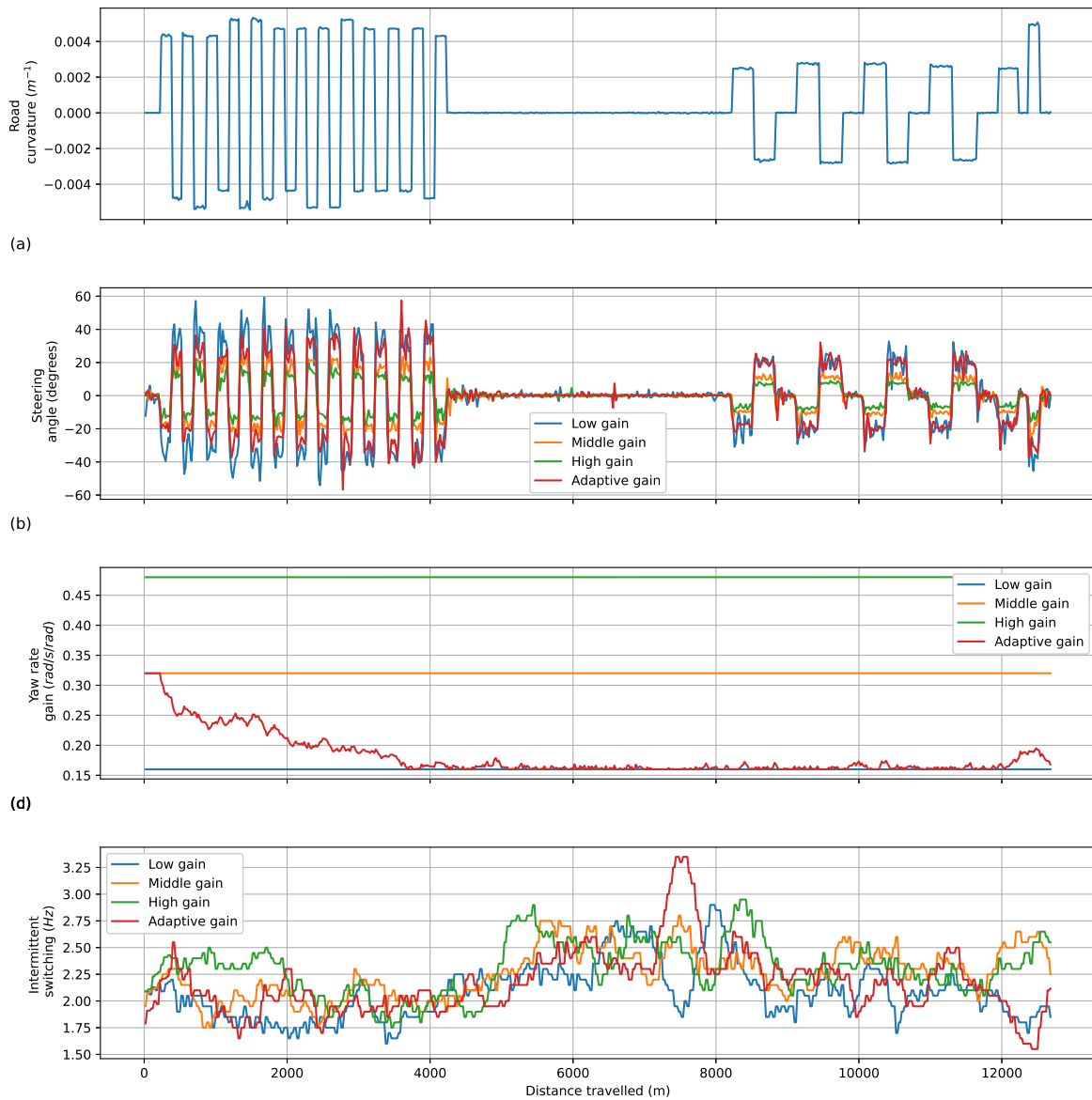


Figure I.4: Raw participant data on the experiment trials (participant 4).

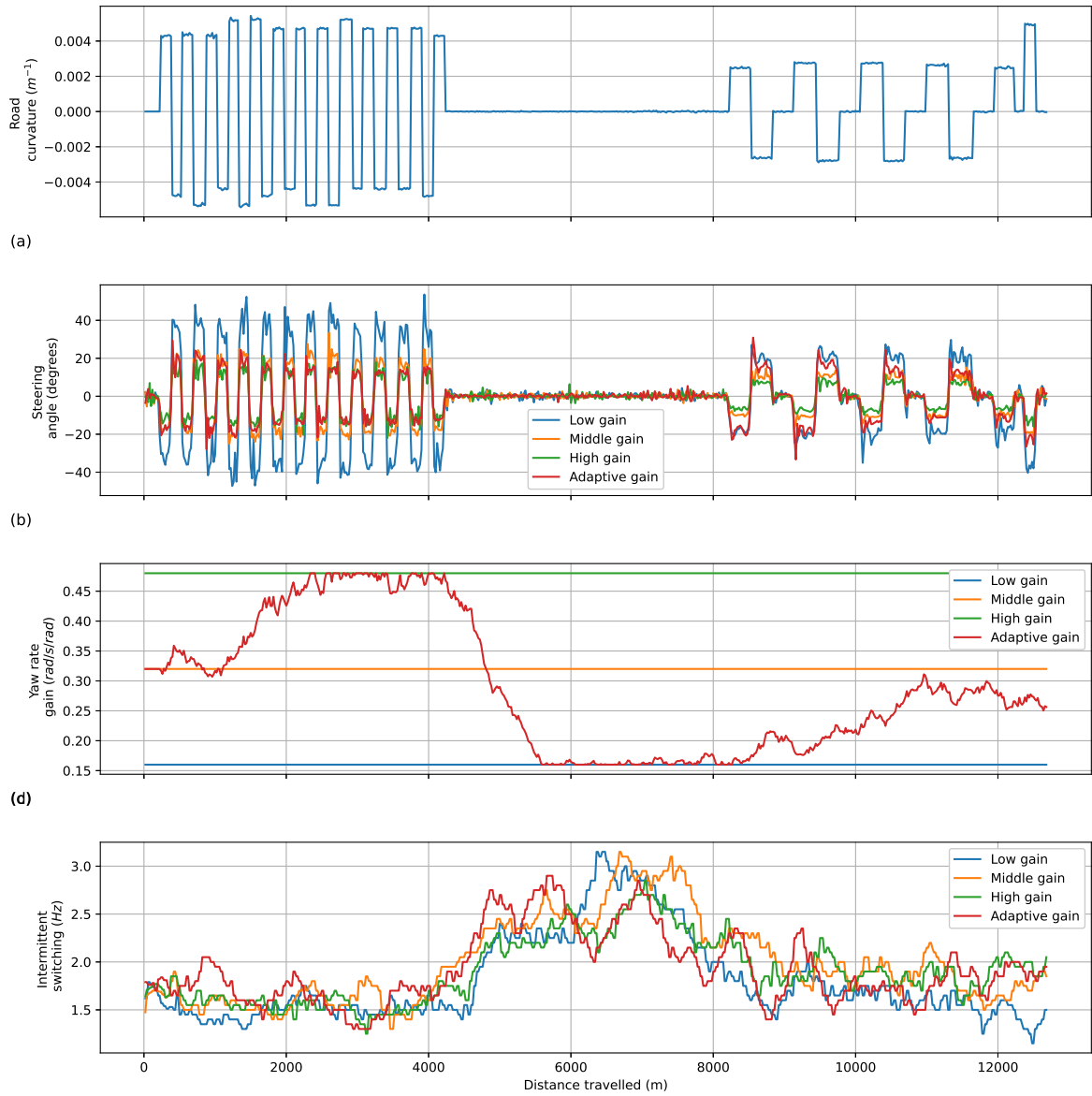


Figure I.5: Raw participant data on the experiment trials (participant 5).

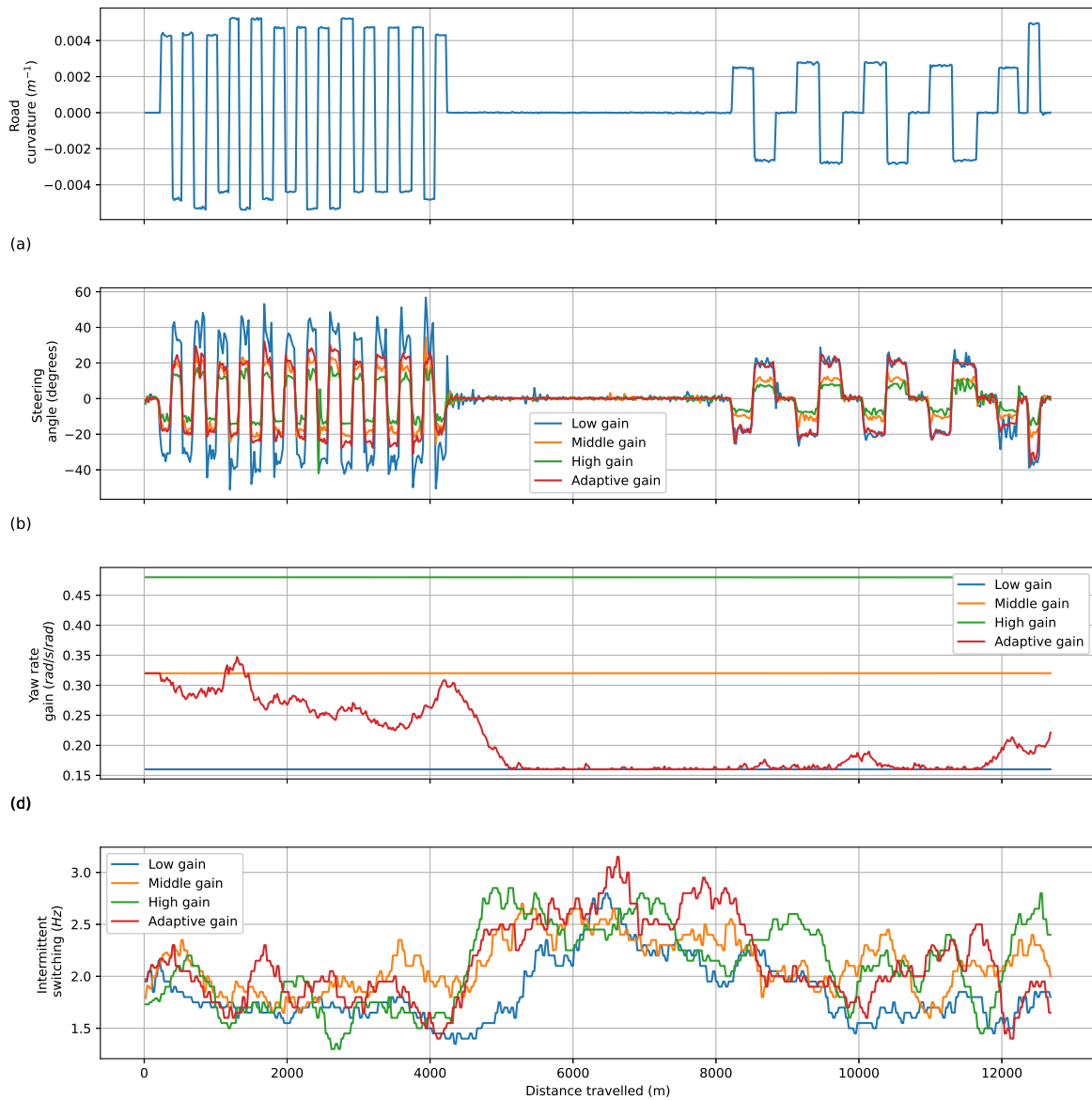


Figure I.6: Raw participant data on the experiment trials (participant 6).

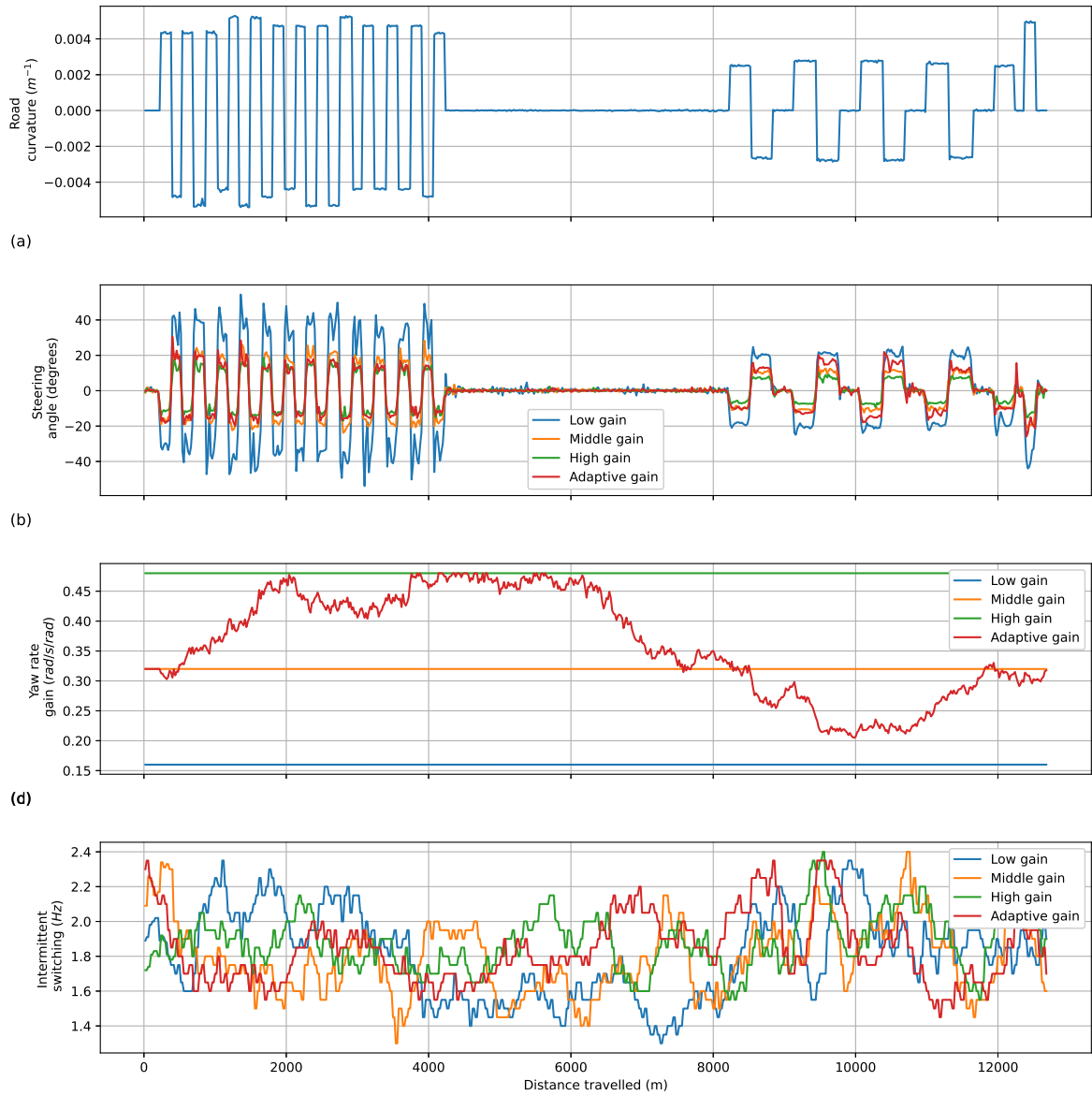


Figure I.7: Raw participant data on the experiment trials (participant 7).

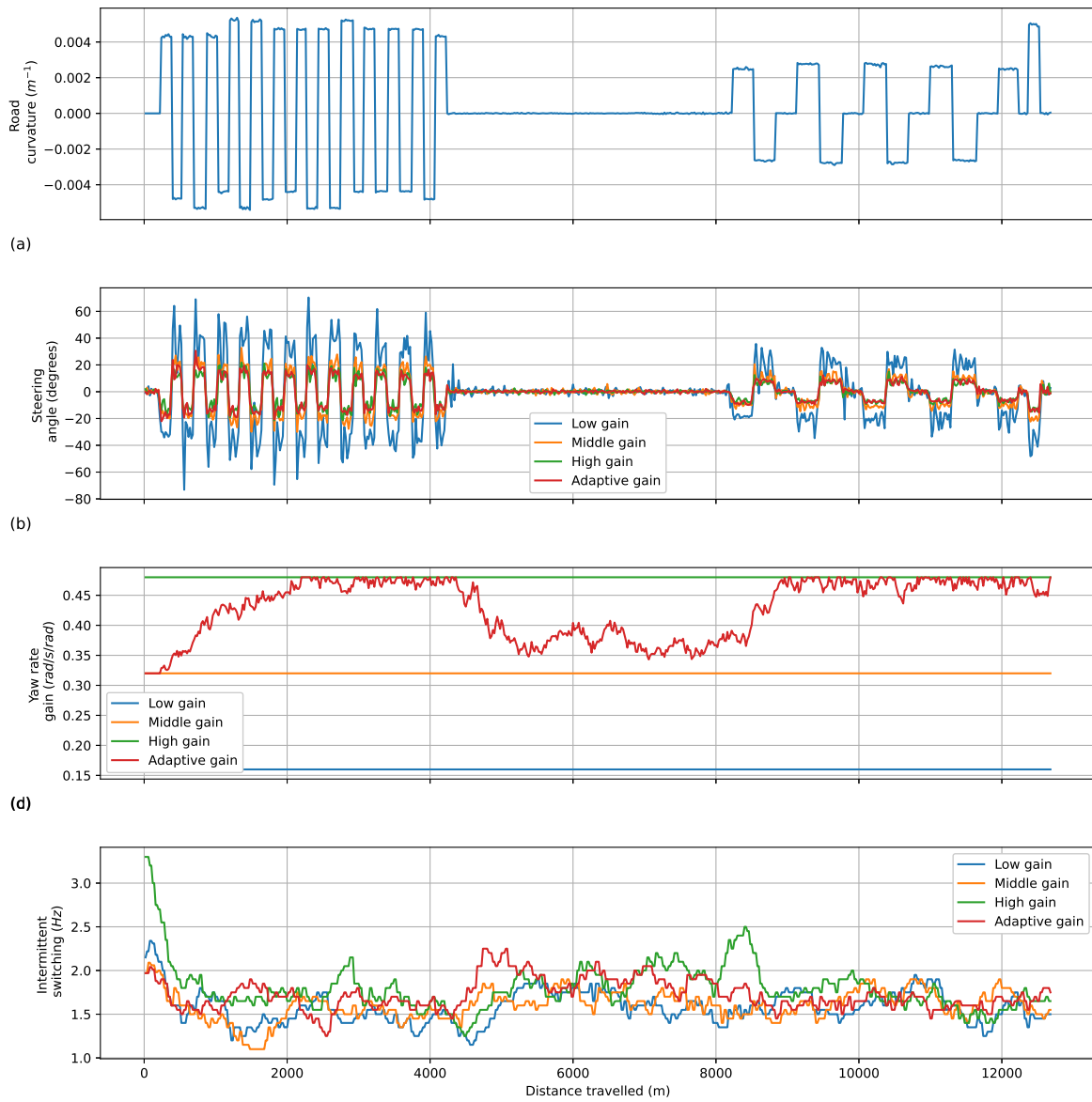


Figure I.8: Raw participant data on the experiment trials (participant 8).

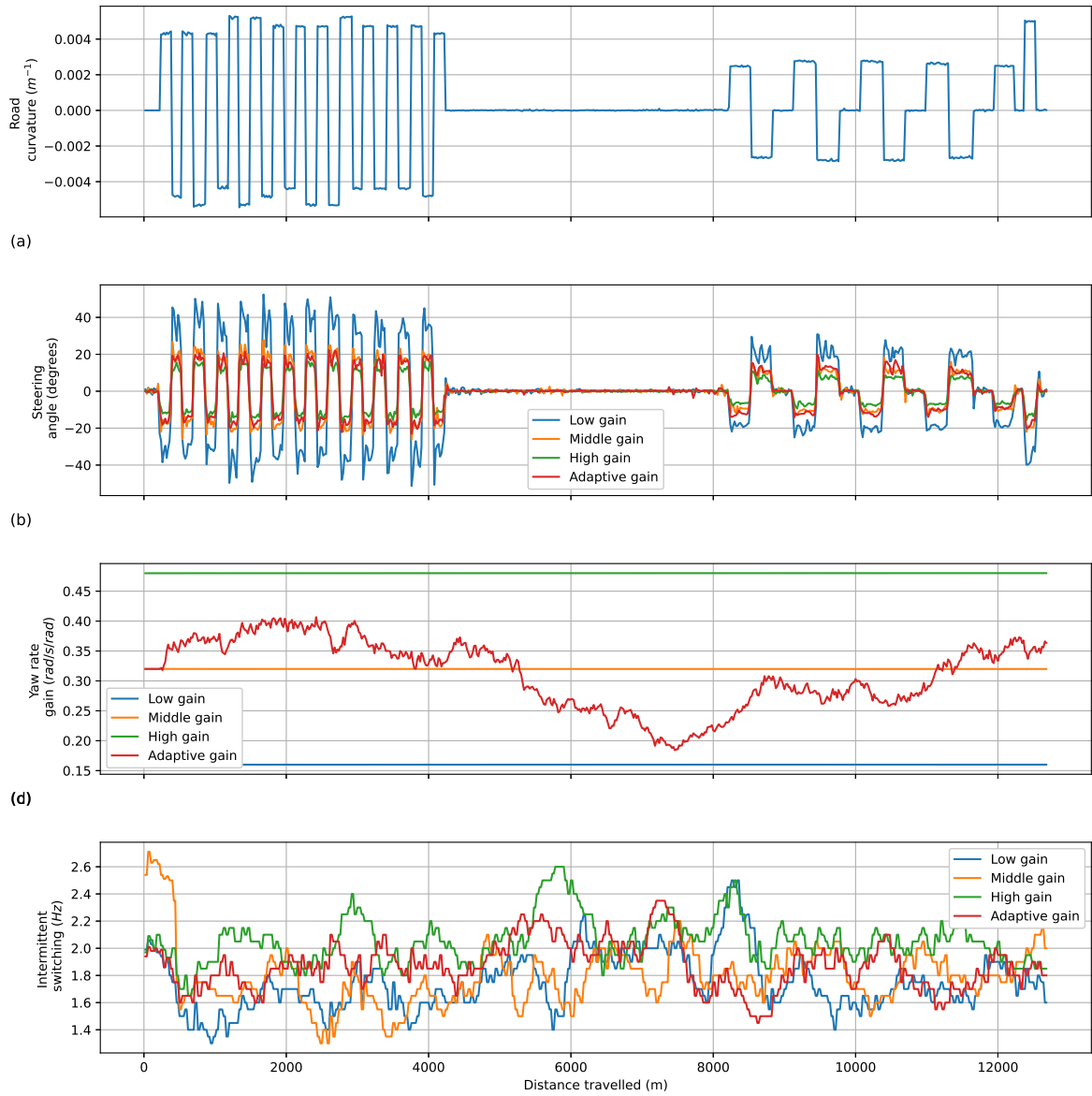


Figure I.9: Raw participant data on the experiment trials (participant 9).

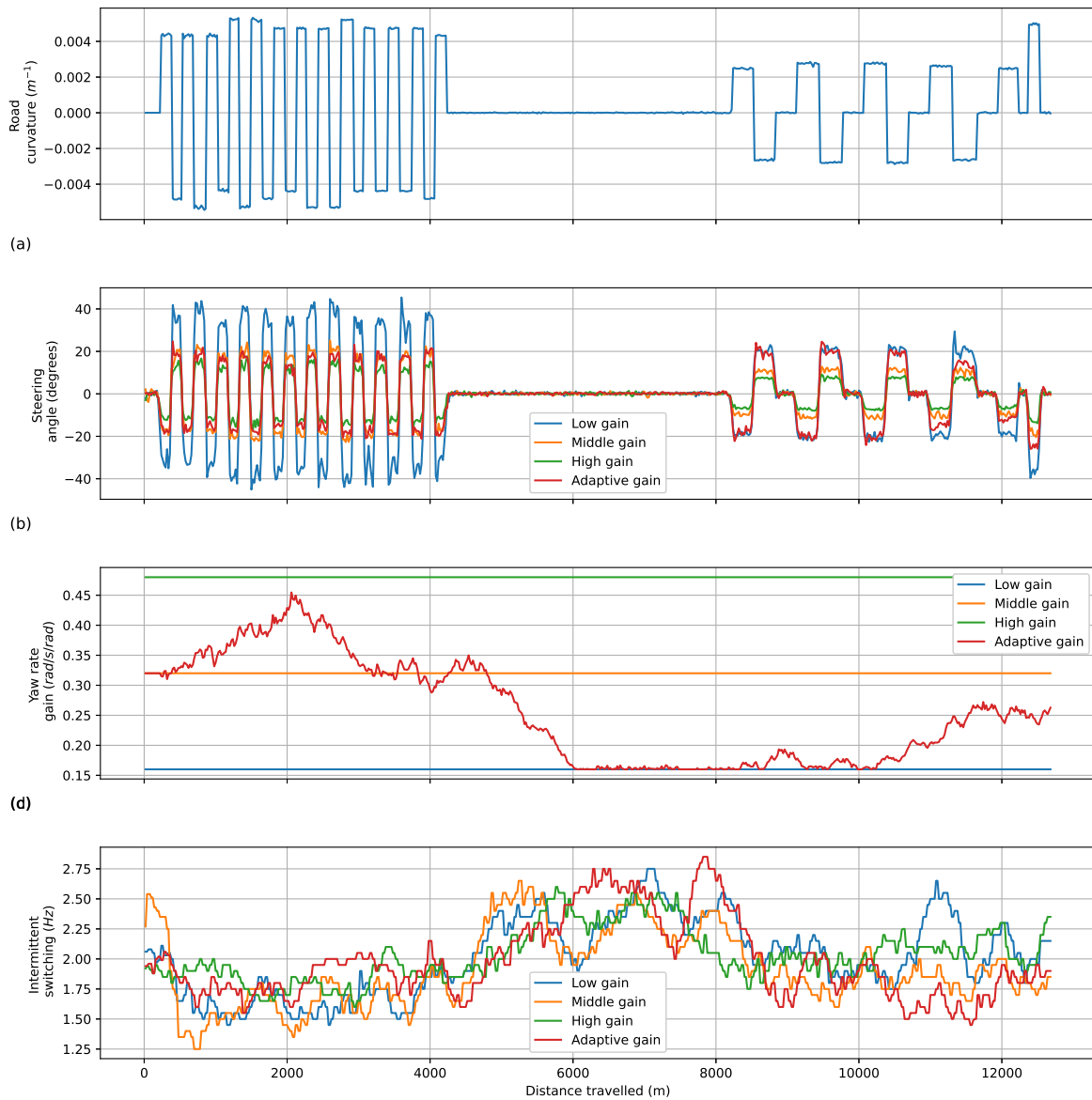


Figure I.10: Raw participant data on the experiment trials (participant 10).

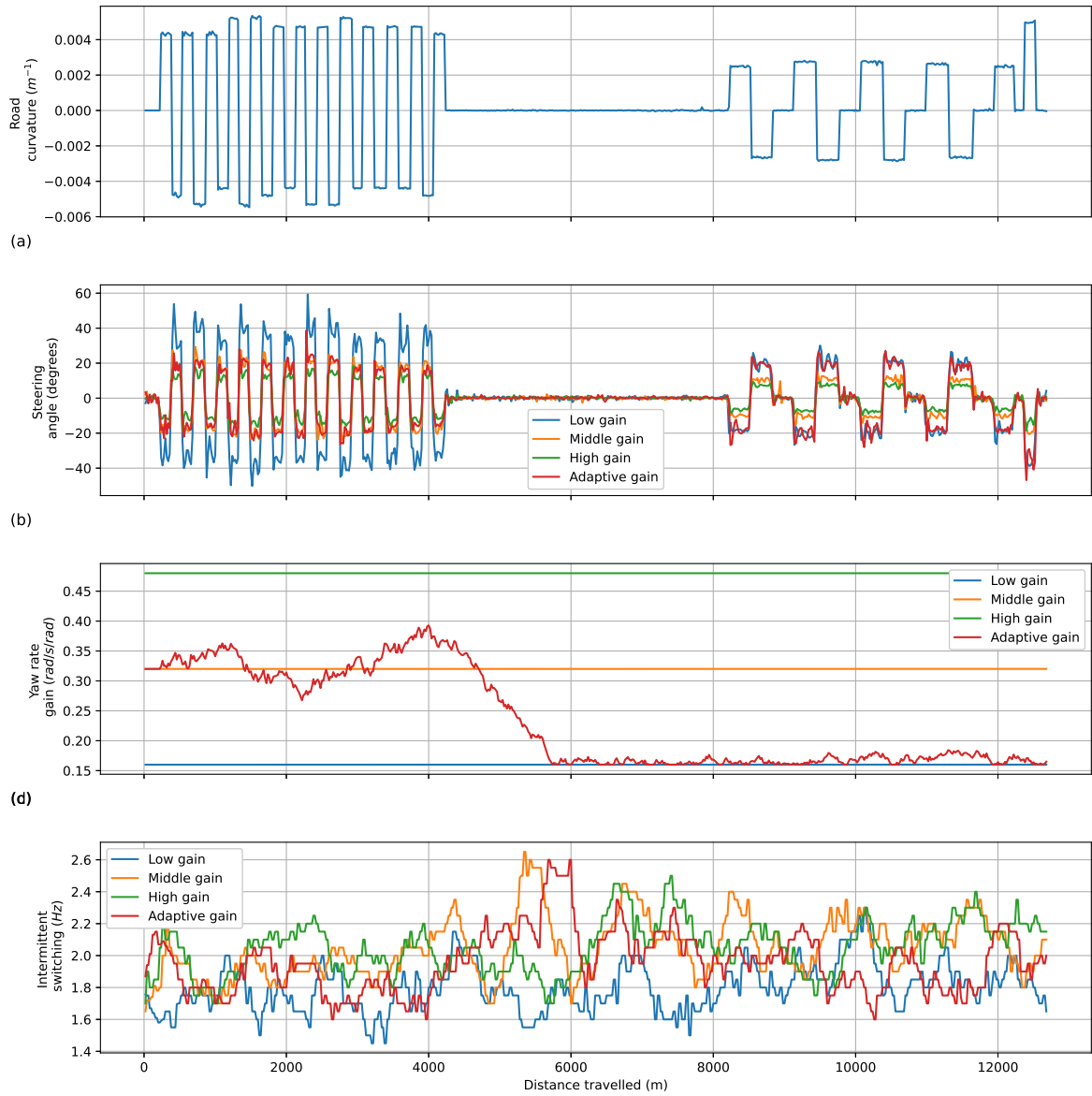


Figure I.11: Raw participant data on the experiment trials (participant 11).

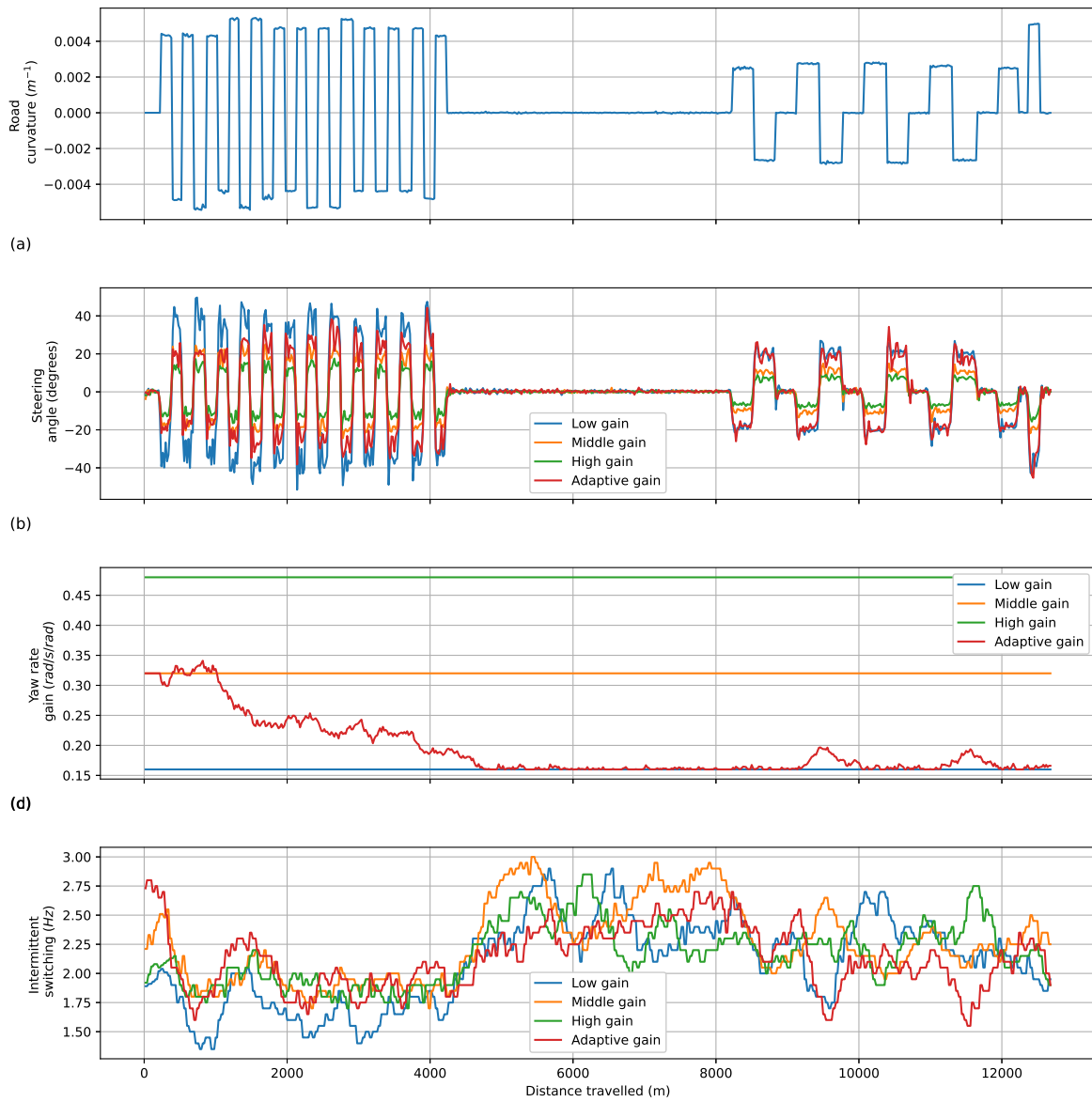


Figure I.12: Raw participant data on the experiment trials (participant 12).

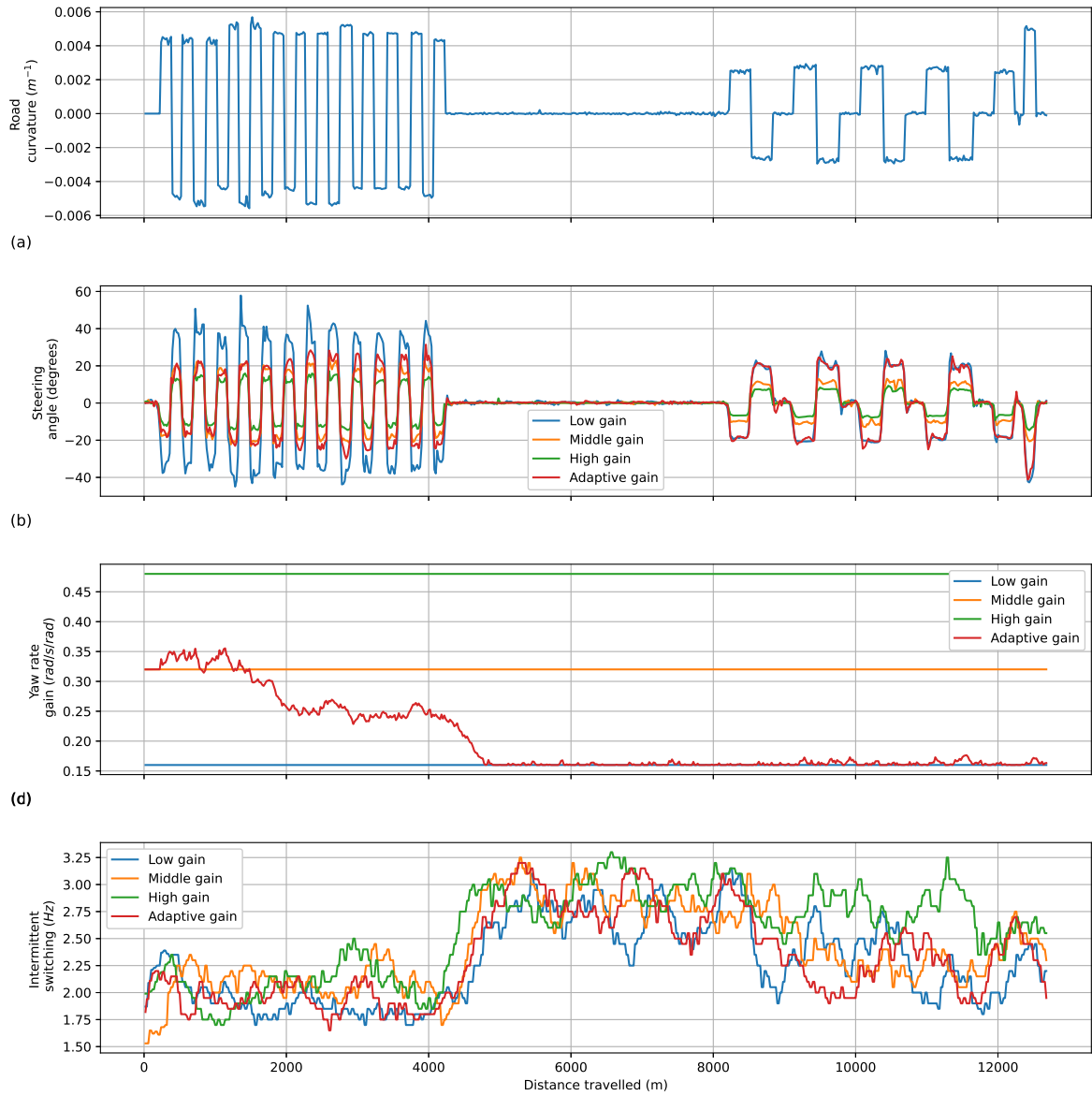


Figure I.13: Raw participant data on the experiment trials (participant 13).

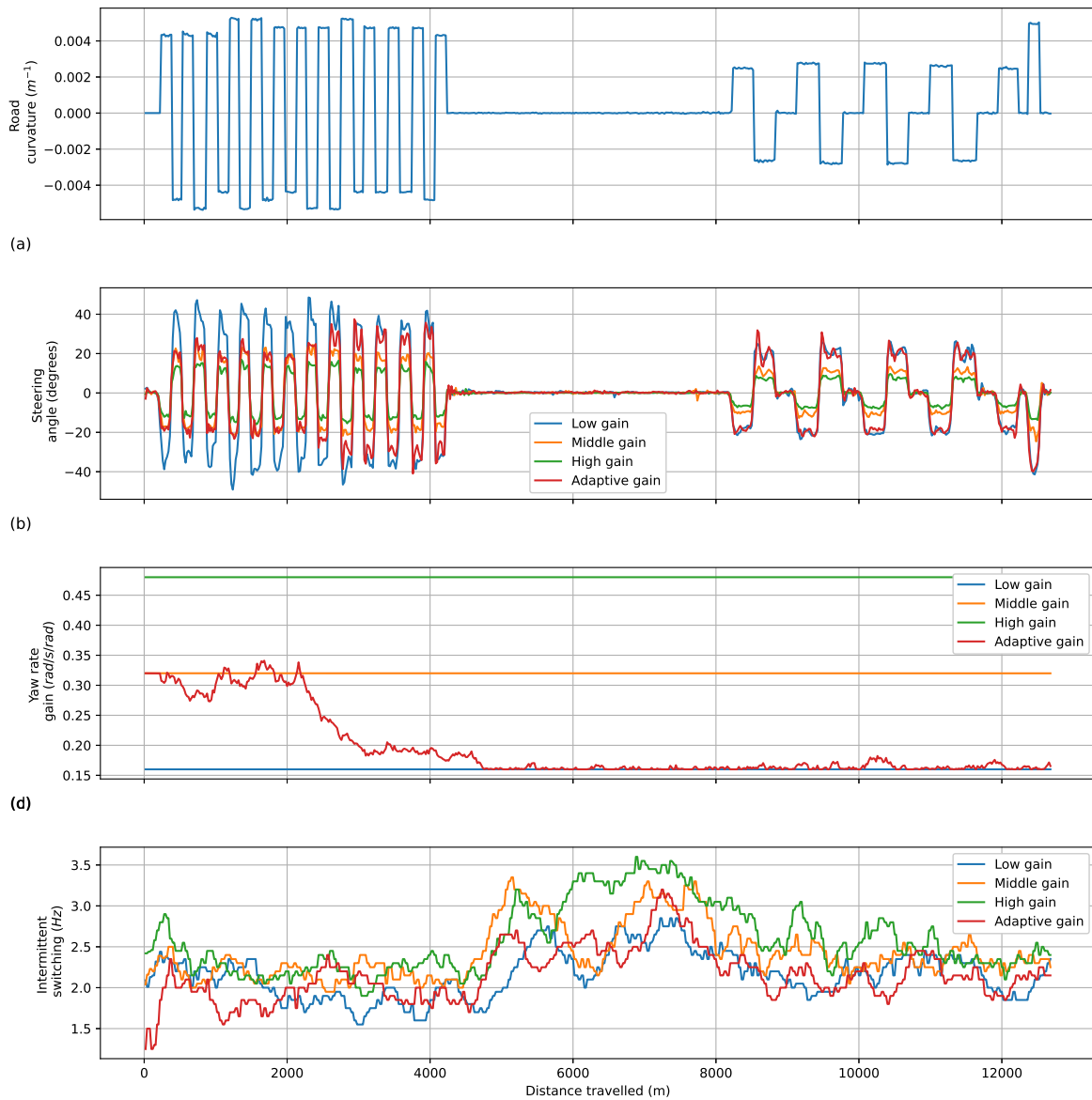


Figure I.14: Raw participant data on the experiment trials (participant 14).

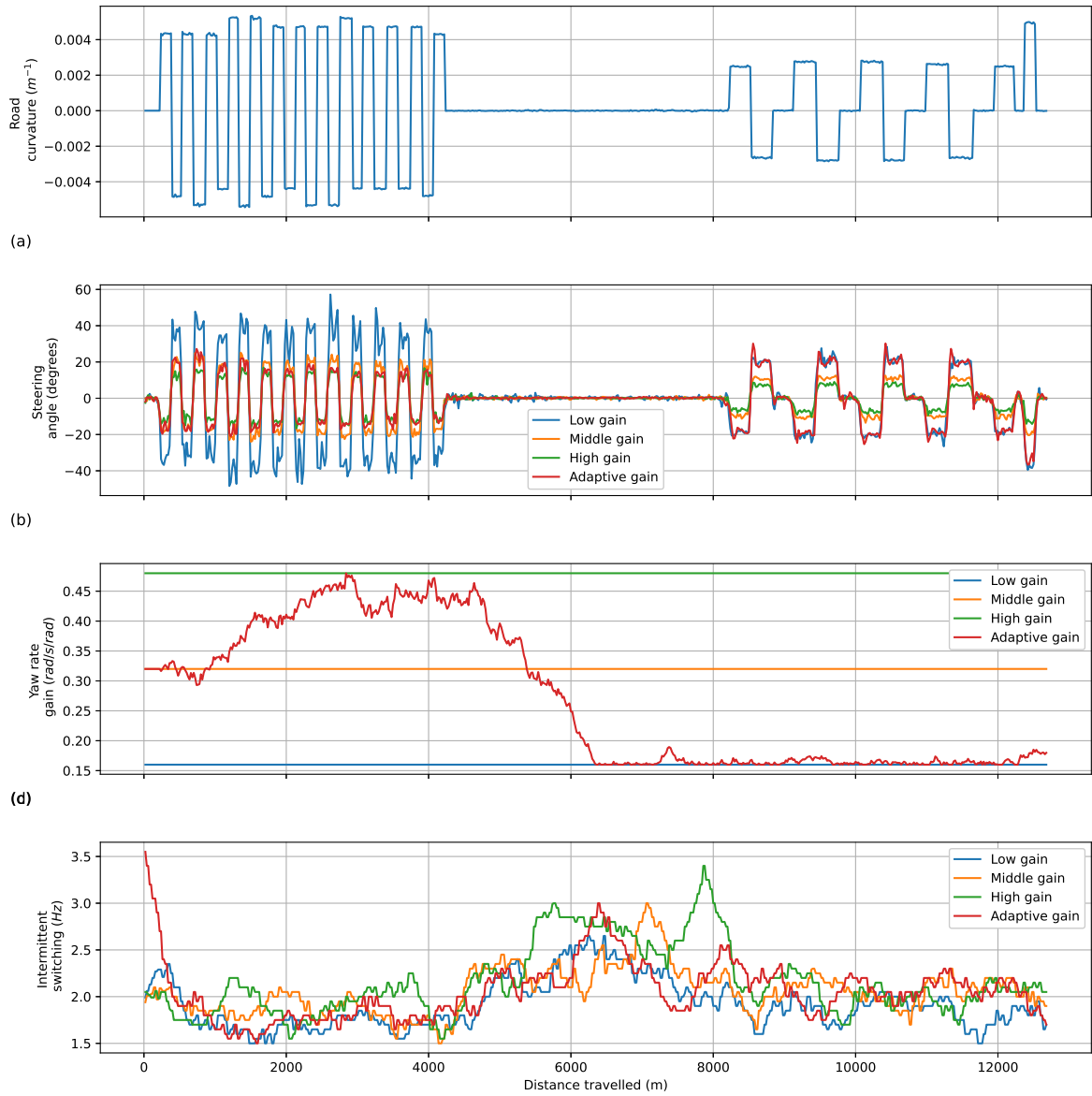


Figure I.15: Raw participant data on the experiment trials (participant 15).

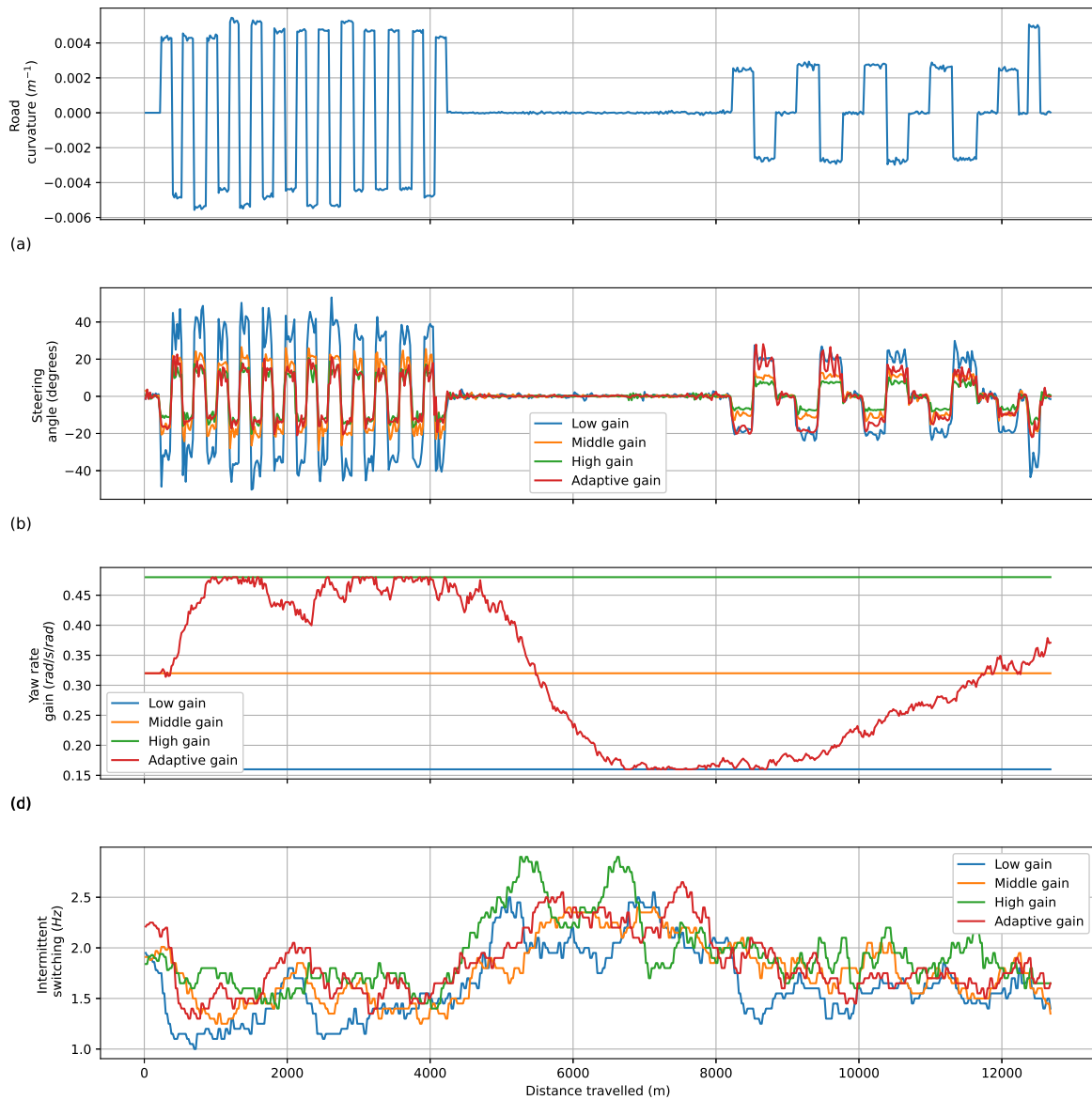


Figure I.16: Raw participant data on the experiment trials (participant 16).

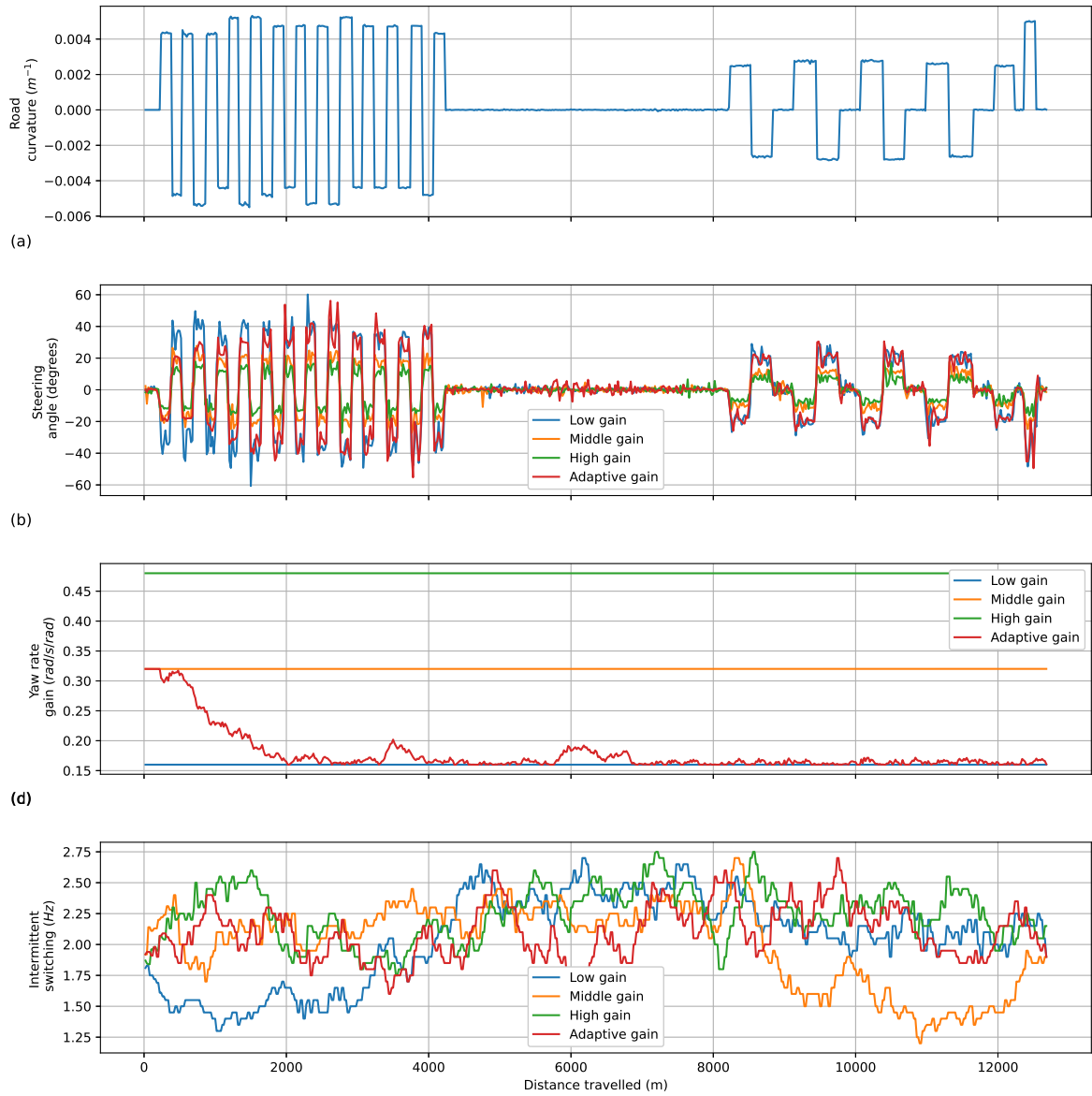


Figure I.17: Raw participant data on the experiment trials (participant 17).

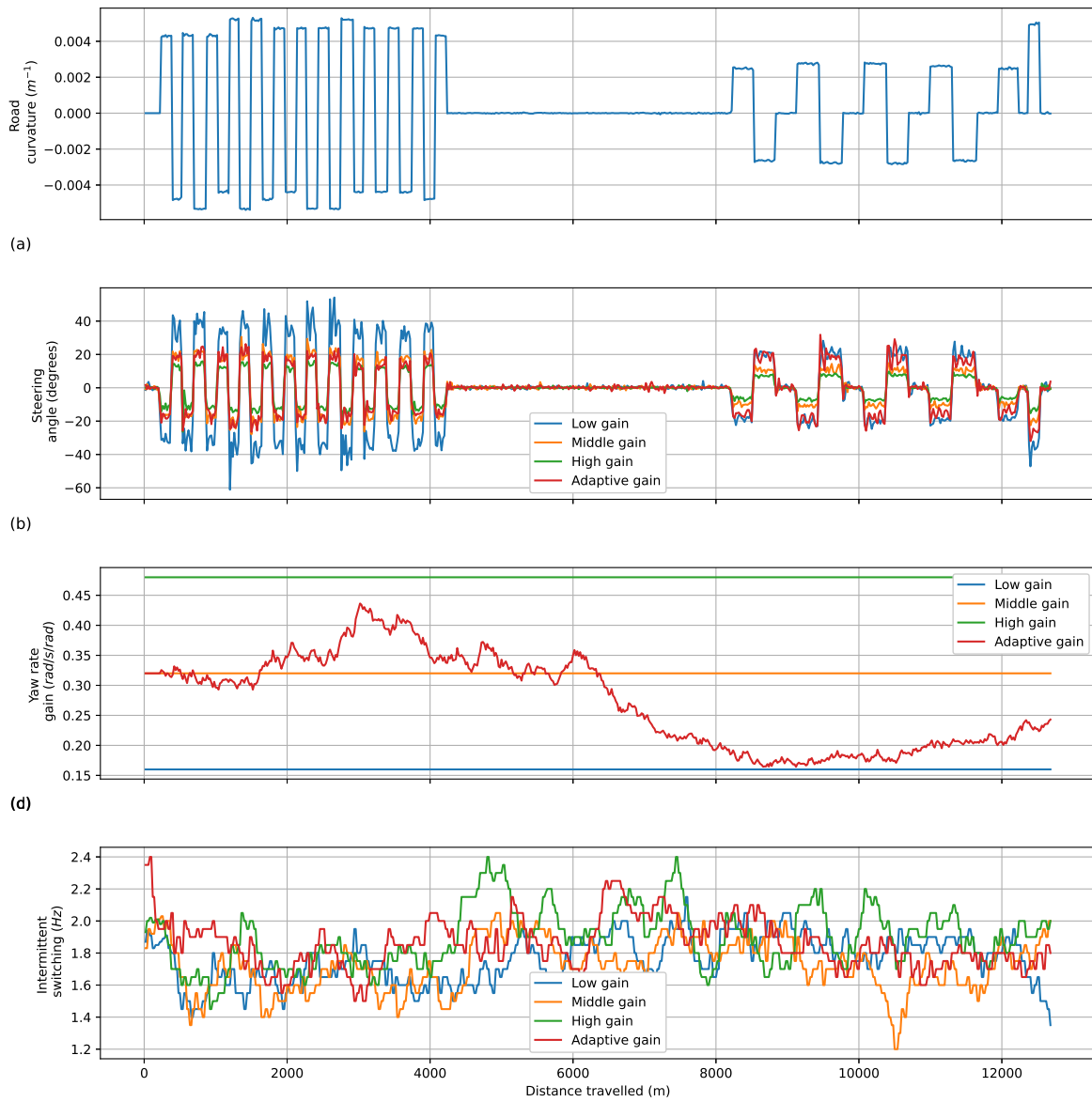


Figure I.18: Raw participant data on the experiment trials (participant 18).

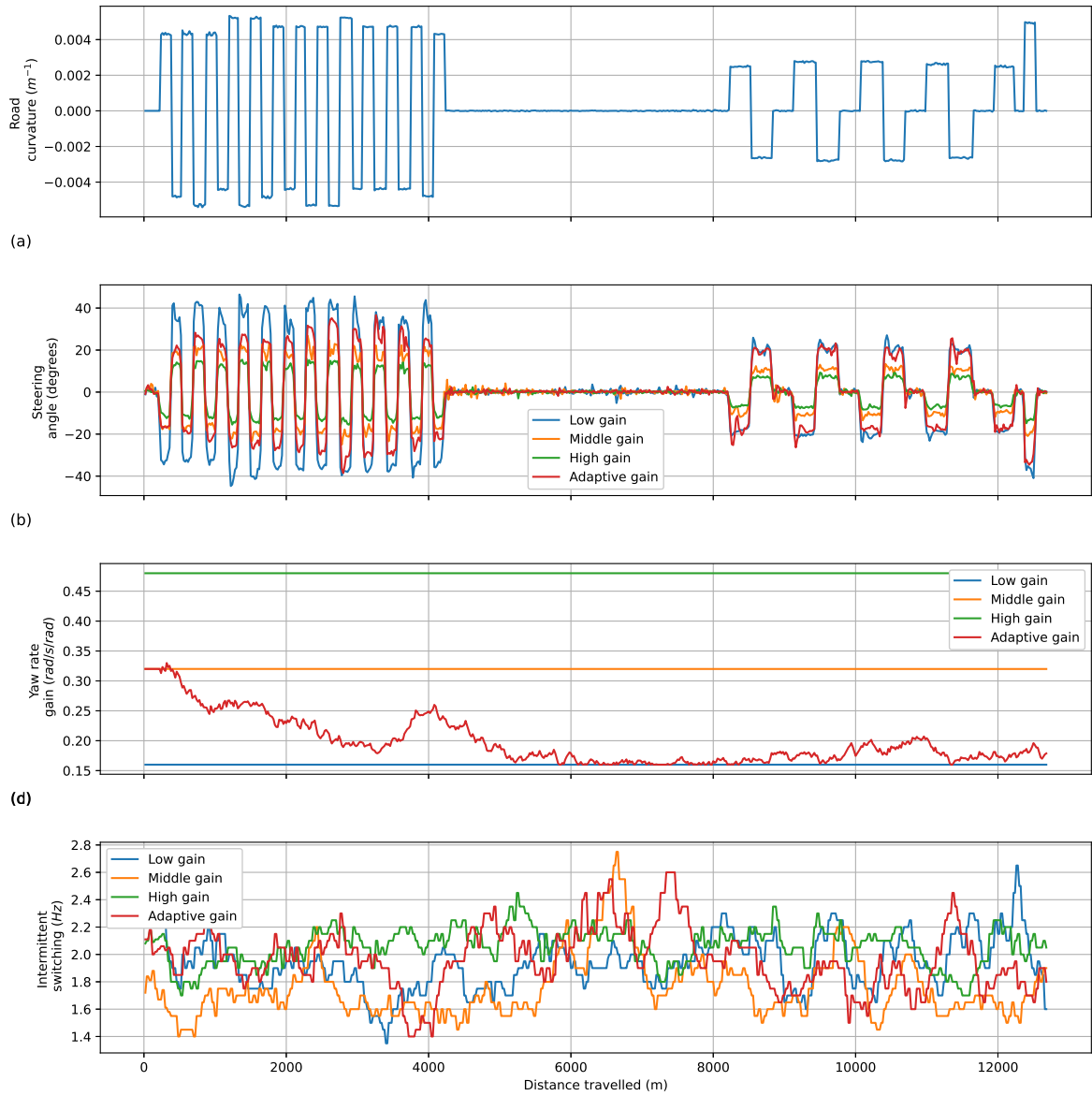


Figure I.19: Raw participant data on the experiment trials (participant 19).

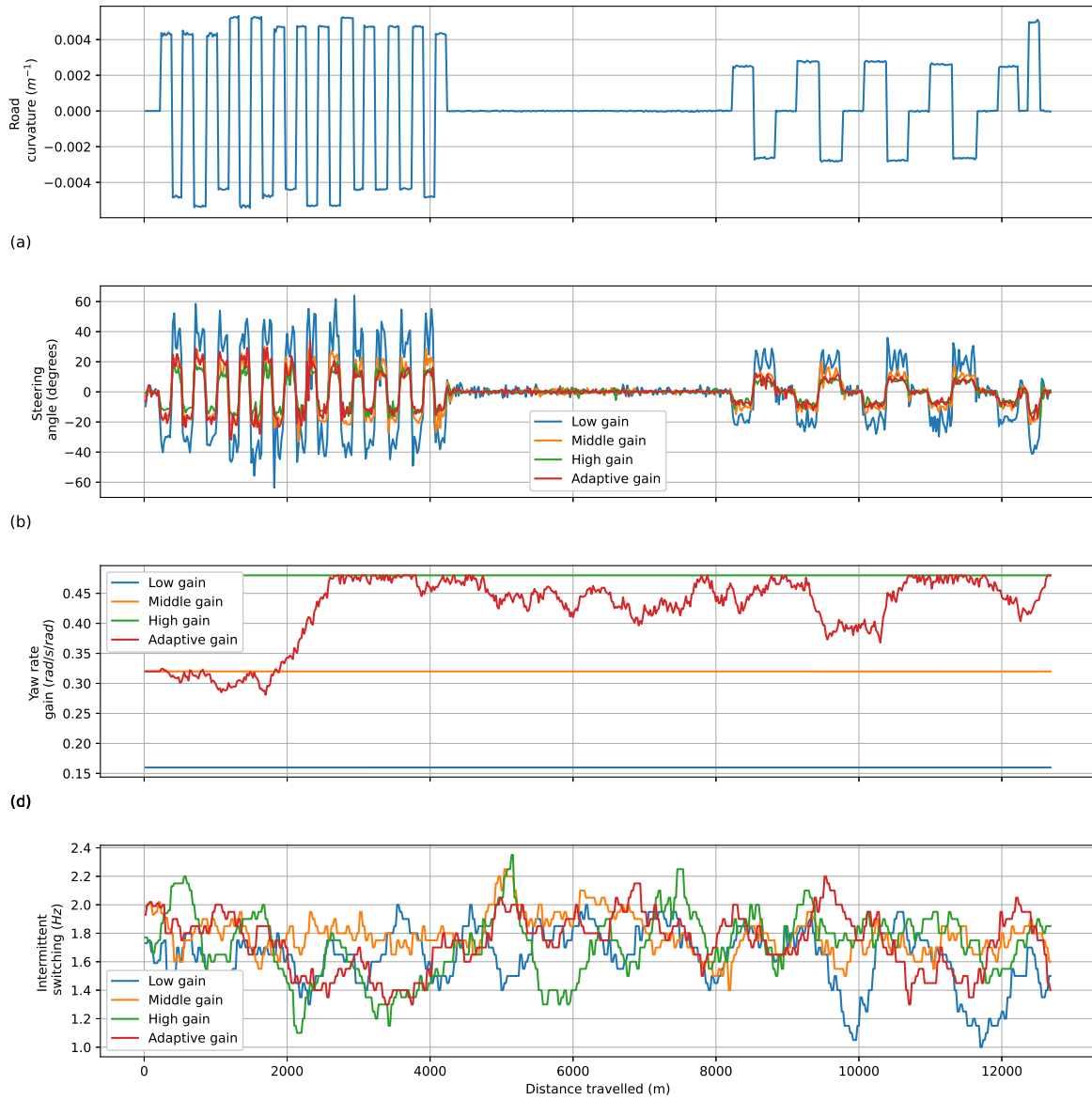


Figure I.20: Raw participant data on the experiment trials (participant 20).

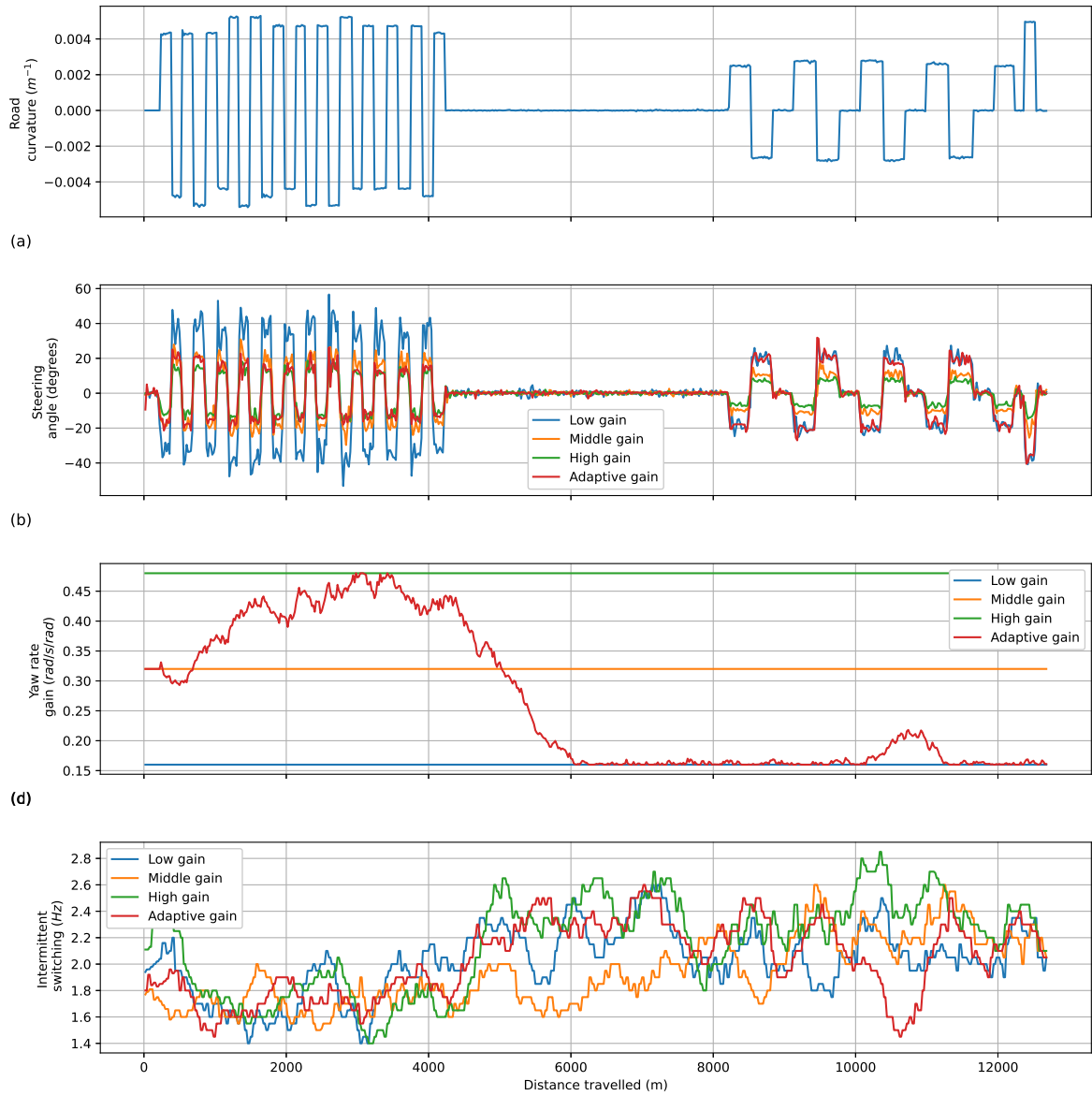


Figure I.21: Raw participant data on the experiment trials (participant 21).

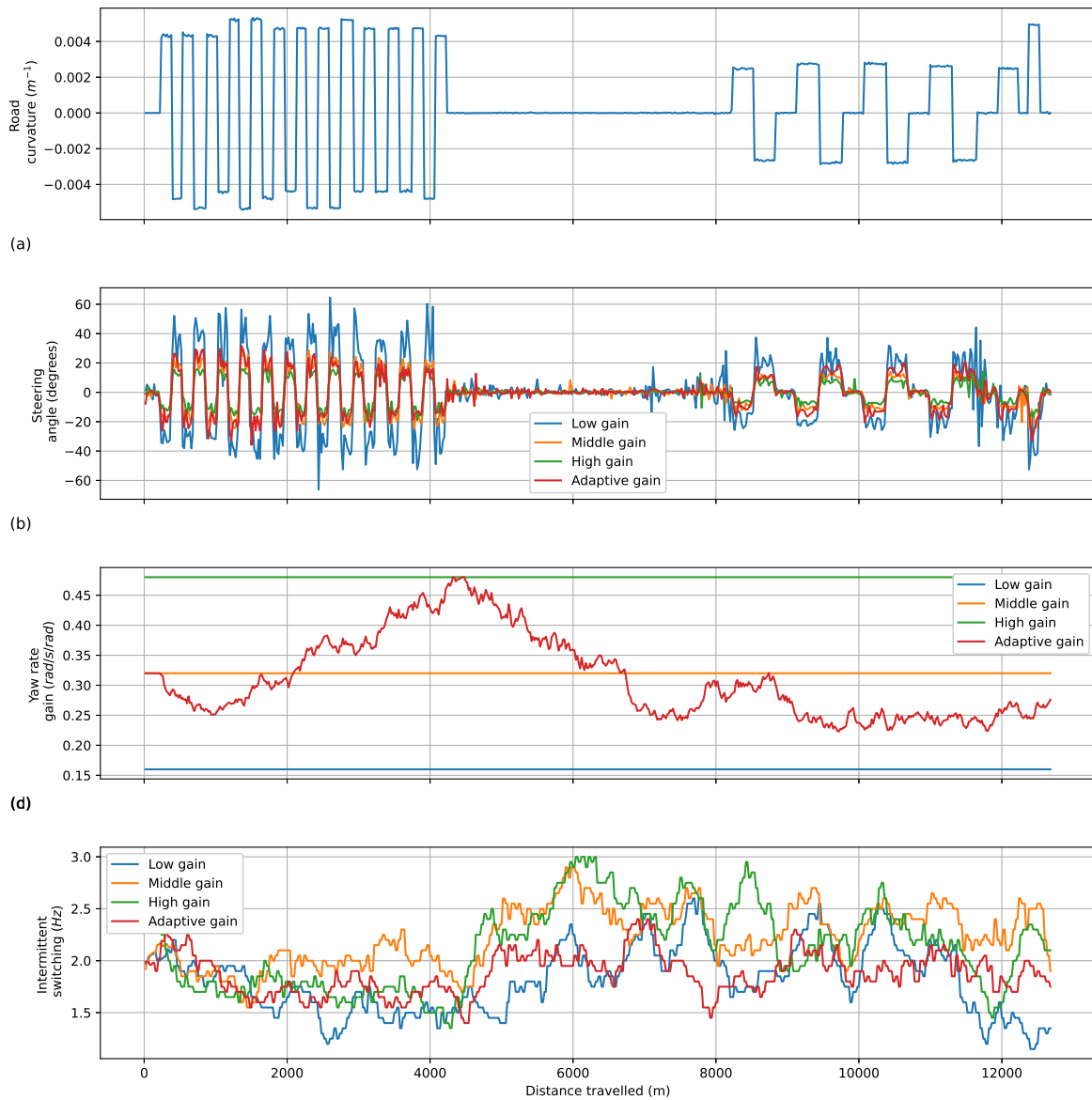


Figure I.22: Raw participant data on the experiment trials (participant 22).

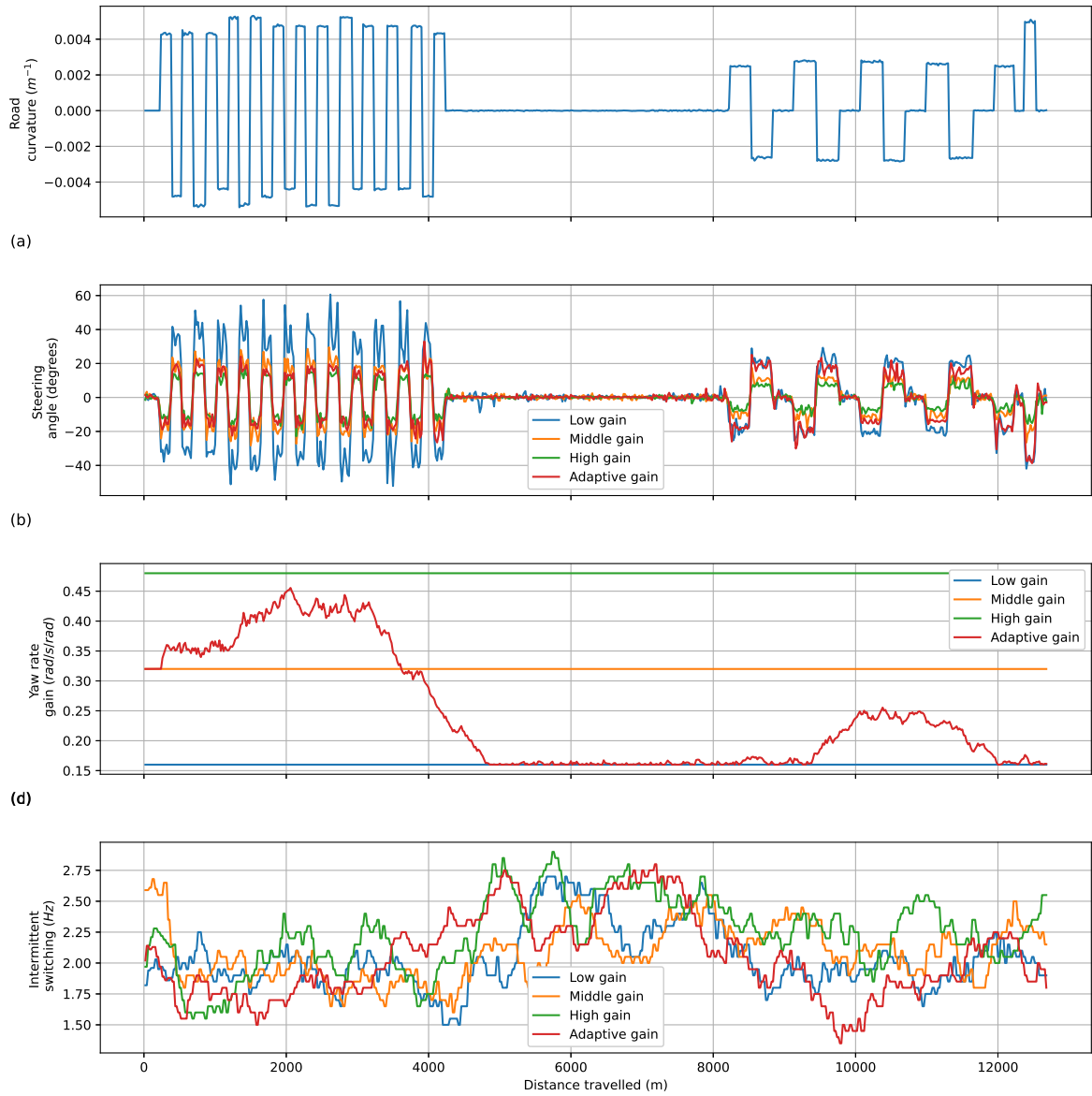


Figure I.23: Raw participant data on the experiment trials (participant 23).

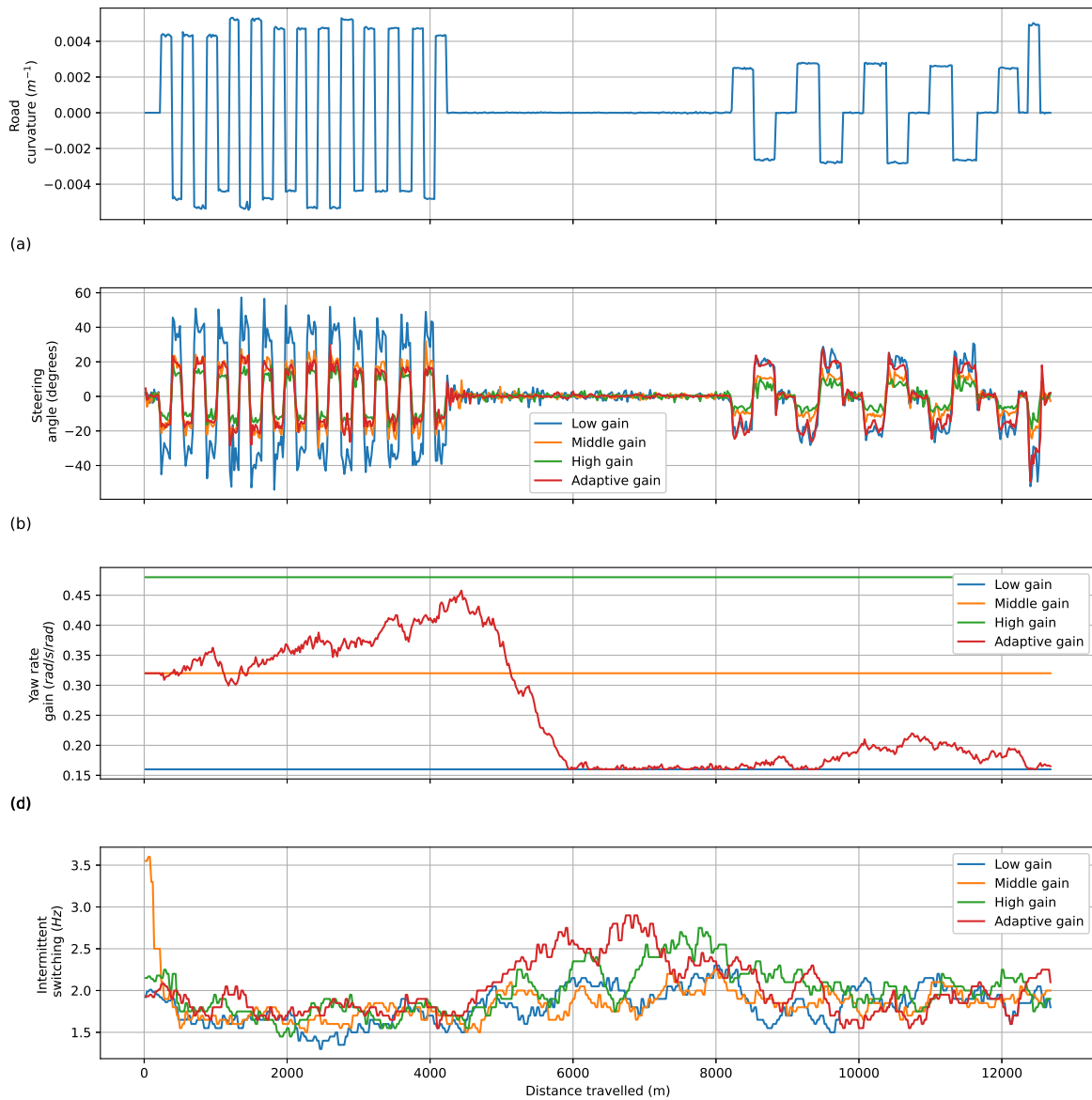


Figure I.24: Raw participant data on the experiment trials (participant 24).